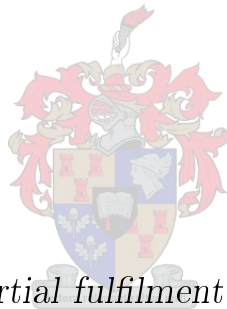


Solar Process Heat Systems: Development of an Open Source Simulation Package

by

Dylan Michael Fourie



Thesis presented in partial fulfilment of the requirements for the degree of Master of Engineering (Mechanical) in the Faculty of Engineering at Stellenbosch University

Supervisor: Prof. T. Harms

Co-supervisor: Dr. S. Hess

April 2019

Declaration

By submitting this thesis electronically, I declare that the entirety of the work contained therein is my own, original work, that I am the sole author thereof (save to the extent explicitly otherwise stated), that reproduction and publication thereof by Stellenbosch University will not infringe any third party rights and that I have not previously in its entirety or in part submitted it for obtaining any qualification.

Date: April 2019

Copyright © 2019 Stellenbosch University
All rights reserved.

Plagiarism Declaration

1. Plagiarism is the use of ideas, material and other intellectual property of another's work and to present it as my own.
2. I agree that plagiarism is a punishable offence because it constitutes theft.
3. I also understand that direct translations are plagiarism.
4. Accordingly all quotations and contributions from any source whatsoever (including the internet) have been cited fully. I understand that the reproduction of text without quotation marks (even when the source is cited) is plagiarism.
5. I declare that the work contained in this assignment, except where otherwise stated, is my original work and that I have not previously (in its entirety or in part) submitted it for grading in this module/assignment or another module/assignment.

17773695 Student number	 Signature
DM Fourie Initials and surname	04/02/2019 Date

Abstract

Solar Process Heat Systems: Development of an Open Source Simulation Package

D. Fourie

*Department of Mechanical and Mechatronic Engineering,
University of Stellenbosch,
Private Bag X1, Matieland 7602, South Africa.*

Thesis: MEng (Mech)

April 2019

Heat is a commonly used form of energy in industrial processes. Solar process heat or SPH is a field of renewable energy that can supply heat to industrial processes using the sun as a source of energy. SPH systems generally entail large investment costs.

A system designer, end-user and investor would naturally want to know how such a system would perform. This project focuses on the further development of previously established open-source pre-assessment software package for SPH systems named SolGain. This included modelling of flat plate, evacuated tube and parabolic trough collectors, pipes, heat exchangers, storage tanks and financials. Making SolGain user-friendly with easy user-inputs and graphic and relevant outputs was also a major focus of the project.

The accuracy of components modelled in SolGain was tested against TRNSYS (a widely trusted simulation package for SPH systems). All components of SolGain provided accuracy within 5% of TRNSYS. For system validation, the SolGain system's accuracy was within 10% of TRNSYS with SolGain underestimating energy outputs. These accuracy values can be considered satisfactory for a pre-assessment tool.

Uittreksel

Sonproshitte Stelsels: Ontwikkeling van 'n Oopbronsagteware Simulasiepakket

D. Fourie

*Departement Meganiese en Megatroniese Ingenieurswese,
Universiteit van Stellenbosch,
Privaatsak X1, Matieland 7602, Suid Afrika.*

Tesis: MIng (Meg)

April 2019

Hitte word dikwels as 'n vorm van energie in nywerheidsprosesse gebruik. Sonproshitte (SPH) is 'n tipe hernubare energie wat die son as energiebron benut om hitte aan nywerheidsprosesse te verskaf. Tog behels SPH-stelsels gewoonlik aansienlike beleggingskoste.

'n Stelselontwerper, eindgebruiker en belegger sal natuurlik wil weet hoe so 'n stelsel presteer. Hierdie projek handel oor die verdere ontwikkeling van die bestaande oopbronsagtewarepakket SolGain vir die voorafbeoordeling van SPH-stelsels. Dit het die modellering van verskillende soorte sonabsorbers (plat plate, lugleë buise en paraboliese trôe), hitteruilers, opgaartenks en finansies ingesluit. Nóg 'n belangrike doel van die projek was om SolGain gebruikervriendelik te maak met maklike gebruikertoevoer sowel as grafiese en relevante afvoer.

Die akkuraatheid van die komponente wat in SolGain gemodelleer is, is getoets aan die hand van TRNSYS ('n wyd beproefde en betroubare simulasiepakket vir SPH-stelsels). Nie een komponent van SolGain het met meer as 5% van TRNSYS afgewyk nie. Wat algehele stelselstaving betref, het die SolGain-stelsel met hoogstens 10% van TRNSYS verskil, met SolGain wat energielewe-

ring onderskat het. Hierdie akkuraatheidswaardes kan as bevredigend beskou word vir 'n voorafbeoordelingsinstrument.

Acknowledgements

Firstly I would like to thank **my parents** for their support during the duration of my masters. My reason for doing masters was definitely questionable at best, but you guys have supported me massively in pursuit of my dreams. It is a big blessing to have parents that are supportive of my dreams, while keeping my feet grounded.

Secondly I would like to thank my supervisor **Professor Harms** and co-supervisor **Dr Hess**. I gained valuable insight into grammar, spelling and compiling academic documents from you, Professor Harms. Dr Hess, it was always a pleasure contacting you over skype and email. I valued your inputs into my project over electronic communication and know that I would have learned a lot more from you had I been at the same institution as you.

Lastly I would like to acknowledge my God, **Jesus Christ**. I want this document and everything that I do to manifest Your glory. I want to honour You in everything I do and acknowledge that I need You and trust in You.

Dedications

"Work willingly at whatever you do, as though you were working for the Lord rather than for people. Remember that the Lord will give you an inheritance as your reward, and that the Master you are serving is Christ."

Colossians 3:23-24

Contents

Declaration	ii
Abstract	iv
Uittreksel	v
Acknowledgements	vii
Dedications	viii
List of Figures	xiii
List of Tables	xvii
Nomenclature	xviii
1 Introduction	1
1.1 Background	1
1.2 Objectives	2
1.3 Motivation	2
1.4 Overview of Report Structure	3
2 Literature Study	4
2.1 Viability of Solar Process Heat	4
2.2 Introduction to Solar Process Heat Systems	5
2.3 Solar Thermal Collectors	6
2.3.1 Flat plate collectors	6
2.3.2 Evacuated tube collectors	6
2.3.3 Parabolic trough collectors	7
2.4 Software Packages Similar to SolGain	8
2.4.1 Commercial packages	8
2.4.2 Open-source packages	11
2.5 Chapter Conclusion	12
3 Theoretical Background	13

3.1	Solar Radiation Theory	13
3.1.1	Position of the sun	13
3.1.2	Angles between sun and collector	15
3.1.3	Radiation components	17
3.2	Collector Theory	20
3.2.1	Efficiency curve	21
3.2.2	Incidence angle modifiers	22
3.2.3	Incidence angle modifier for beam irradiance	22
3.2.4	Calculation of specific useful power	24
3.2.5	Considerations for parabolic trough collectors	24
3.3	Thermal Energy Storage Theory	26
3.3.1	Multinode variable inlet tank model	28
3.3.2	Choice of number of nodes	30
3.4	Theory on Miscellaneous System Components	31
3.4.1	Heat exchangers	31
3.4.2	Pipes	32
3.5	Weather Data	33
3.6	System Performance Measurements	33
3.6.1	System efficiency and solar fraction	33
3.6.2	Financial methods of analysing renewable projects	35
3.7	Chapter Conclusion	37
4	Initial State of SolGain	38
4.1	The Original Aim of SolGain	38
4.2	User-Interface	39
4.2.1	Data input spreadsheet	39
4.2.2	Weather data spreadsheet	40
4.2.3	Heat demand profile	40
4.2.4	Results spreadsheet	41
4.3	Parameter Assumptions	41
4.3.1	Collector data	41
4.3.2	Specific heats	42
4.3.3	Collector aperture size	42
4.3.4	Storage parameters	42
4.3.5	Mass flow rate in the collector loop	43
4.3.6	Pipe surface	43
4.4	Component Validation	43
4.4.1	Pipe losses	44
4.4.2	Heat exchanger	44
4.4.3	Tank model	44
4.4.4	Collector	44
4.5	Chapter Conclusion	47
5	Modifications to SolGain	48

5.1	Rewriting SolGain Code	48
5.2	User Interface and Parameter Assumptions	50
5.3	Sun Position	51
5.4	Collector Modelling	52
5.5	System Controls	53
5.5.1	Calculation of collector side heat exchanger temperatures	54
5.5.2	Calculation of collector inlet and outlet temperatures . .	55
5.5.3	Calculation of collector loop mass flow rate	55
5.6	Tank Model	56
5.7	System Performance Measurements	56
5.7.1	Manual collector inputs	57
5.7.2	Automatic collector inputs	57
5.8	Chapter Conclusion	58
6	Component Validation	59
6.1	Angle of Incidence	59
6.2	Radiation on the Collector	61
6.3	Collector Model Testing	63
6.3.1	Flat plate collector	63
6.3.2	Evacuated tube collector	64
6.3.3	Parabolic trough collector	65
6.4	Pipes	66
6.5	Heat Exchanger	68
6.6	Thermal Energy Storage Tank	69
6.7	Chapter Conclusion	71
7	System Validation	72
7.1	System with Non-concentrating Collectors	72
7.2	System with Concentrating Collectors	74
7.3	Chapter Conclusion	76
8	Conclusion and Recommendations	77
8.1	Conclusion	77
8.2	Recommendations	77
	Appendices	79
A	Userforms and Parameter Assumptions	80
A.1	Geographical Inputs Userform	81
A.2	Process Information Userform	81
A.3	Daily, Weekly and Monthly Demand Userforms	82
A.4	First Collector Input Userform	83
A.5	Manual Collector Inputs Userform	84
A.6	Collector Tilt and Azimuth Userform	85

A.7	Collector Field Layout Userform	86
A.8	Miscellaneous System Inputs Userform	86
A.9	Financial Inputs Userform	89
A.10	Heat Transfer Fluid in the Collector Loop	89
B	SolGain 2.0 Program Structure	91
C	Heat Transfer Fluids Properties	93
C.1	Water and Glycol	93
C.2	<i>Therminol 66</i>	94
D	Collector Datasheets	95
D.1	Flat Plate Collector	96
D.2	Evacuated Tube Collector	97
D.3	Parabolic Trough Collector	99
	List of References	104

List of Figures

1.1	Pampa Elvira SPH plant, Chile. Picture: Arcon-Sunmark (2017) . . .	1
2.1	Electricity generation around the world by source pie chart. Picture: International Energy Agency (2017)	4
2.2	A typical basic SPH system, also the system setup that is modelled by SolGain 2.0.	5
2.3	An illustration of a flat plate collector. Picture: Ilchmann (2016) . . .	6
2.4	An illustration of an evacuated tube collector. Picture: Ilchmann (2016)	7
2.5	An illustration of a parabolic trough collector. Picture: Ilchmann (2016)	8
2.6	A basic TRNSYS simulation model of a solar preheating application. Left: TRNSYS black-box visual of simulation system Right: A schematic of the same simulation system. Picture: Solar Energy Laboratory (2007)	9
2.7	A screen-shot of a typical SPH system diagram in Polysun.	10
2.8	The monthly heat production visual generated by SHIPcal. Screen shot taken from Frassetto (2016)	12
3.1	Illustration of angles used to define the position of the sun	14
3.2	Angles used to define the position of a collector. Top left: Collector tilt β Right: Collector azimuth γ Bottom left: Tube orientation (Only for ETCs)	16
3.3	Incidence angle θ decomposed into longitudinal θ_l and transverse θ_t components. Picture: Theunissen and Beckman (1985)	17
3.4	Two models of sky and ground reflected irradiance. Yellow arrows: G_{st} and G_{rt} according to the isotropic model. Blue curve: G_{st} according to the Perez model. Picture: adapted from Hess (2014)	18
3.5	An illustration of the cosine-effect. Picture: Hess (2014)	19
3.6	Generic collector output curves for different collector types. Incidence angles are equal to perpendicular. Picture: Hess (2014)	21

3.7	Left: One-dimensional collector (FPC) and Right: Two-dimensional collector (ETC) with the angle of incidence θ decomposed into transversal θ_t and longitudinal θ_l components. Picture: Carvalho <i>et al.</i> (2007)	23
3.8	Graphical representation of the incidence angle for a parabolic trough, where $\theta = \theta_l$. It can be seen that $\theta > 0$ will result in end losses . . .	25
3.9	A stratified tank. The temperature profile and appropriate parameters divided by Pizzolato <i>et al.</i> (2015) are displayed.	27
3.10	A five-node variable inlet tank model. $T_{s,2} > T_{co} > T_{s,3}$ and therefore the fluid entering is assumed to flow to node 3. Picture: Duffie and Beckman (2013)	27
3.11	A three-node tank displaying all heat flows and relevant parameters. Picture: Duffie and Beckman (2013)	28
3.12	System efficiency and solar fraction vs system size. Picture: adapted from Deutsche Gesellschaft für Sonnenenergie (2010)	34
3.13	A graphical representation of IRR. NPV is on the y-axis and discount rate, d , is on the x-axis. IRR occurs where NPV = 0.	36
3.14	System cost relative to gross collector area. The exchange rate on the date of installation was used ($9.66 < \text{ZAR}/\text{EUR} < 15.3$ from 2007 to 2015). Picture: Joubert <i>et al.</i> (2016)	37
4.1	A visual representation of the initial concept of SolGain. Picture: adapted from Ilchmann (2016)	38
4.2	A screen-shot of the data input spreadsheet in SolGain 1.0. Fields highlighted in red are mandatory for the user to input.	40
4.3	A visual representation of the concept of a heat demand profile . .	41
4.4	SolGain 1.0 calculated angle of incidence on 1 January in Vancouver. Picture: Ilchmann (2016)	45
4.5	SolGain 1.0 irradiance on a collector (tilted) on 5 February for Vancouver Left: Beam irradiance (G_{bt}) Right: Diffuse sky irradiance (G_{dt}) Bottom: Ground reflected irradiance (G_{rt}). Picture: Ilchmann (2016)	46
4.6	SolGain 1.0 collector output test results for Vancouver on 26 February. Picture: Ilchmann (2016)	47
5.1	SolGain 2.0's userform structure	50
5.2	A userform (<i>Miscellaneous System Inputs</i>) used for user inputs in SolGain 2.0	51
5.3	Collectors in series and parallel	52
5.4	An isolated part of the SolGain 2.0 system relevant for storage charging using solar means	53
5.5	Target temperature mass flow control strategy	54
5.6	Pipe inlet temperature calculation from pipe outlet temperature . .	55
5.7	Simulation results in SolGain 2.0	58

6.1	Angle of incidence for 1 January Left: Cape Town Right: London	60
6.2	Angle of incidence for 12 May Left: Cape Town Right: London . .	61
6.3	Angle of Incidence for 26 October Left: Cape Town Right: London	61
6.4	Total Irradiance onto collector Left: 1 January (clear day) Right: 20 June (overcast day)	62
6.5	FPC outlet temperature ($T_{col,out}$) Left: 1 January (clear day) Right: 20 June (overcast day)	64
6.6	ETC outlet temperature ($T_{out,col}$) Left: 1 January (clear day) Right: 20 June (overcast day)	66
6.7	PTC outlet temperature ($T_{out,col}$) Left: 1 January (clear day) Right: 20 June (overcast day)	67
6.8	Schematic representation of the system modelled in TRNSYS for pipe tests	67
6.9	Schematic representation of the system modelled in TRNSYS for heat exchanger tests	68
6.10	Schematic representation of the system modelled in TRNSYS for storage tank tests	69
6.11	Tank model node temperatures on the 5th of March Top left: node one (i.e. $T_{pro,in}$) Top right: node three Bottom left: node eight Bottom right: node twelve (i.e. $T_{HE,tank,in}$)	70
7.1	Schematic representation of the system modelled in TRNSYS for pipe tests	72
7.2	Monthly heat supplied to the process by a non-concentrating col- lector system for TRNSYS and SolGain 2.0	74
7.3	Monthly heat supplied to the process by a concentrating collector for TRNSYS and SolGain 2.0	75
A.1	A screen-shot of the <i>Weather Data</i> spreadsheet in SolGain 2.0 . . .	80
A.2	A screen-shot of the <i>Geographical Inputs</i> userform in SolGain 2.0 .	81
A.3	A screen-shot of the <i>Process Information</i> userform in SolGain 2.0 .	81
A.4	A screen-shot of the <i>Weekly Demand</i> userform in SolGain 2.0 . . .	82
A.5	A screen-shot of the <i>First Collector Input</i> userform in SolGain 2.0 .	83
A.6	A screen-shot of the <i>Manual Collector Inputs</i> userform in SolGain 2.0	84
A.7	A screen-shot of the <i>Evacuated Tube Collector Tilt and Azimuth</i> userform in SolGain 2.0	85
A.8	A screen-shot of the <i>Parabolic Trough Collector Tilt and Azimuth</i> userform in SolGain 2.0	85
A.9	A screen-shot of the <i>Concentrating Collector Field Layout</i> userform in SolGain 2.0	86
A.10	A screen-shot of the <i>Miscellaneous System Inputs</i> userform in Sol- Gain 2.0	87
A.11	A screen-shot of the <i>Financial Inputs</i> userform in SolGain 2.0 . . .	89

B.1 Flow structure of a year simulation in SolGain 2.0 92

List of Tables

3.1	Terms used for radiation based on the work of Iqbal (1983)	13
4.1	Input data breakdown of SolGain 1.0 (Ilchmann, 2016)	39
4.2	Input Data for angle of incidence testing in SolGain 1.0 (location: Vancouver)	44
4.3	Input data for collector output testing of SolGain 1.0	47
4.4	IAM references for collector output testing of SolGain 1.0	47
5.1	Physical object classes in SolGain 2.0	49
5.2	Non-physical object classes in SolGain 2.0	50
6.1	Input data for angle of incidence testing in the southern hemisphere (location: Cape Town)	60
6.2	Input data for angle of incidence testing in the northern hemisphere (location: London)	60
6.3	Input data for FPC testing	63
6.4	IAM references for FPC testing	63
6.5	Input data for ETC testing	65
6.6	IAM references for ETC testing	65
6.7	Input data for PTC testing	66
6.8	Input data for PTC testing.	67
6.9	Input data for Pipe testing	68
6.10	Input data for heat exchanger testing	69
6.11	Input data for thermal storage tank testing	69
7.1	Input data for system with non-concentrating collectors testing . .	73
7.2	Changes made to input data contained in Table 7.1 for system validation with concentrating collectors	75
C.1	Glycol and water mixtures and there freezing points (Alvarez, 2010)	93

Nomenclature

Abbreviations

CFD	Computational fluid dynamics
DHI	Diffuse horizontal irradiance
DNI	Diffuse normal irradiance
ETC	Evacuated tube collector
FPC	Flat plate collector
GHI	Global horizontal irradiance
HTF	Heat transfer fluid
HVAC	Heating, ventilation and air conditioning
IAM	Incidence angle modifier
IRR	Internal rate of return
LCOH	Levelised cost of heat
NPV	Net present value
NTU	Number of transfer units
PTC	Parabolic trough collector
SAURAN	South African universities radiometric networks
SPH	Solar process heat

STERG	Solar thermal energy research group
TMY	Typical meteorological year
VBA	Visual basic for applications

Greek Variables

α_s	Solar elevation angle	[°]
β	Collector tilt	[°]
γ	Collector orientation	[°]
γ_s	Solar azimuth angle	[°]
δ	Declination angle	[°]
ϵ	Heat exchanger effectiveness	[–]
η	Efficiency	[–]
η_0	Intercept efficiency of collector	[–]
θ	Angle of incidence	[°]
θ_l	Longitudinal projection of angle of incidence . . .	[°]
θ_t	Transversal projection of angle of incidence . . .	[°]
θ_z	Solar zenith angle	[°]
ρ_{grd}	Ground reflectance	[–]
ϕ	Local latitude	[°]
ψ	Local longitude	[°]
$\psi_{timezone}$	Timezone longitude	[°]
ω	Hour angle	[°]

Latin Variables

A	Area	[m ²]
C	Cash flow	[currency]
c_{eff}	Collector effective heat capacity	[J/(m ² K)]
C_{max}	Maximum heat capacity rate	[W/K]
C_{min}	Minimum heat capacity rate	[W/K]
c_p	Specific heat at constant pressur	[J/(kg K)]
d	Diameter	[m]
d_{local}	Day of the year	[-]
dr	Discount rate	[-]
EOT	Equation of time	[min]
G	Irradiance (power)	[W/m]
h	Height	[m]
h_{local}	Hour of the day	[-]
I	Irradiation (energy)	[kW h/m ²]
IRR	Internal rate of return	[-]
K	Incidence angle modifier	[-]
L	Length	[m]
M	Mass	[kg]
\dot{M}	Mass flow rate	[kg/s]
\dot{m}	Specific mass flow rate per unit collector aperture area	[kg/(s m ²)]
N	Number of an item	[-]

n	Year number	[–]
NPV	Net present value	[currency]
NTU	Number of transfer units	[–]
Q	Heat	[kW h]
\dot{Q}	Heat transfer rate	[W]
\dot{q}	Specific heat transfer rate per unit collector aperture area	[W/m ²]
r	Radius	[m]
SF	Solar fraction	[–]
T	Temperature	[°C]
t	Time	[s]
$\Delta t_{internal}$	Internal time step	[s]
U	Heat transfer coefficient	[W/(m ² K)]
w	Width	[m]

Subscripts

a	Ambient
aux	Auxiliary heater
avg	Average
b	Beam
col	Collector
d	Diffuse
$endGain$	End gains
$endLoss$	End loss

<i>fl</i>	Fluid
<i>fo</i>	Focal
<i>gap</i>	Gap between collectors
<i>gain</i>	Collector gain
<i>HE</i>	Heat exchanger
<i>in</i>	Inlet
<i>nodes</i>	Tank nodes
<i>out</i>	Outlet
<i>par</i>	Parallel
<i>p</i>	Pipe
<i>pro</i>	Process
<i>r</i>	Ground reflected
<i>ref</i>	Reference
<i>s</i>	Sky diffuse
<i>ser</i>	Series
<i>sol</i>	Solar
<i>sys</i>	System
<i>t</i>	Tilted surface
<i>tank</i>	Storage tank
<i>tot</i>	Total
<i>to</i>	Turnovers
<i>use</i>	Useful

Superscripts

c	Collector
p	Process
$'$	Tank

Chapter 1

Introduction

1.1 Background

Heat is a commonly used form of energy for many industrial processes (e.g. food cooking, sugar milling, cleaning, drying, heating ventilation and cooling (HVAC)). In recent years a field of renewable energy has opened up, whereby solar energy is collected and used to provide process heat. These systems are generally large scale and entail large investment costs.



Figure 1.1: Pampa Elvira SPH plant, Chile. Picture: Arcon-Sunmark (2017)

A designer, end-user and possible investor of solar process heat (SPH) systems would naturally want a pre-assessment estimation of the performance of such a system. This could include, amongst others, the expected temperatures, energy output, solar fraction and financial performance measurements. For this reason a trustworthy, user-friendly way of modelling SPH systems could be of much value to the renewable energy industry.

The main purpose of this thesis is to further develop an existing software package, SolGain, that currently partially performs the aforementioned functions. SolGain is programmed using Microsoft Excel and Visual Basic Applications (VBA). The software package will be open-source and will be free to download from the Solar Thermal Energy Research Group (STERG) webpage.

1.2 Objectives

The objectives of this project are to further develop the current SolGain 1.0 software to be ready for release on the STERG web page. This entails improving SolGain in the following ways:

- **Functionality:**
 - Model a number of commonly used SPH collectors.
 - Develop a financial model.
 - Allow a user more control over the system model.
- **Accuracy:**
 - Develop a more detailed simulation model (including collectors, storage and heat exchangers).
 - Improve heat flow tracking.
- **User-friendliness:**
 - Include descriptive and insightful visuals.
 - Implement user warnings and error messages.

1.3 Motivation

In the solar thermal industry there are open-source software packages available to model small-scale, domestic solar thermal systems. However, no such open-source software package exists for large-scale, industrial applications.

This thesis will provide a solution to the above problem. SolGain will be advantageous for the industry image of STERG and Stellenbosch University, as individuals using the software package will associate the product with STERG and Stellenbosch University.

1.4 Overview of Report Structure

Chapter 2 contains a literature study to provide a background to solar process heat systems and their simulation packages. This is followed by Chapter 3, which contains all the theoretical background needed for the development of SolGain 2.0. Chapter 4 is a review of SolGain 1.0 as documented by Ilchmann (2016). The work completed on SolGain (to create SolGain 2.0) during this project is then documented in Chapter 5. Test results from component and system validation are contained in Chapter 6 and 7 respectively. The report is then concluded in Chapter 8 and recommendations for further development are given.

The Appendices of this report contain important documentation. Appendix A provides a walk-through of the user interface developed for SolGain 2.0. Various assumptions made based on the user's preference are outlined in this appendix. Appendix B contains a flow chart of SolGain 2.0's main subroutine. The fluid properties of heat transfer fluids used in SolGain 2.0 are discussed in Appendix C. Finally the collector datasheets of collectors implemented in SolGain 2.0 are contained in Appendix D.

Chapter 2

Literature Study

A literature study of solar process heat (SPH) systems is contained in this chapter. An introduction to solar process heat systems is given, followed an introduction to solar collectors. Finally a few software systems similar to SolGain are reviewed.

2.1 Viability of Solar Process Heat

The renewable sector has grown substantially in recent times (refer to Figure 2.1), possibly due to a global wide realization that more sustainable sources of energy are needed. Rising prices of fuel and health issues caused by fossil fuel emissions have also resulted in increased investment into renewable energy (Joubert *et al.*, 2016).

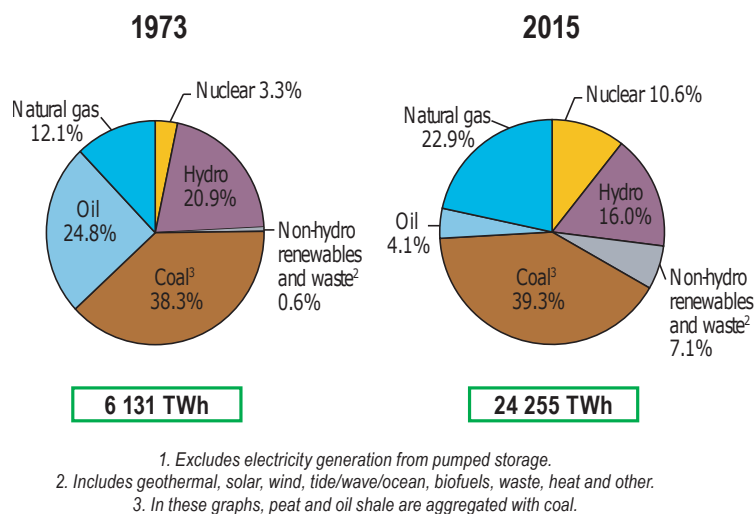


Figure 2.1: Electricity generation around the world by source pie chart. Picture: International Energy Agency (2017)

A technology that is particularly useful in the generation of heat for industrial processes is solar thermal technology. Solar thermal technologies in industrial applications have a high potential in South Africa. In 2016, South Africa consumed 122.3 t of oil worth in energy, which was 27.8% of Africa's total energy usage for the same year (British Petroleum, 2017), meaning that South Africa is a highly energy intensive country.

According to the Energy Research Centre (2013), 44% of South Africa's energy demand goes towards heat generation. South Africa also has abundant solar resources with global horizontal irradiation (GHI) in South Africa around 2000 kWh/(m² a) for industrial areas, compared to 1200 kWh/(m² a) in central Europe (Joubert *et al.*, 2016). The above factors make solar process heat a highly attractive and viable option in South Africa.

2.2 Introduction to Solar Process Heat Systems

This section will describe the operation of a standard SPH system to allow the reader to contextualise this project. A typical basic SPH system is displayed below in Figure 2.2. It consists of a solar field of collectors, a heat exchanger, a thermal storage tank, an auxiliary heater and piping to connect all system components.

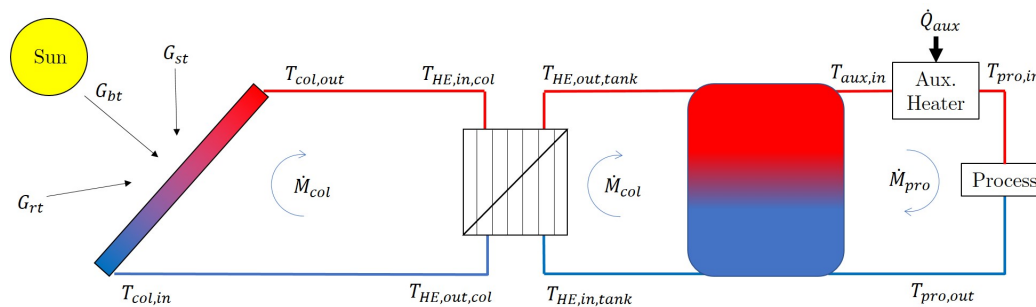


Figure 2.2: A typical basic SPH system, also the system setup that is modelled by SolGain 2.0.

The heat transfer fluid (HTF) in the collector loop is heated up by the sun as it passes through the collector. The HTF is then transported to a heat exchanger where its heat is transferred to the HTF in the tank loop. The HTF in the tank loop then is transported to the tank for thermal storage. HTF is drawn from the tank to support the process. Before it is sent to the process the HTF is heated by an auxiliary heater to the exact process inlet temperature.

This is a simplified model of an SPH system. It is sufficient for the purposes of introducing SPH systems to the reader and is also a sufficient model for the purposes of SolGain 2.0 as a pre-assessment tool.

2.3 Solar Thermal Collectors

A major aspect of this project entails modelling different collector types. For this reason a literature review was done in order to gain insight into different collectors and their operating principles.

2.3.1 Flat plate collectors

A flat plate collector (FPC) is the most commonly used solar collector according to AEE - Institute for Sustainable Technologies (2009*b*). The collector consists of a transparent cover, absorber, pipes holding the heat transfer fluid (HTF), insulation and a frame. Irradiation from the sun passes through the cover and is absorbed by the absorber. This heat is then transferred to the HTF in the pipes. An illustration of a flat plate collector can be seen below in Figure 2.3.

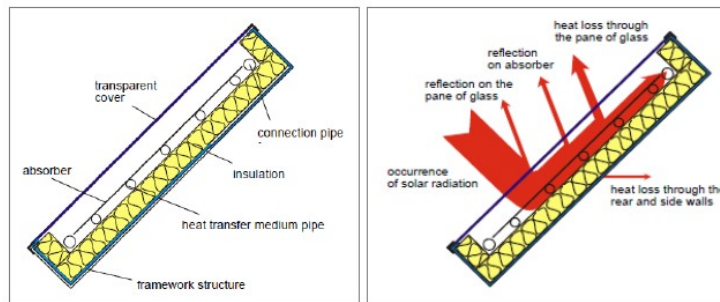


Figure 2.3: An illustration of a flat plate collector. Picture: Ilchmann (2016)

Heat loss occurs due to the imperfect transmissivity of the cover and absorptivity of the absorber. Radiation and convection losses occur to the environment from all collector components, although the glass cover reduces convection heat transfer losses and the insulation reduces conduction heat transfer losses.. These collectors can reach temperatures up to 100 °C (AEE - Institute for Sustainable Technologies, 2009*b*).

2.3.2 Evacuated tube collectors

There are various different designs of evacuated tube collectors (ETCs) available, with similar operating principles. The main component of an ETC is the evacuated tube itself. The tube consists of an outer glass tube, with an inner

tube made of a material with a high conductivity (usually copper). The space between the inner and outer tube is a vacuum (or as close to a vacuum as possible). This is to minimize further convection heat loss to the environment from the inner tube (Ilchmann, 2016). An illustration of an evacuated tube collector can be seen below in Figure 2.4.

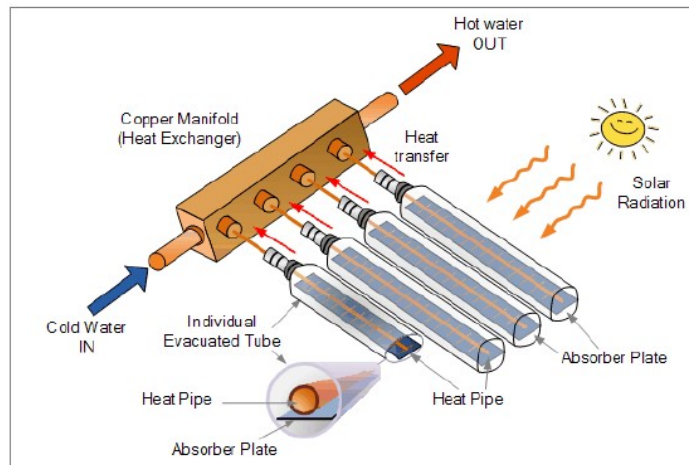


Figure 2.4: An illustration of an evacuated tube collector. Picture: Ilchmann (2016)

Although the exact operating procedure of ETCs differs, the aforementioned main principle of preventing heat loss to the environment applies to all ETCs. These kinds of collectors can reach temperatures of up to 130 °C (AEE - Institute for Sustainable Technologies, 2009b).

2.3.3 Parabolic trough collectors

The parabolic trough collector (PTC) is the first kind of collector addressed in this text that is a concentrating collector. This means that they concentrate the sun's irradiation to reach higher temperatures. The collector makes use of a reflective parabolic surface to concentrate almost parallel irradiation beams from the sun to a single line. This requires tracking of the sun around the north-south axis or east-west axis (AEE - Institute for Sustainable Technologies, 2009b).

At the location of the concentrated line, a pipe with a high absorptivity is placed. The HTF is transported through the pipe from one end of the parabolic trough to the other, heating up along the way (Ilchmann, 2016). Temperatures up to 450 °C are attainable using parabolic trough collectors (AEE - Institute for Sustainable Technologies, 2009b).

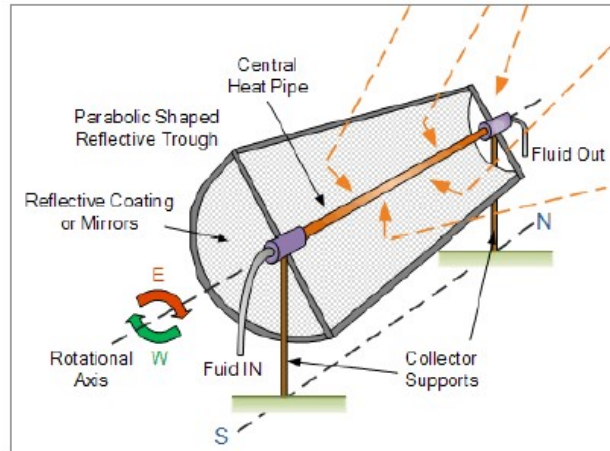


Figure 2.5: An illustration of a parabolic trough collector. Picture: Ilchmann (2016)

2.4 Software Packages Similar to SolGain

A study was completed on existing software packages performing similar functions to those envisaged in SolGain. The successes as well as failures of these packages are investigated with the aim of learning from them. In order to not reinvent the wheel, SolGain 2.0 was developed with these in mind.

2.4.1 Commercial packages

Commercial software packages provide system designers with accurate simulations of SPH systems. They supply designers with invaluable insights into projects. They are also a great way of marketing SPH to possible investors as many of them supply financial modelling.

They are usually expensive and/or complex, meaning that they are of little use to end-users of SPH systems who invariably have little solar thermal experience. Source code of commercial packages is also not available for external development. The above two factors necessitate the need for an open-source alternative.

Nevertheless valuable insights can be gained by reviewing these software packages. In this literature study TRNSYS version 16 (Solar Energy Laboratory, 2007) and Polysun version 10.2 (Vela Solaris, 2017) will be reviewed. From now on TRNSYS 16 will be referred to as TRNSYS and Polysun 10.2 as Polysun.

A brief introduction to TRNSYS and Polysun will now be given. The introduction to these software packages will serve the function of assisting the reader in acquainting themselves with TRNSYS and Polysun.

TRNSYS

TRNSYS, which is shorthand for TRaNsient SYstems Simulation software uses a graphic user interface to facilitate simulating transient systems. These systems are mostly thermal and electrical systems. TRNSYS is often used to simulate solar thermal systems (Solar Energy Laboratory, 2007).

The simulation package models components as black-boxes with various inputs and outputs. The user can set up a simulation by selecting from a list of components that have been developed by Solar Energy Laboratory (2007). These components can be arranged as the user requires.

Connections between components can be made by the user. These connections represent certain outputs from a component being used as inputs for the next component. This can be visually seen below in Figure 2.6.

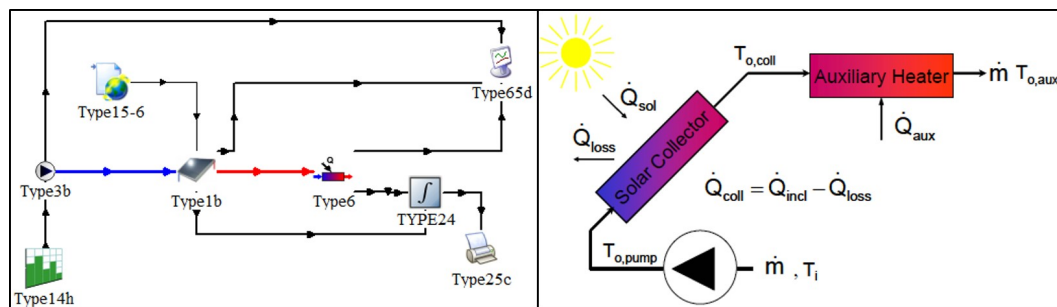


Figure 2.6: A basic TRNSYS simulation model of a solar preheating application. **Left:** TRNSYS black-box visual of simulation system **Right:** A schematic of the same simulation system. Picture: Solar Energy Laboratory (2007)

TRNSYS contains a library of weather data from locations around the world. This can be used as the weather input data for a simulation or alternatively the user can input weather data using a traditional weather data file such as a TMY2 file (Solar Energy Laboratory, 2007).

A very useful function of TRNSYS is that it contains a platform for users and third-party developers to add their own black-box components. This can be done using all common programming languages. TRNSYS can also interface with other applications before and after simulations (Solar Energy Laboratory, 2007).

TRNSYS does not contain any financial modelling. For this reason a software package containing a financial modelling tool will now be examined.

Polysun

Polysun is a simulation software that can be used to simulate solar thermal, photovoltaic and geothermal systems (Vela Solaris, 2017). Simulations can also include more than one energy source (i.e. solar thermal, solar photovoltaic or geothermal) in an integrated system.

The software package groups systems for a set of consumers at a set location into a *project*. A project contains various *system diagrams*, which describe a specific energy system. Polysun also includes templates of common energy systems that can be used as a starting point for a designer.

A system diagram contains all components and connections that are contained in the energy system. Polysun models systems in a similar fashion to TRNSYS (i.e. as black-boxes); however, less effort is required in setting up Polysun simulations. This is due to Polysun only connecting energy flows (in the form of heat or electricity) between components. A typical Polysun system diagram can be seen in Figure 2.7.

Project Project - System diagram 58a: Process heat (solar thermal)

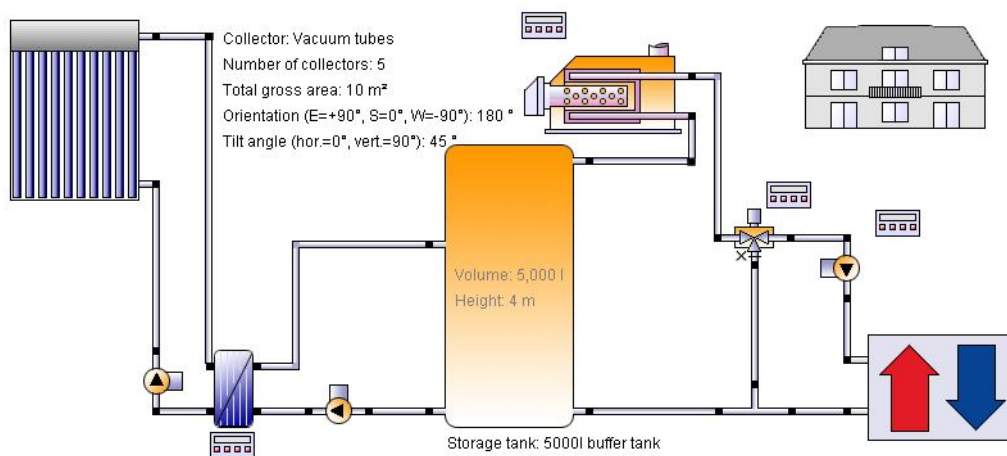


Figure 2.7: A screen-shot of a typical SPH system diagram in Polysun.

After a simulation has been completed, a user can view the performance indicators of the simulation graphically. This is a powerful tool in Polysun as several systems can be compared to one another using various performance indicators.

Once a user has completed a simulation and is satisfied by the preliminary energy output results provided by Polysun, the user can generate a PDF report. The user can specify which details of the simulation he would like to be in

the report. This can include amongst others solar fraction, system efficiency, energy generation categorized by source, and financial indicators.

These reports include powerful graphics that allow deeper insight into system performance. They are an ideal marketing tool to present to customers.

2.4.2 Open-source packages

Open-source software packages for simulating SPH systems will allow a possible investor to perform rough simulations. This could lead them to contacting solar manufacturers and ultimately drive the solar thermal industry. It is thus crucial that open source software packages are easy-to-use for prospective end-users (i.e. decision makers) of SPH systems.

Another added advantage of open-source software is their flexibility offered. This feature allows field experts to develop and change parts of the code to suit their needs.

In this literature review a single open-source SPH simulation package will be discussed, namely SHIPcal developed by Frassetto (2016).

SHIPcal

Solar Heat for Industrial Processes Calculator or SHIPcal was developed to be an end-user orientated online calculator (OC) for SPH simulations. The main motivation for this project was to make SPH simulations more accessible to end-users and decision makers (Frassetto, 2016). OCs have been used widely in the photovoltaic industry (Frassetto, 2016), and have large potential to promote SPH due to the ease of access they offer.

Two simulation modes are included in SHIPcal. The first is a simplified annual performance model. This is a coarse annual model and uses an hourly simulation of one characteristic day per month to determine system performance. In this simulation mode results can be viewed online.

With the simplified annual performance, SHIPcal generates visuals to represent the results of a simulation. Perhaps the most useful of these for an end-user is the monthly heat production plot. An example of this plot can be seen below in Figure 2.8. To view all the visuals generated by SHIPcal the reader is referred to Frassetto (2016).

The second of the two modes is an annual hourly performance model. In this mode a more detailed simulation of every hour in a year is performed. This is a more traditional approach that can be found in software such as TRNSYS



Figure 2.8: The monthly heat production visual generated by SHIPcal. Screen shot taken from Frassetto (2016)

and Polysun. Results from this mode of simulation are sent via email to the user.

SHIPcal can model three types of collectors, namely flat plate, parabolic trough and linear Fresnel collectors. Like SolGain 1.0 (refer to Section 4.3.1), SHIPcal assumes the performance coefficients of a type of collector to be the same for all variations of that collector type. The performance curve coefficients that SHIPcal uses were obtained from work done by IDAE (2015), which recommends generic performance parameters for different collector types.

For processes with temperatures less than 110°C the FPC model is automatically selected. Above 110°C the parabolic trough is selected, unless the user states that the solar field will be on a rooftop. In this case the linear Fresnel collector is used.

The minimum number of user-inputs required for a simulation in SHIPcal is four. Depending on which inputs are provided, SHIPcal employs different design strategies to determine the missing details. SHIPcal then optimises the solar field parameters to give the highest energy yield.

While providing a highly accessible simulation tool, SHIPcal has various flaws. A major flaw is that simulation results are not represented in a way that is easily understandable to most end-users. This could be improved by including a financial model. Weather data cannot be entered into this tool and as a result it can only be used for preprogrammed locations.

2.5 Chapter Conclusion

The viability of SPH was studied followed by a brief introduction to SPH. Selected solar thermal collector's were introduced to the reader. The need for an open-source pre-assessment simulation package for SPH systems was outlined by reviewing software packages similar to SolGain.

Chapter 3

Theoretical Background

The theoretical background required to program SolGain 2.0 is laid out in this chapter. The topics that are reviewed are solar radiation, collector modelling, thermal energy storage, miscellaneous solar process heat (SPH) system components and finally SPH system performance measurements.

3.1 Solar Radiation Theory

To simulate SPH systems an accurate model of the sun needs to be developed. This section aims at laying down the framework to accurately determine radiation intensity on a collector. Before starting with theory it will be helpful to define the terminology that will be used to describe radiation throughout the rest of this document. The definitions that will be used can be found below in Table 3.1. The term "radiation" will be used whenever units do not matter.

Table 3.1: Terms used for radiation based on the work of Iqbal (1983)

Term	Unit	Meaning
Radiation	-	Used when units are irrelevant
Irradiance	W/m ²	Incident radiation per time per unit area (i.e. power)
Irradiation	kW h/m ²	Incident radiation per unit area (i.e. energy)

Determining irradiance on a collector is a two step process. Firstly the position of the sun relative to the collector needs to be determined. Secondly a sky model needs to be implemented to model the different components of radiation.

3.1.1 Position of the sun

The position of the sun can be defined at any time using the zenith angle θ_z and azimuth angle γ_s (refer to Figure 3.1). Before delving into the formulas

to determine zenith and azimuth angles, it is necessary to define a set of auxiliary angles. Unless otherwise stated the formulas and definitions used are from Duffie and Beckman (2013):

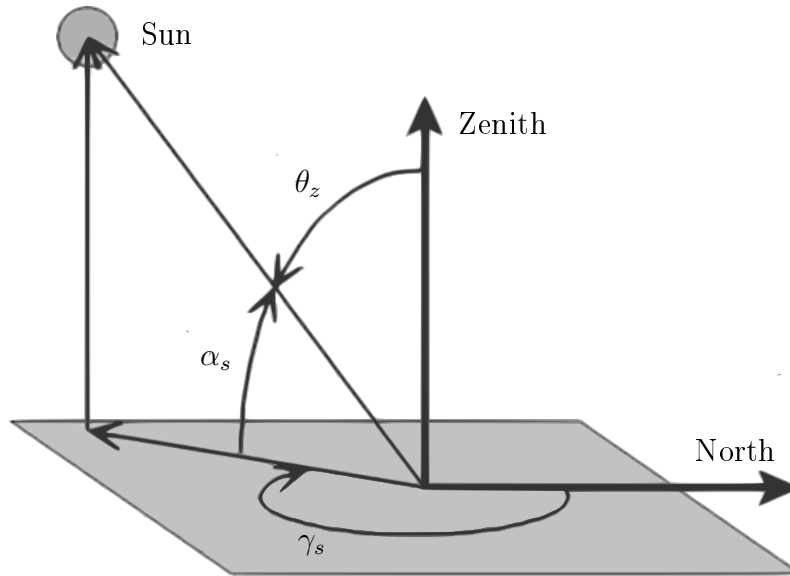


Figure 3.1: Illustration of angles used to define the position of the sun

ω **Hour angle**, the angular position of the sun in the east-west direction due to the rotation of the earth. It is negative in the morning and positive in the evening. An hours rotation is represented 15° . Dependent on the solar time, t_{sol} , hour angle can be calculated using Equation 3.1:

$$\omega = (t_{sol} - 12)15^\circ \quad (3.1)$$

Solar time is the apparent time at a location based on the angular position of the sun (Duffie and Beckman, 2013: 11). Solar noon occurs when the sun crosses the meridian of the observer. Assuming that there are no daylight savings, solar time can be calculated using Equation 3.2 (Stine and Geyer, 2001):

$$t_{sol} = h_{local} + \frac{EOT}{60} - \frac{(\psi - \psi_{timezone})}{15^\circ} \text{ [hours]} \quad (3.2)$$

Where EOT is the equation of time, which is the difference between *mean solar time* and *true solar time*. An approximation of EOT that is accurate to 30 seconds or less is contained below in Equation 3.3 (Stine and Geyer, 2001):

$$EOT = 0.258 \cos(x) - 7.416 \sin(x) - 3.648 \cos(2x) - 9.228 \sin(2x) \text{ [minutes]} \quad (3.3)$$

Where angle x is defined as:

$$x = \frac{360(d_{local} - 1)}{365.241} \text{ [degrees]}$$

δ **Declination**, the angular position of the sun at solar noon (i.e. when the sun is highest in the sky) measured from the zenith axis (refer to Figure 3.1 to visualise the zenith axis). Dependent on the day of the year, d_{local} . Calculated using Equation 3.4:

$$\delta = 23.45 \sin\left(360 \frac{284 + d_{local}}{365}\right) \quad (3.4)$$

Now that the necessary definitions have been made, the methods for determining the **zenith and azimuth angles** will be covered. The zenith angle can be calculated by using Equation 3.5:

$$\theta_z = 90^\circ - \arcsin(\cos \delta \cos \omega \cos \phi + \sin \delta \sin \phi) \quad (3.5)$$

Where ϕ is the latitude coordinate, which is an angle. Before moving onto calculating the azimuth angle, a convention should be defined for how it is specified in this text.

The azimuth angle γ_s will be measured clockwise from due north, as seen in Figure 3.1. It can be determined using Equation 3.6. The $\text{sign}(\omega)$ function is equal to +1 if ω is positive and equal to -1 if ω is negative.

$$\gamma_s = \text{sign}(\omega) \left| \arccos\left(\frac{\cos \theta_z \sin \phi - \sin \delta}{\sin \theta_z \cos \phi}\right) \right| \quad (3.6)$$

Now that the necessary theory to determine the sun's position has been described, radiation will now be investigated.

3.1.2 Angles between sun and collector

Before delving into determining the angles between the sun and collector it is necessary to define a set of angles to specify the collector's position. These angles are displayed below in Figure 3.2. They are namely collector tilt β ,

collector azimuth γ and tube orientation for evacuated tube collectors. The tube orientation of an ETC can either be horizontal or vertical.

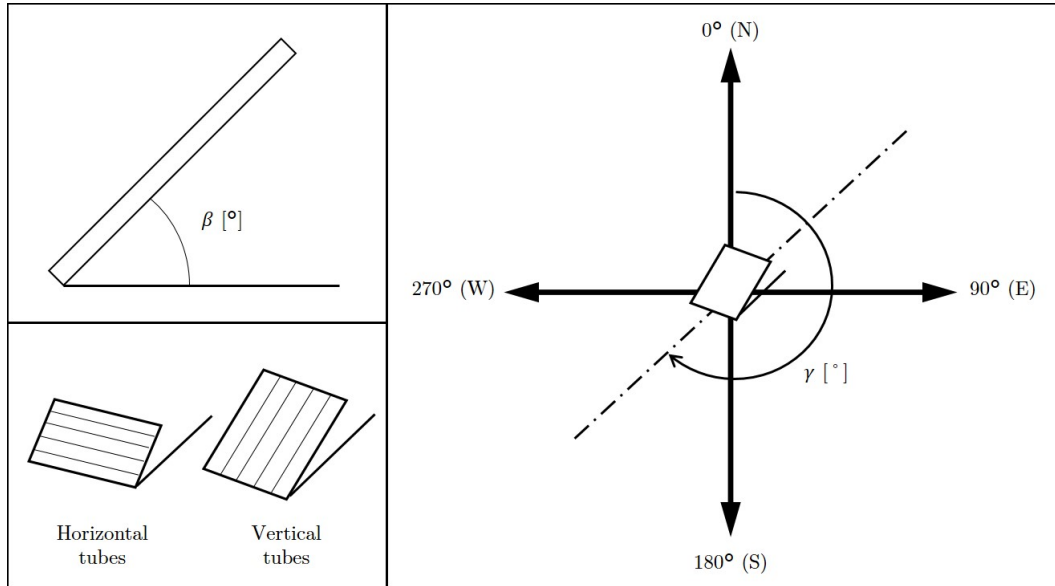


Figure 3.2: Angles used to define the position of a collector. **Top left:** Collector tilt β **Right:** Collector azimuth γ **Bottom left:** Tube orientation (Only for ETCs)

The angle of incidence θ is defined as the angle between the normal of the collector and radiation striking the collector (as displayed below in Figure 3.3). For a non-tracking collector this can be determined using Equation 3.7:

$$\theta = \arccos(\cos \theta_z \cos \beta + \sin \theta_z \sin \beta \cos(\gamma_s - \gamma)) \quad (3.7)$$

For a single axis tracking collector (i.e. a parabolic trough collector or PTC) the incidence angle can be calculated using Equation 3.8 (Wagner and Gilman, 2011):

$$\theta = \arccos \sqrt{1 - [\cos(\alpha_s - \beta) - \cos \beta \cos \alpha_s (1 - \cos(\gamma_s - \gamma))]^2} \quad (3.8)$$

Where $\alpha_s = 90^\circ - \theta_z$ is the elevation angle (as displayed in Figure 3.1).

For certain collectors the incidence angle θ needs to be decomposed into two components for determining collector performance. This is discussed in further detail in Section 3.2.3. For now it is just necessary to know that the two decomposed components are a projection onto the longitudinal plane θ_l and a projection onto the transversal plane θ_t (refer to Figure 3.3).

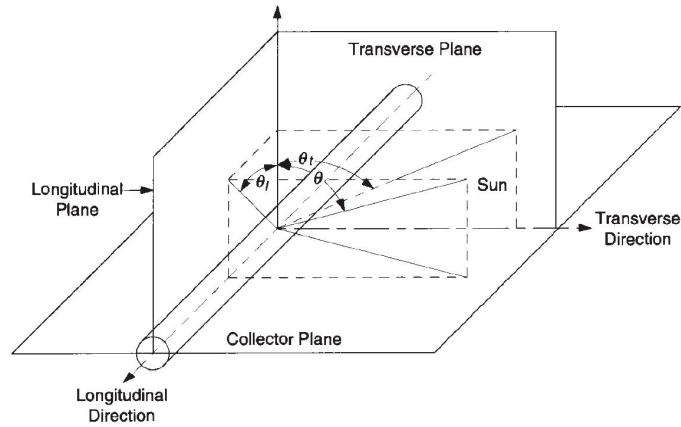


Figure 3.3: Incidence angle θ decomposed into longitudinal θ_l and transverse θ_t components. Picture: Theunissen and Beckman (1985)

The longitudinal projection of the incidence angle can be calculated according to Equation 3.9 (Theunissen and Beckman, 1985):

$$\theta_l = \arctan(\tan \theta \cos(\gamma_s - \gamma)) \quad (3.9)$$

While the transversal projection can be calculated using Equation 3.10 (Theunissen and Beckman, 1985):

$$\theta_t = \arctan(\tan \theta \sin(\gamma_s - \gamma)) \quad (3.10)$$

It is important to note that for parabolic trough collectors the incidence angle will be exactly on the longitudinal plane. This means that $\theta_l = \theta$ and there is no transversal projection of the incidence angle.

Now that the necessary theory required to determine the position of the sun relative to a collector has been laid down, the theory on solar radiation can be addressed.

3.1.3 Radiation components

Radiation can be divided into three separate components (Duffie and Beckman, 2013). The first of these is beam radiation, G_b . Beam radiation represents sun rays coming directly from the sun, i.e. not reflected. The other two radiation components are diffuse sky radiation, G_s , and reflected ground radiation, G_r . These three components can be seen visually in Figure 3.4.

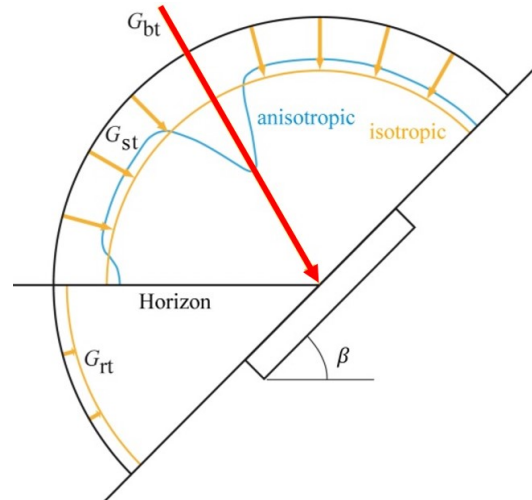


Figure 3.4: Two models of sky and ground reflected irradiance. **Yellow arrows:** G_{st} and G_{rt} according to the isotropic model. **Blue curve:** G_{st} according to the Perez model. Picture: adapted from Hess (2014)

A typical weather data file (TMY2 or similar) will supply three measurements of radiation that can be used to determine G_b , G_s and G_r . These are global horizontal irradiance G (GHI), direct normal irradiance G_{bn} (DNI) and diffuse horizontal irradiance G_d (DHI). For a horizontally orientated collector (zero tilt), GHI contains all of the aforementioned components of radiation (G_b , G_s and G_r). However, on a tilted surface further calculation is necessary to determine these components. Determining each of these components will now be addressed.

Irradiance on tilted planes

In order to simulate radiation on a tilted collector it is necessary to determine G_{bt} , G_{st} and G_{rt} from the weather data (the subscript "t" in G_{bt} , G_{st} and G_{rt} represents *tilted surface*). To view the different components of radiation on a tilted surface the reader is referred to Figure 3.4 above. The methods for determining the components of radiation on a tilted surface will now be discussed.

G_{bt} **Beam irradiance** on a tilted surface can be calculated using Equation 3.11 (Hess, 2014):

$$G_{bt} = G_{bn} \cdot \cos \theta = G_{bn} \cdot A_1/A_2 \quad (3.11)$$

The $\cos \theta$ term in Equation 3.11 above is to include the so-called cosine-effect. It accounts for the diminishing intensity of beam radiation at increasing incidence angle θ . Figure 3.5 displays this phenomenon.

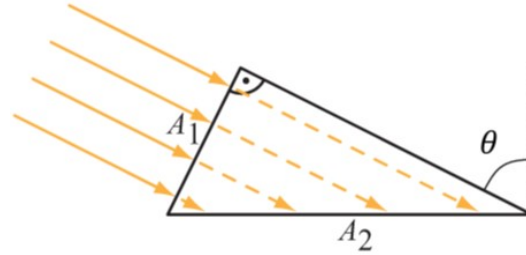


Figure 3.5: An illustration of the cosine-effect. Picture: Hess (2014)

G_{rt} **Diffuse ground reflected irradiance** needs to be accounted for when the collector is tilted (for a collector tilt of zero the radiation from the ground does not land on the collector). Hess (2014) states that this component of radiation is usually assumed to be isotropic, i.e. it does not vary with angular location. Figure 3.4 above displays the isotropic nature of radiation reflected from the ground.

Diffuse ground reflected irradiance originates from reflected GHI G and can be calculated using Equation 3.12 (Hess, 2014):

$$G_{rt} = \frac{G \cdot \rho_{grd}}{2 \cdot (1 - \cos \beta)} \quad (3.12)$$

Where ρ_{grd} is the reflectivity of the ground also known as albedo, and β is the collector tilt. The value of albedo ρ_{grd} is usually not known and is commonly assumed to be 0.2 (Hess, 2014).

G_{st} **Diffuse sky irradiance** accounts for all radiation that is emitted from the sky dome excluding the angle of 6° with the sun as its centre (Hess, 2014). Various sky models have been developed to model this component of radiation. A very simple sky model is the **isotropic sky model**, which assumes that all parts of the sky dome emit the same irradiance. Using this model the diffuse sky irradiance can be calculated using Equation 3.13 (Frasquet, 2016):

$$G_{st} = G_d \cdot 0.5 \cdot (1 + \cos \beta) \quad (3.13)$$

The isotropic sky approach is a coarse model and more accurate models have been developed. A model that accounts for the varying intensity of radiation from different parts of the sky is termed an anisotropic sky model. The main reason for anisotropy occurring is brightening of diffuse radiation near the sun and near the horizon (Hess, 2014).

The **Perez sky model** is a commonly used sky model that was developed by Perez *et al.* (1987). This model uses a description of the circumsolar zone and horizon zone superimposed onto an isotropic model (Perez

et al., 1987). This sky model will provide higher energy yields than an isotropic sky model (Duffie and Beckman, 2013).

For this work the isotropic model will be implemented, due to its simplicity. As previously mentioned, the isotropic sky model generally produces more conservative energy yields than the Perez model. It was thus considered satisfactory for the purposes of SolGain 2.0.

Once the different components of irradiance have been calculated, the total irradiance falling on a tilted collector can be determined. This is done by simply summing the components:

$$G_t = G_{bt} + G_{st} + G_{rt} \quad (3.14)$$

3.2 Collector Theory

A major aspect of SolGain 2.0 is modelling of solar collectors. This section will focus on the theory of modelling collectors.

The heating power that a solar thermal collector provides per unit aperture area \dot{q}_{use} , is described conceptually as:

$$\dot{q}_{use} = \frac{\dot{Q}_{use}}{A_{col}N_{par}} = \eta \cdot G_t \approx \dot{M} \cdot c_p \cdot (T_{out} - T_{in}) \quad (3.15)$$

Where A_{col} is the aperture area of a single collector, N_{par} is the number of collector flow loops in parallel, η is the collectors overall efficiency, \dot{m} is the specific mass flow rate of the HTF, c_p is the specific heat of the HTF, and T_{in} and T_{out} are the inlet and outlet temperatures. The main losses that occur in a solar collector are (Hess, 2014):

- Radiation losses including reflection and absorption at the transparent cover, reflection from the absorber and radiation from the absorber.
- Convection between the collector and its surroundings.
- Conduction between absorber and other collector components.
- Concentrating collectors have other losses associated with concentration, i.e. end losses and shading losses.

It is not practical to model all of these heat losses analytically. Instead collectors are characterised using empirical data from tests following the international collector testing standard (ISO 9806:2017, 2017). The effects of thermal losses are expressed in the form of a collector efficiency curve for perpendicular radiation, incidence angle modifiers (IAMs) to account for the effects of varying incidence angles.

3.2.1 Efficiency curve

According to European standards, efficiency for perpendicular angle of incidence is expressed as a second order polynomial obtained from regression of the form (Hess, 2014):

$$\eta_{\perp} = \eta_0 - c_1 \cdot \frac{T_{fl} - T_a}{G_t} - c_2 \cdot G_t \cdot \left(\frac{T_{fl} - T_a}{G_t} \right)^2 \quad (3.16)$$

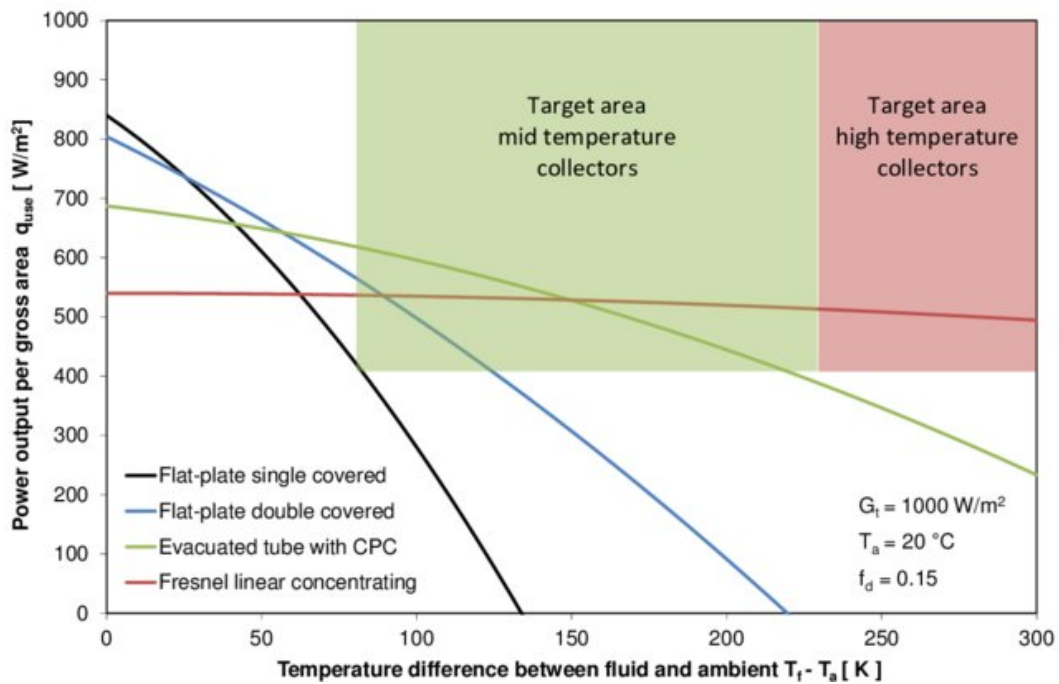


Figure 3.6: Generic collector output curves for different collector types. Incidence angles are equal to perpendicular. Picture: Hess (2014)

Where mean fluid temperature T_{fl} is expressed as:

$$T_{fl} = \frac{T_{in} + T_{out}}{2} \quad (3.17)$$

The conversion factor η_0 is the efficiency when ambient temperature T_a is equal to the mean fluid temperature T_{fl} and radiation incidence is perpendicular. The first order and second order heat loss coefficients are represented by c_1 and c_2 respectively. It is important to note that these are just variables used to characterize heat loss and are not physical parameters.

3.2.2 Incidence angle modifiers

In order to account for effects of varying incidence angles that are not perpendicular, variables called incidence angle modifiers (IAMs) are used. There are three separate incidence angle modifiers for each of the modes of radiation. $K_b(\theta_l, \theta_t)$ for beam irradiance, K_s for diffuse sky irradiance, K_r for diffuse reflected ground irradiance.

In order to calculate the specific power gain per unit aperture area \dot{q}_{gain} the following equation is used:

$$\dot{q}_{gain} = \eta_0 \cdot [K_b(\theta_l, \theta_t) \cdot G_{bt} + K_s \cdot G_{st} + K_r \cdot G_{rt}] - c_1 \cdot (T_{fl} - T_a) - c_2 \cdot (T_{fl} - T_a)^2 \quad (3.18)$$

The values of K_b , K_s and K_r are determined during collector testing. Determination of K_s and K_r will be addressed first with K_b in the following section.

It is standard procedure for state-of-the-art collector simulation to assume that both K_s and K_r are equal to some constant IAM for diffuse irradiation K_d . This value is provided by collector testing reports and is independent of the angle of incidence.

3.2.3 Incidence angle modifier for beam irradiance

This section will focus on the general procedures for determining K_b from collector testing reports. Before delving into the procedures it is important to note that collectors are categorized into two types of collectors for these calculation, namely one-dimensional and two-dimensional collectors. This is aptly displayed below in figure 3.7, with an FPC being one-dimensional and an ETC being two-dimensional.

Collector test reports generally contain reference points for IAM determination (Carvalho *et al.*, 2007):

- **One-dimensional collectors:** a single IAM value for 50° incidence angle, i.e. $K_b(50^\circ)$.

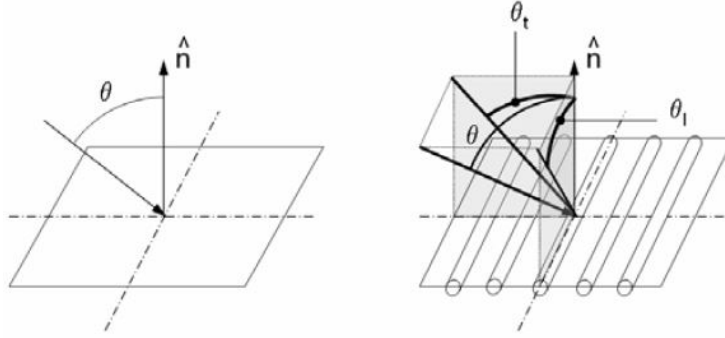


Figure 3.7: **Left:** One-dimensional collector (FPC) and **Right:** Two-dimensional collector (ETC) with the angle of incidence θ decomposed into transversal θ_t and longitudinal θ_l components. Picture: Carvalho *et al.* (2007)

- **Two-dimensional collectors:** one IAM reference value in the longitudinal plan at 50° i.e. $K_b(50^\circ, 0)$, and three IAM references for the transverse plane at 20° , 40° and 60° i.e. $K_b(0, 20^\circ)$, $K_b(0, 40^\circ)$ and $K_b(0, 60^\circ)$.

In order to determine the IAM for a specific incidence angle (decomposed as θ_l and θ_t) various approximations must be made. These approximations will now be addressed.

One-dimensional and Longitudinal IAMs

One-dimensional collector IAMs and longitudinal IAMs of two-dimensional collectors are grouped together, as they can be approximated in the same way. Carvalho *et al.* (2007) suggests the use of the following equation for approximating the IAM:

$$K(\theta_l, 0) \approx \left[1 + b_0 \left(\frac{1}{\cos(\theta_l)} - 1 \right)^c \right]^+ \quad (3.19)$$

The positive exponent in Eq. 3.19 is to express that only positive and zero values should be accepted. In order to calculate the value of coefficients b_0 and c from Equation 3.19 two IAM references are required. If only the single mandatory reference is provided by the collector test report (at $\theta_l = 50^\circ$ or $\theta = 50^\circ$) then another reference can be assumed to be a value of 0.05 for $K(85, 0)$.

The coefficients b_0 and c can then be calculated using:

$$c = \log_{\left(\frac{c_1}{c_2}\right)} \left(\frac{1 - K(\theta_1, 0)}{1 - K(\theta_2, 0)} \right) \quad (3.20)$$

Where:

$$C_n = \frac{1}{\cos(\theta_n) - 1} \quad (3.21)$$

$$b_0 = \frac{1 - K(\theta_1, 0)}{C_1^c} = \frac{1 - K(\theta_2, 0)}{C_2^c} \quad (3.22)$$

Transverse IAM

For calculations of transverse IAMs Carvalho *et al.* (2007) suggests the use of a simple linear connection between the reference IAMs. Two additional theoretical points can be added to the test sheet ones: $K(0, 0) = 1$ and $K(0, 90) = 0$. From this linear interpolation an accurate approximation of transverse IAMs can be made (Carvalho *et al.*, 2007).

Composed IAM

In order to compose an approximated IAM for longitudinal and transverse effects, an equation was proposed by McIntire (1982):

$$K(\theta) \equiv K(\theta_l, \theta_t) \approx K(\theta_l, 0) \cdot K(0, \theta_t) \quad (3.23)$$

This is the standard way of composing an approximated IAM and is used by most collector models (Carvalho *et al.*, 2007).

3.2.4 Calculation of specific useful power

By using the effective collector heat capacity c_{eff} specified by the test report, the specific useful power can now be calculated using:

$$\dot{q}_{use} = \dot{q}_{gain} - c_{eff} \cdot \frac{dT_{fl}}{dt} \quad (3.24)$$

3.2.5 Considerations for parabolic trough collectors

The procedure for determining PTC performance is the same as for non-concentrating collectors bar a few exceptions. These exceptions and their implications will now be addressed.

The first thing to be noted when determining PTC performance is that, because the collector tracks exactly along the longitudinal plane, there is **no transversal projection of the incidence angle** i.e. $\theta = \theta_l$ (refer to Figure

3.8 below and Equation 3.8). This means that only a longitudinal IAM for beam irradiance $K_b(\theta_l, 0)$ needs to be determined.

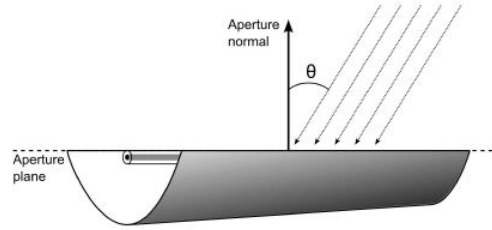


Figure 3.8: Graphical representation of the incidence angle for a parabolic trough, where $\theta = \theta_l$. It can be seen that $\theta > 0$ will result in end losses

The second consideration is **end losses** that occur due to solar radiation not striking directly normal to the collector. This is due reflected radiation at the end of a collector row not reaching the receiver tube. From Figure 3.8 it can be seen that end losses occur when $\theta > 0$. End loss efficiency $\eta_{endLoss}$ for a collector can be calculated using Equation 3.25 (Wagner and Gilman, 2011):

$$\eta_{endLoss} = 1 - \frac{L_{fo,avg} \tan \theta}{L_{col}} + \eta_{endGain} \quad (3.25)$$

End losses are partially recovered through *end gain* that occurs when reflected radiation from the end of a collector lands on the adjacent collector's receiver. End gain efficiency $\eta_{endGain}$ is equal to zero if there is no adjacent collector to recover the solar radiation. In the case that there is an adjacent collector, Equation 3.26 can be used to calculate end gain efficiency (Wagner and Gilman, 2011):

$$\eta_{endGain} = \frac{L_{fo,avg} \tan \theta - L_{gap}}{L_{col}} \quad (3.26)$$

In the two equations above, L_{col} is the net length of the collector aperture, L_{gap} is the distance between the collector its adjacent collector, and $L_{fo,avg}$ is the average surface-to-focus path length. The value of $L_{fo,avg}$ can be calculated using the focal length L_{fo} and the collector width w_{col} , which are usually provided by collector datasheets. This is done using Equation 3.27 (Wagner and Gilman, 2011):

$$L_{fo,avg} = \sqrt{\frac{\left[4L_{fo}^2 + \left(\frac{w_{col}}{2}\right)^2\right]^2}{L_{fo}^2}} \cdot \frac{12L_{fo}^2 + \left(\frac{w_{col}}{2}\right)^2}{12\left[4L_{fo}^2 + \left(\frac{w_{col}}{2}\right)^2\right]} \quad (3.27)$$

The last consideration when modelling parabolic troughs is **row shadowing**. This occurs when the shadow of a collector is cast onto another collector's aperture. For the purposes of SolGain 2.0 as a pre-assessment tool, modelling of row shadowing was seen as unnecessary. A model where these losses are not considered was deemed to be accurate enough for SolGain 2.0.

3.3 Thermal Energy Storage Theory

Many SPH systems include storage tanks so that heat can be used on demand, even when there is no solar energy resource. Most thermal energy storage systems used in SPH applications are stratified/thermocline tanks. Stratified refers to the fact that the tank contains hot water at the top and cold water at the bottom (refer to Figure 3.9). This literature study will only include a study of stratified tanks.

The most complex and computationally expensive way of modelling stratified tanks is by using computational fluid dynamics (CFD). According to Pizzolato *et al.* (2015), this is a highly accurate way to model these systems, but for the purposes of this project such a high level of accuracy is not necessary nor practical.

A novel approach using CFD to deduce an analytical equation for a thermocline was completed by Pizzolato *et al.* (2015). The equation to describe the temperature profile can be seen in Figure 3.9. This approach was studied in detail by the author, but was disregarded due to it not being an industry established way of modelling thermal storage. Polysun and TRNSYS for example use alternative methods for modelling thermoclines.

Duffie and Beckman (2013) states that when modelling stratified storage tanks there are two categories that tank models fall into. The **multinode** approach divides the tank into N nodes at uniform temperature. Energy balances are written for each node. Thus N differential equations are solved to determine the temperature of each node for a specific time step.

The second approach is the **plug flow** method. Using this model, the stratified tank is once again divided into segments of uniform temperature. The difference with the plug flow approach being that the segments are assumed to move through the tank in plug flow manner (as opposed to remaining still in

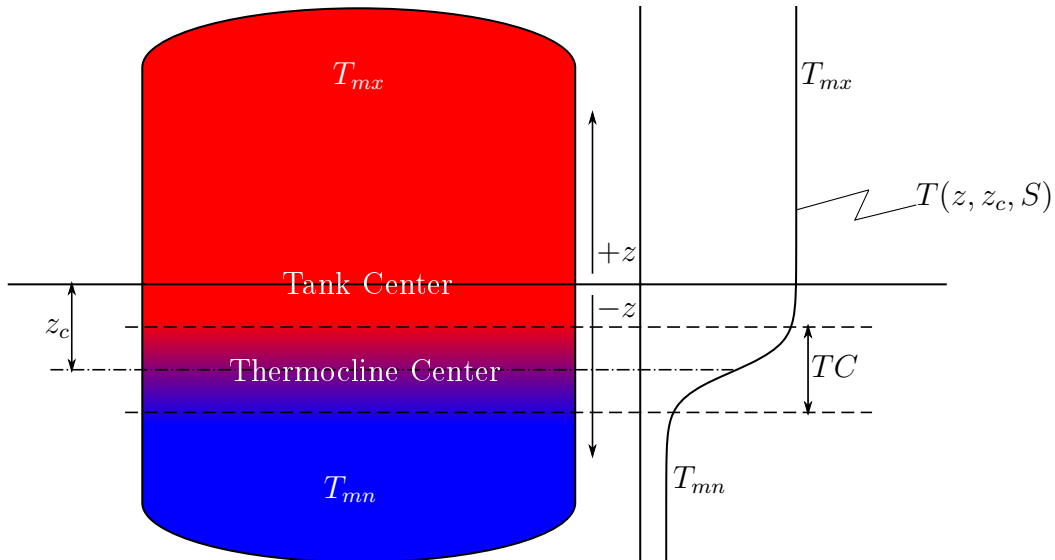


Figure 3.9: A stratified tank. The temperature profile and appropriate parameters divided by Pizzolato *et al.* (2015) are displayed.

the multinode approach). Segments are also not constant in size and depend on mass flow rate and temperature of fluid entering the tank (Kleinbach *et al.*, 1993).

Kleinbach *et al.* (1993) mention that in addition to classifying a model as multinode or plug flow, a model may use fixed or variable inlet positions. A fixed inlet position specifies that fluid from the heat source always enters the top of the tank and fluid from the heat sink always the bottom. With a variable inlet position, fluid entering the tank is assumed to find its way to a node or segment that nearly matches its density. The reader is referred to Figure 3.10 to visualize a five-node variable inlet tank.

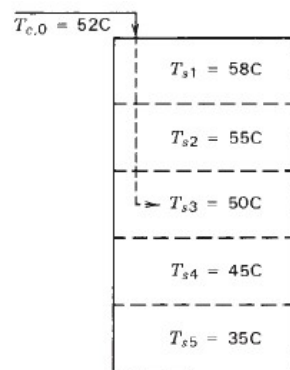


Figure 3.10: A five-node variable inlet tank model. $T_{s,2} > T_{c,0} > T_{s,3}$ and therefore the fluid entering is assumed to flow to node 3. Picture: Duffie and Beckman (2013)

A study on the performance of storage tank models by Kleinbach *et al.* (1993) suggests the use of a multinode model with variable inlets. This model gave the higher accuracy than the plug flow model with the plug flow model overpredicting energy quantities. Using variable inlets resulted in higher computational efficiency than fixed inlets without sacrificing accuracy.

TRNSYS contains both a plug flow model and a multinode model, while Polysun uses only a multinode model. Thus a multinode variable inlet model was selected for implementation in SolGain 2.0. Further discussion on thermal energy storage will be confined to this tank model.

3.3.1 Multinode variable inlet tank model

The energy flows that are accounted for in a multinode variable inlet tank model are displayed in Figure 3.11. These are namely: heat to and from the collector, heat to and from the load, heat transfer from mass flows between nodes and convective heat losses to the environment. A convective mix between nodes is ignored.

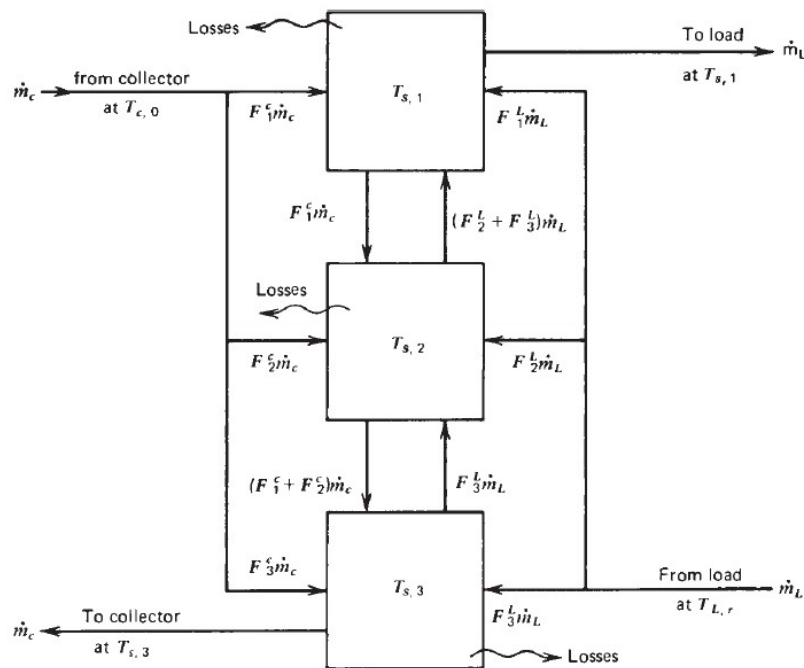


Figure 3.11: A three-node tank displaying all heat flows and relevant parameters. Picture: Duffie and Beckman (2013)

A collector control function is used to determine which node the fluid from the collector flows into. It is defined below as (Duffie and Beckman, 2013):

$$F_i^c = \begin{cases} 1 & \text{if } i = 1 \text{ and } T_{col,0} > T_1 \\ 1 & \text{if } T_{i-1} \geq T_{col,0} > T_i \\ 0 & \text{otherwise} \end{cases} \quad (3.28)$$

Where T_i is the uniform temperature of a node, and $T_{col,0}$ is the temperature of fluid returning from the collector.

It should be noted that only a single node's control function can be equal to 1 at any time step. Similarly a load control function is also used to determine which node receives the fluid returning from the load (Duffie and Beckman, 2013):

$$F_i^p = \begin{cases} 1 & \text{if } i = N \text{ and } T_{pro,r} < T_N \\ 1 & \text{if } T_{i-1} \geq T_{pro,r} > T_i \\ 0 & \text{otherwise} \end{cases} \quad (3.29)$$

Where $T_{pro,r}$ is the temperature of fluid returning from the load, and N is the number of nodes used to divide the tank up.

To calculate the heat transfer between nodes by mass flow, a net flow rate between node i and $i - 1$ is defined \dot{M}_i . This net flow can either be up or down. It is calculated using Equation 3.30 (Duffie and Beckman, 2013):

$$\dot{M}_i = \dot{M}_{col} \sum_{j=1}^{i-1} F_j^c - \dot{M}_{pro} \sum_{j=i+1}^N F_j^p; \quad i = 2, 3, \dots, N \quad (3.30)$$

A simple energy balance can now be used to derive a differential equation for each node at any time step (Duffie and Beckman, 2013):

$$M_i \frac{dT_i}{dt} = \left(\frac{UA}{c_p} \right)_i (T_a - T_i) + F_i^c \dot{M}_{col} (T_{col,0} - T_i) + F_i^p \dot{M}_{pro} (T_{pro,r} - T_i) + \begin{cases} \dot{M}_i (T_{i-1} - T_i) & \text{if } \dot{M}_i > 0 \\ \dot{M}_{i+1} (T_i - T_{i+1}) & \text{if } \dot{M}_{i+1} < 0 \end{cases} \quad (3.31)$$

Where A is the surface area of the node, U is the heat transfer coefficient between the node and the environment, and c_p is the specific heat of fluid in the node.

The first term on the right hand side of Equation 3.31 accounts for the losses to ambient temperature T'_a . The second and third terms account for the net energy gain from collector and load inlet respectively. The final term accounts for the net mass flow between nodes \dot{M}_i .

A study on solving the differential equation in Equation 3.31 for TRNSYS was completed by Newton (1995). The study prescribes the use of a Crank-Nicolson method for solving Equation 3.31. For this to be done, the differential equation is rearranged to the form of Equation 3.32 (Newton, 1995):

$$\frac{dT_i}{dt} = a_i T_{i-1} + b_i T_i + c_i T_{i+1} + d_i \quad (3.32)$$

Where a_i , b_i , c_i and d_i are coefficients from the rearranged Equation 3.31. The node temperatures are then solved iteratively using the Crank-Nicolson method in Equation 3.33 (Newton, 1995):

$$T_i = \Delta t_{internal} \left(\begin{array}{l} \frac{a_i}{2} (T_{i-1,prev} + T_{i-1}) + \frac{b_i}{2} (T_{i,prev} + T_i) \\ + \frac{c_i}{2} (T_{i+1,prev} + T_{i+1}) + d_i \end{array} \right) + T_{i,prev} \quad (3.33)$$

The subscript *prev* refers to the node temperature at the previous time step. According to Newton (1995), a smaller internal time step is required for solving the differential equation. Newton (1995) advises a time step of 1/10 of the critical Euler time step:

$$\Delta t_{internal} = \frac{1}{10} \cdot \text{minimum} \left(\frac{-1}{b_i} \right)_{i=1, N_{nodes}} \quad (3.34)$$

3.3.2 Choice of number of nodes

The number of nodes used by the tank model has an impact on the simulation results. A large number of nodes represents a more stratified tank and can over-predict energy yields. A limited number of nodes represents a low degree of stratification and under-predicted yields i.e. a single node tank represents a fully mixed tank. For this reason it is crucial to use a number of nodes that will most accurately model the actual tank.

Kleinbach *et al.* (1993) completed a study to determine which variables of an SPH system influenced the accuracy of a multinode model with a specific number of nodes. It was found that the only variable that impacted the accuracy of

a multinode model was the mean number of tank turnovers N_{to} . A function to determine the required number of nodes for a fixed inlet model was determined from experimental data as Kleinbach *et al.* (1993):

$$N_{nodes} = 45.8N_{to}^{-1.218} \quad (3.35)$$

Simulations using the proposed value of N_{nodes} above showed less than 13% deviation from experimental results (Kleinbach *et al.*, 1993). Polysun uses a tank model with 12 nodes/layers (Vela Solaris, 2017). This value could be used as a reference while developing a tank model.

3.4 Theory on Miscellaneous System Components

Theory on other components that are generally used in SPH systems will now be studied. This includes a study on heat exchangers, and pipes.

3.4.1 Heat exchangers

A common way of calculating heat exchanger performance is the effectiveness-NTU(number of transfer units) method. The heat transferred between a hot and a cold fluid is dependent on the heat exchanger effectiveness ϵ , the minimum heat transfer capacity C_{min} and the temperature difference between the hot and cold inlets ($T_{hi} - T_{ci}$). Using the NTU-effectiveness method, this can be calculated using Duffie and Beckman (2013):

$$\dot{Q}_{HE} = \epsilon C_{min}(T_{in,col} - T_{in,tank}) \quad (3.36)$$

with (the subscript *col* and *tank* denote collector side and tank side respectively):

$$C_{min} = \begin{cases} (\dot{M}c_p)_{col} & \text{if } (\dot{M}c_p)_{col} < (\dot{M}c_p)_{tank} \\ (\dot{M}c_p)_{tank} & \text{if } (\dot{M}c_p)_{tank} < (\dot{M}c_p)_{col} \end{cases} \quad (3.37)$$

The effectiveness is defined as the ratio of the actual heat transfer Q_{HE} to the maximum possible heat transfer Q_{max} and can be calculated using Equation 3.38 (Duffie and Beckman, 2013):

$$\epsilon = \frac{Q_{HE}}{Q_{max}} = \begin{cases} \frac{1 - e^{-NTU(1 - \frac{C_{min}}{C_{max}})}}{1 - (\frac{C_{min}}{C_{max}})e^{-NTU(1 - \frac{C_{min}}{C_{max}})}} & \text{if } \left(\frac{C_{min}}{C_{max}}\right) < 1 \\ \frac{NTU}{1 + NTU} & \text{if } \left(\frac{C_{min}}{C_{max}}\right) = 1 \end{cases} \quad (3.38)$$

where NTU is the number of transfer units:

$$NTU = \frac{UA}{C_{min}} \quad (3.39)$$

With U being the heat transfer coefficient and A being the heat transfer area. C_{max} is the maximum heat transfer capacity defined as:

$$C_{max} = \begin{cases} (\dot{M}c_p)_{col} & \text{if } (\dot{M}c_p)_{col} > (\dot{M}c_p)_{tank} \\ (\dot{M}c_p)_{tank} & \text{if } (\dot{M}c_p)_{tank} > (\dot{M}c_p)_{col} \end{cases} \quad (3.40)$$

The above described process was developed for a countercurrent heat exchanger. The method can, however, be used for different heat exchangers, by using a different expression for effectiveness of the specific heat exchanger (Duffie and Beckman, 2013).

3.4.2 Pipes

In the design of a solar thermal energy system, the selection of pipe diameter as well as insulation can impact the performance of a system considerably. Vela Solaris (2017) gives a guideline when selecting pipe diameter, which is summarized by the following points:

- A large pipe diameter results in a large surface area, which inturn leads to increased heat losses.
- However a large diameter can result in laminar flow, which decreases heat losses.
- Higher flow rates can be achieved with a larger pipe diameter.
- A system with large pipe diameters is more inert than one with smaller diameters, due to more fluid mass being in the system at any given time.

Vela Solaris (2017) goes on to conclude that a smaller pipe diameter is therefore optimal. A criterion for a suitable pressure loss is suggested as the final selection consideration.

According to Duffie and Beckman (2013) the decrease in temperature across a pipe ΔT_p can be calculated by using:

$$\Delta T_p = \frac{UA(T_{in} - T_a)}{\dot{M}c_p} \quad (3.41)$$

Where U is the pipe heat loss coefficient, A is the pipe outer surface area, T_{in} is the inlet temperature, T_a is the ambient temperature, \dot{M} is the mass flow rate and c_p is the HTF specific heat.

3.5 Weather Data

Simulations of solar thermal systems require weather data as an input. This data would include the ambient temperature, and radiation measurements. A common way of representing weather data is in the form of a TMY (typical meteorological year) or TMY2 (second version of the TMY2) file (Duffie and Beckman, 2013). Both TMY and TMY2 files use historical data from a specific location to estimate hourly values for an average year.

The METEONORM software developed by Meteotest *et al.* (2017) has a database of more than 7000 weather stations around the world. A METEONORM user can generate a data file with monthly, daily or hourly values for a surface at any orientation.

In Southern Africa, a free to use weather database was compiled by Brooks *et al.* (2015) named the Southern African Universities Radiometric Network (SAURAN). Weather data can be obtained online from the SAURAN website. Similar data services can be expected for other regions.

3.6 System Performance Measurements

It is necessary to translate solar thermal system gains into tangible metrics for a possible investor to understand. These measures include system efficiency, solar fraction and financial parameters. This section contains a brief discussion of system efficiency and solar fraction followed by an in-depth study of financial metrics.

3.6.1 System efficiency and solar fraction

These are two simple methods for analysing an SPH system. System efficiency η_{sys} is the efficiency at which solar radiation is converted into useful process heat. This can be calculated by Equation 3.42:

$$\eta_{sys} = \frac{Q_{sol,pro}}{I_{tot}} \quad (3.42)$$

Where $Q_{sol,pro}$ is the total amount of energy (in kWh) provided to the process over a year and I_{tot} is the total amount irradiation (in kWh) that strikes the collector over the whole year.

The solar fraction is the amount of energy provided to the process by solar means over the total energy provided to the process by all means. This is shown in Equation 3.43:

$$SF = \frac{Q_{sol,pro}}{Q_{tot,pro}} \quad (3.43)$$

$Q_{sol,tot}$ is the total energy provided to the process by any means (i.e. solar or auxiliary heater).

System efficiency decreases with increasing system size (as heat losses increase with increasing HTF temperature), while solar fraction increases with increasing system size. Conventional SPH system understanding suggests that the optimum system size in financial terms occurs in the region where the solar fraction and solar efficiency overlap (Deutsche Gesellschaft für Sonnenenergie, 2010). This concept is displayed below in Figure 3.12.

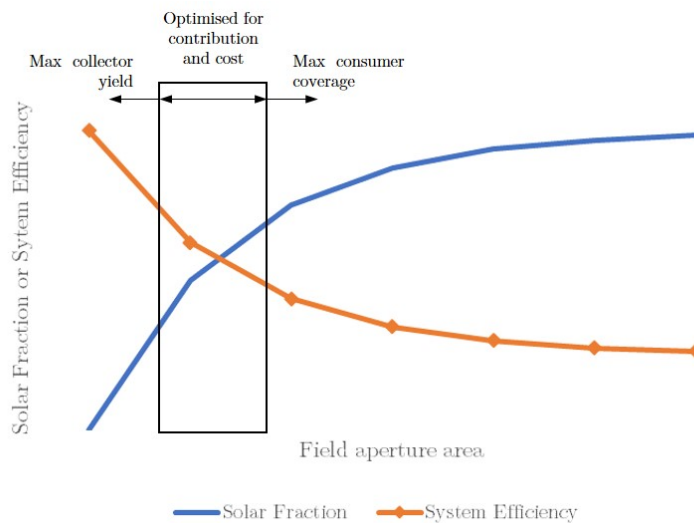


Figure 3.12: System efficiency and solar fraction vs system size. Picture: adapted from Deutsche Gesellschaft für Sonnenenergie (2010)

3.6.2 Financial methods of analysing renewable projects

The various methods to analyse renewable projects from a financial point of view will now be discussed. Four specific indicators will be studied, namely Net Present Value (NPV), Internal Rate of Return (IRR), Payback Period, and Levelized Cost of Heat (LCOH). NPV and LCOH are good indicators for the full returns of the project over its entire lifespan, while IRR and Payback Period are useful to determine the risk involved with the project.

Net present value

Net Present Value or NPV is a measure of the returns of a project over its entire lifetime (Short *et al.*, 1995). The most basic description of NPV would be the sum of all cash flows over the lifetime of a project. In order to account for the time value of money a discount rate dr is applied. Joubert *et al.* (2016) specifies the formula to calculate NPV as below in Equation 3.44:

$$NPV = \sum_{n=0}^N \frac{C_n}{(1 + dr)^n} \quad (3.44)$$

C_n is the cash flow for a specific year (subscript n referring to the year counted from the commencement of the project). The cash flows in Equation 3.44 (above) are assumed to occur once a year, starting with a large investment for the SPH installation that will be a negative cash flow. This will be followed by yearly income as a result of gains from the SPH system. These will reflect as positive cash flows.

If the calculated NPV is a positive value then the project will result in value being added to the business, while if it is negative the project will result in a net loss. For a graphical representation of NPV the reader is referred to Figure 3.13 below.

Internal rate of return

The Internal Rate of Return or IRR is the discount rate at which the NPV of a project is equal to zero. This is aptly displayed Figure 3.13 and by Equation 3.45 taken from Short *et al.* (1995).

$$0 = NPV = \sum_{n=0}^N \frac{C_n}{(1 + IRR)^n} \quad (3.45)$$

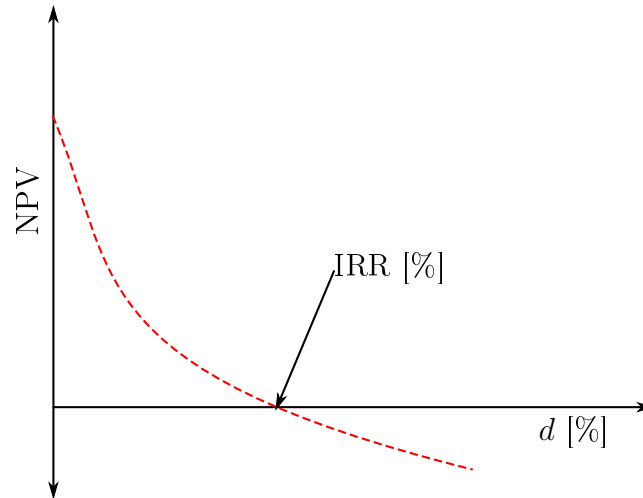


Figure 3.13: A graphical representation of IRR. NPV is on the y-axis and discount rate, d , is on the x-axis. IRR occurs where $NPV = 0$.

This method is useful for gauging the risk of a project. This is because it allows financial decision makers to measure the extent to which external factors will influence the project.

Payback period

Payback Period is another way of gauging the risk of an SPH project. It is also simple to understand and quick to calculate. Payback is defined as "the number of years necessary to recover the project cost of an investment under consideration" by Short *et al.* (1995). This can be applied by using nondiscounted cash flows (Simple Payback) or by using discounted cash flows (Discounted Payback).

Levelized cost of heat

Levelized Cost of Heat or LCOH is a method that allows alternative technologies for generating heat to be compared. There are numerous ways to calculate LCOH, but for the purposes of SolGain 2.0, a formula contained in Joubert *et al.* (2016) was deemed most appropriate. This formula can be seen below in Equation 3.46:

$$LCOH = \frac{\sum_{n=0}^N \frac{C_n}{(1+dr)^n}}{\sum_{n=1}^N \frac{Q_n}{(1+dr)^n}} \quad (3.46)$$

Where Q_n is the heat production for the year n and C_n is the cash flow for the year n .

This method is a good way of gauging long term benefits of an SPH project. It is particularly useful in comparing traditional fossil fuel methods to renewable methods (Short *et al.*, 1995).

Cost of solar process heat in South Africa

In order for SolGain 2.0 to calculate the financial performance indicators discussed above, it is necessary to estimate the cost of an SPH system. A "Large-scale Solar Thermal Heating Systems Database" was previously set up at Stellenbosch University (Joubert *et al.*, 2016). The data base considers systems with gross collector areas of more than 10 m² as large-scale.

Included in the data base are the costs of each specific system in EUR. Joubert *et al.* (2016) generated a scatter plot for this data. A line of best fit was fitted to the data so that estimations for SPH systems can be made based on their gross collector area. This plot and line of best fit can be seen below in Figure 3.14

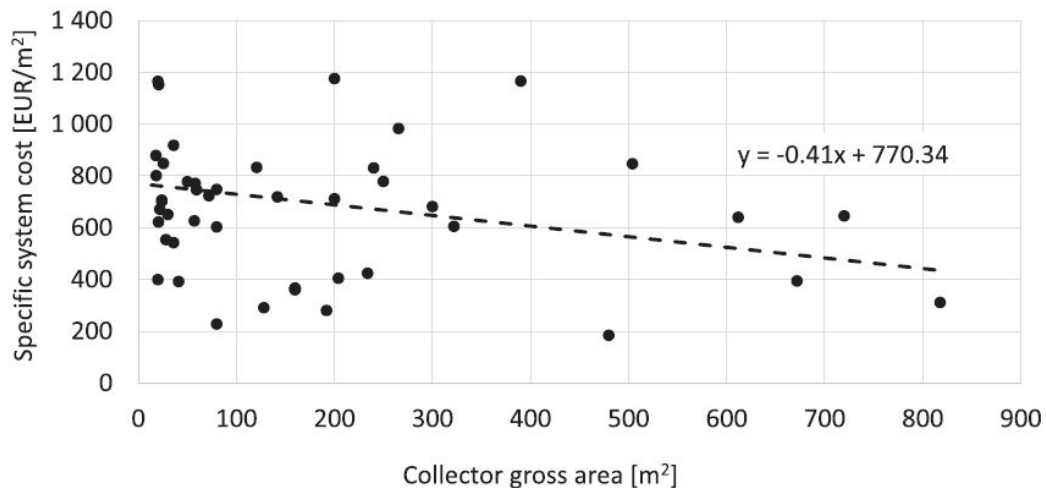


Figure 3.14: System cost relative to gross collector area. The exchange rate on the date of installation was used ($9.66 < \text{ZAR}/\text{EUR} < 15.3$ from 2007 to 2015). Picture: Joubert *et al.* (2016)

3.7 Chapter Conclusion

The necessary theoretical background needed to understand SolGain was laid out in this chapter. The theory contained in this chapter was used for the development of SolGain 2.0. All coding that was completed on SolGain 2.0 was based on this theory.

Chapter 4

Initial State of SolGain

This chapter will aim at accessing the initial state of SolGain (version 1.0) at the commencement of this project. A review of the work completed on SolGain by Ilchmann (2016) will be documented. This includes defining limitations of this state of SolGain and analysing its functionality, accuracy and user-friendliness.

4.1 The Original Aim of SolGain

The original concept of SolGain was to model and characterize SPH systems using hourly and static inputs. This concept can be seen below in Figure 4.1.

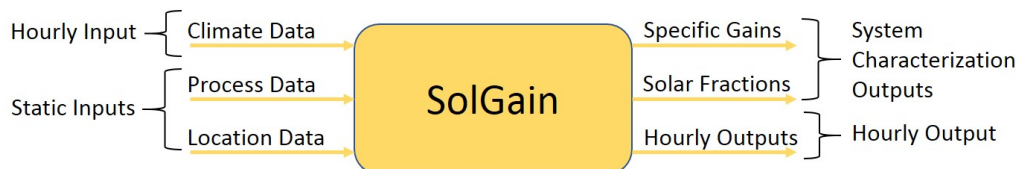


Figure 4.1: A visual representation of the initial concept of SolGain. Picture: adapted from Ilchmann (2016)

In order to make the software as user friendly as possible, SolGain 1.0 was developed so that the user would have to enter minimal data for a simulation (Ilchmann, 2016). The user input data has been separated into three categories, namely climate, process and location data. The data inputs that each of these categories include can be seen in Table 4.1.

The input variables in Table 4.1 will now be briefly explained. In the location data category latitude and hemisphere refer to the geographical location of the SPH system. Area, A , refers to a user input that is either the collector area

Table 4.1: Input data breakdown of SolGain 1.0 (Ilchmann, 2016)

Location Data	Climate Data (Hourly Input)	Process Data
Latitude	G_d	\dot{M} or \dot{Q}
Hemisphere (N or S)	G_b (DNI)	$T_{pro,in}$
A	T_a	$T_{pro,out}$
		c_p
		Load Profile

or available space for collectors. The user can input either one of these (refer to Figure 4.2 to see the Data Input Spreadsheet.).

The climate data inputs are hourly changing values that can be obtained in a typical meteorological year (TMY) or similar file for the site location. G_d and G_b are the global diffuse and direct normal irradiation respectively. T_a is the ambient temperature.

Process data inputs are entered for the specific process that the SPH system will support. These include the mass flow rate (\dot{M}) or heat flow rate (\dot{Q}) to the process, the input and output temperatures ($T_{pro,in}$ and $T_{pro,out}$), the process's working fluid's specific heat (c_p) and the load profile for heat supply to the process.

4.2 User-Interface

SolGain 1.0 contains four visible spreadsheets and one hidden spreadsheet (Ilchmann, 2016). The user will either input data into or obtain results from each of the visible spreadsheets.

Each of the visible spreadsheets will now be briefly discussed.

4.2.1 Data input spreadsheet

The previously discussed location and process data inputs are specified by the user in this spreadsheet. The user can either input the values manually into the spreadsheet or an entry can be made into a form which is opened when clicking the *Data Entry* button (refer to Figure 4.2). Using forms only for data entries in future versions of SolGain could be advantageous, as queries could be written to prevent the user from entering erroneous data.

B	C	D	E	F	G	H	I	J	K	L	M	N	O	P	Q	R
Location Cape Town	Heat Demand Type Pre Heating	Data Entry		Collector Type Flat Plate Collector	Calculation Data											
Latitude 33.58	Process Feed Temperature 60 °C	Calculate		Collector Tilt 30 °	Tracking	Range	Max		Min		Ground Reflection 0.2		Iteration: max diff. for temperature 0.01			
Hemisphere S	Process Return Temperature 45 °C			Collector Orientation 180 °	Tracking	Range	Max		Min		Maximum Collector Power Production per m ² Collector 700 W/m ²		Heat Exchanger UA 6500 W/K			
Available Space m ²	Heat Capacity of the Process Medium kJ/(kg*K)			Collector Area Size m ²							Pipe and Duct Heat Loss Coefficient 0.8 W/m ²		Distance between collector and process 2 m			
	Massflow of the Process Medium 250 kg/h			Heat Carrier Fluid in the Collector Glycol 20%												
	Energy Consumption of the Process kW															
Heat Storage No	Storage Volume m ³															
	Heat Storage Heat Loss Coefficient 0.5 W/(m ² *K)															

Figure 4.2: A screen-shot of the data input spreadsheet in SolGain 1.0. Fields highlighted in red are mandatory for the user to input.

4.2.2 Weather data spreadsheet

Here the user must input the aforementioned climate data. Hourly values over the whole year for G_d , G_b and T_a should be input into their respective columns. The user can acquire these values from a TMY file. There should be 8760 data entries into each column, representing each of the hours in a year.

4.2.3 Heat demand profile

Here the user can enter the heat demand profile for the process. The user should input percentages of the previously specified heat demand, \dot{Q} . This is done for each hour of the day, each day of the week and each week of the year. This can be seen visually in Figure 4.3.

In the example in Figure 4.3 it can be seen that on a normal working day the heat demand is zero between 12pm and 6am. The demand on Saturdays and Sundays is 50%. In weeks 25 and 26 the load is 50%.

SolGain 1.0 uses the following formula to calculate the heat demand for a specific hour of the year:

$$\dot{Q}_{need} = \dot{Q}(x_{hour} x_{day} x_{week}) \quad (4.1)$$

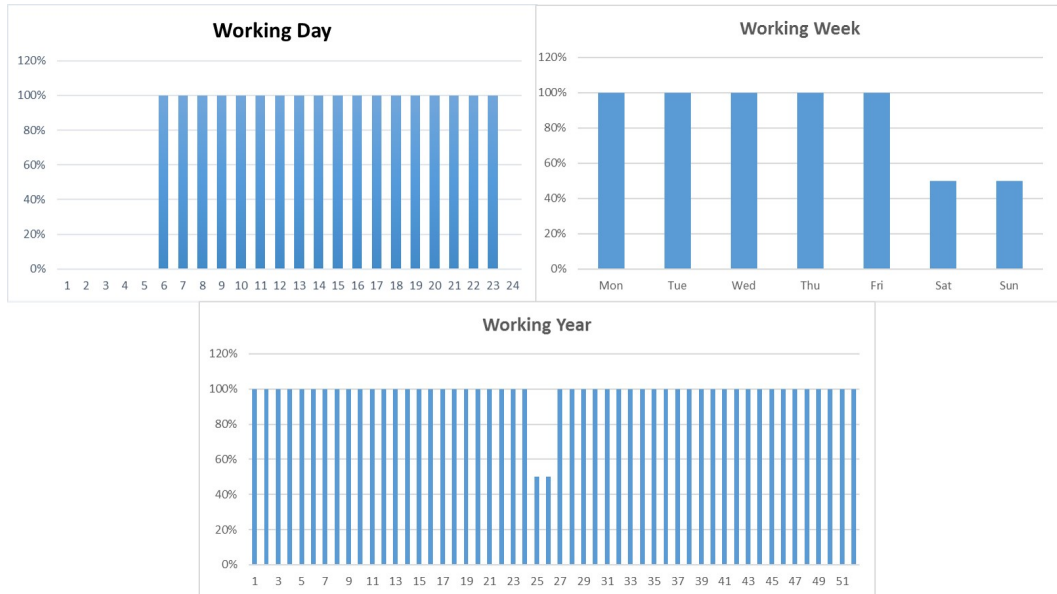


Figure 4.3: A visual representation of the concept of a heat demand profile

4.2.4 Results spreadsheet

This is the place where a user can view the results of a simulation. This includes system characterization outputs, such as specific heat gains and solar fraction of the proposed system.

Hourly outputs are also displayed here for each hour of the simulation year. The specific values shown here are collector heat gains, \dot{Q}_{gain} ; collector input and output temperature, $T_{col,in}$ and $T_{col,out}$; heat exchanger outlet temperature on the process side, $T_{HE,out,tank}$; tank temperature, T_{tank} ; energy demand of the process, Q_{need} , and lastly the energy supplied to the process, Q_{pro} .

4.3 Parameter Assumptions

In order to make the program as user friendly as possible, SolGain 1.0 was developed to have few input values (Ilchmann, 2016). The result of this is that SolGain 1.0 makes various assumptions to determine other necessary values. This section will focus on explaining these assumptions.

4.3.1 Collector data

SolGain 1.0 simulates two types of collectors namely flat plate and evacuated tube collectors (ETCs). SolGain 1.0 assumes the performance parameters for all FPCs to be the same and for all ETCs to be the same (refer to Section 3.2 for theory on collector performance). These parameters are based on a generic

FPC and ETC. It should be mentioned that Ilchmann (2016) did not use a valid procedure for modelling ETCs as outlined in Section 3.2, nor was the model validated.

4.3.2 Specific heats

SolGain 1.0 contains two separate loops where two different heat transfer fluids (HTFs) flow, namely the collector loop and the process loop. For the collector loop, the user can choose between different mixtures of glycol and water for the HTF. SolGain 1.0 then selects the matching specific heat, $c_{p,col}$.

On the process side the user can input a value for the specific heat, $c_{p,pro}$. If this field is left open, SolGain 1.0 assumes that the HTF on the process side is water. It is thus assumed that $c_{p,pro} = 4.18 \text{ kJ}/(\text{kg K})$.

4.3.3 Collector aperture size

The user may input a collector aperture size, A_{col} . In the case that the user is inexperienced with selecting this size, SolGain 1.0 assumes a value for A_{col} if one is not supplied by the user. This is done by applying the following formula (Ilchmann, 2016):

$$A_{col} = \frac{\dot{Q}_{need}}{\dot{q}_{col,max}} \quad (4.2)$$

Where \dot{Q}_{need} is the user-defined maximum heat demand and $\dot{q}_{col,max}$ is the user-defined collector peak power. The value of $\dot{q}_{col,max}$ is automatically set to $700 \text{ W}/\text{m}^2$ if no user-input is supplied (Ilchmann, 2016).

4.3.4 Storage parameters

If no input is given by the user for storage volume, SolGain 1.0 assumes the tank to have a volume of 100 litres per square meter aperture size (Ilchmann, 2016). It is assumed that the storage tank is cylindrical. Heat losses from the tank will be minimized if the surface area of the tank is minimized. This occurs when:

$$\frac{r_{tank}}{h_{tank}} = 0.5 \quad (4.3)$$

Where r_{tank} is the radius and h_{tank} is the height of the cylinder. SolGain 1.0 assumes that the above ratio holds true. The surface area is then calculated using Equation 4.4:

$$A_{tank} = 2\pi r_{tank} h_{tank} + 2\pi r_{tank}^2 \quad (4.4)$$

The storage tank is modelled as lumped system, i.e. the temperature is consistent throughout the tank. This is a very coarse way of modelling such storage tanks and is a point for possible improvement.

4.3.5 Mass flow rate in the collector loop

If storage is included, the collector loop specific flow rate is assumed to be $18 \text{ kg}/(\text{m}^2 \text{ h})$ in accordance with the work done by Furbo and Shah (1996). This specific flow rate is used to reach high temperatures at the collector output (Ilchmann, 2016). Without storage in a pre-heating process the collector loop mass flow rate, \dot{M}_{col} , is selected to be equal to the process loop mass flow rate, \dot{M}_{pro} (i.e. $\dot{M}_{col} = \dot{M}_{pro}$).

4.3.6 Pipe surface

It is assumed that the only heat losses during pipe transportation occur between the collector and heat exchanger (refer to Figure 2.2). SolGain 1.0 assumes that the flow in this pipe is laminar (Ilchmann, 2016). This occurs at a Reynold's number, Re , of less than 2300 in a round pipe according to Çengel and Ghajar (2015).

SolGain 1.0 calculates the diameter, d_p , of the pipe so that the maximum Reynold's number is equal to 2000.

4.4 Component Validation

Each component in SolGain 1.0 was tested by Ilchmann (2016) to identify points of inaccuracy within the system. Each component was individually tested from the collector to the storage tank (refer to Figure 2.2). Weather data from Cape Town, South Africa and Vancouver, Canada was used in component validation tests.

The testing was performed by comparing outputs from SolGain 1.0 to TRN-SYS: a commercially available software package that performs the same simulations as SolGain 1.0. It was selected as the datum against which SolGain 1.0 was tested due to its good standing in industry (Ilchmann, 2016).

The results obtained by Ilchmann (2016) suggest that the only component that contains notable errors is the collector. The accuracy of components that provided minimal error will only be briefly discussed. The collector accuracy, however, will be discussed in detail.

4.4.1 Pipe losses

The HTF is transported in pipes from the collector to the heat exchanger (refer to Figure 2.2). This results in heat losses. SolGain 1.0 obtains very similar values to TRNSYS in this part of the simulation. This is shown by differences in daily average temperatures at the end of this pipe in SolGain 1.0 and TRNSYS never exceeding 0.01 °C (Ilchmann, 2016).

4.4.2 Heat exchanger

Heat exchangers are commonly used in SPH systems. The heat exchanger modelled in SolGain 1.0 produced no visible deviations from the TRNSYS model, i.e. the two simulations are almost precisely the same (Ilchmann, 2016). The heat exchanger model can therefore be used by future versions of SolGain.

4.4.3 Tank model

The tank modelled in SolGain 1.0 has only one temperature level, i.e. the tank is at the same temperature throughout. Testing indicated that SolGain 1.0's tank model produces similar values to a single temperature level tank in TRNSYS. However, this kind of a tank is not commonly used in SPH systems and as such the tank in SolGain 1.0 is not sufficient for modelling thermal storage used in SPH systems.

4.4.4 Collector

The first metric that was measured to verify the collector model was the **angle of incidence**, θ . This is dependent on the sun's position relative to the collector. For the sake of brevity only the Vancouver simulation shall be reviewed. The input data for the Vancouver simulation is contained in Table 4.2.

Table 4.2: Input Data for angle of incidence testing in SolGain 1.0 (location: Vancouver)

Term	Value	Unit	Description
ϕ	49.15	degrees	Latitude
ψ	-123.12	degrees	Longitude
β	30	degrees	Collector tilt
γ	180	degrees	Collector azimuth (0=North; 180=South)

The results from the Vancouver test seem to indicate an error in the sun position calculated by SolGain 1.0. This can be seen visually below in Figure 4.4. This is something that should be addressed in future versions of SolGain.

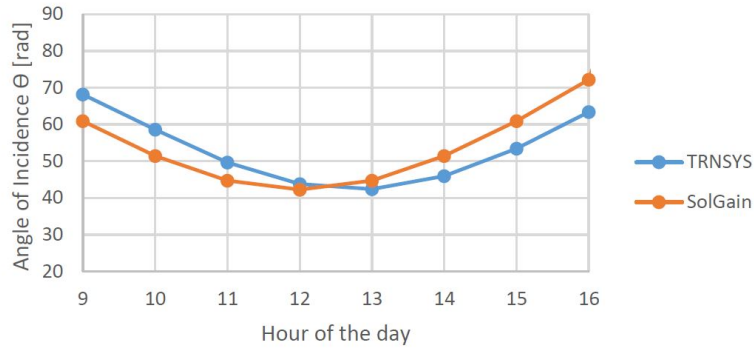


Figure 4.4: SolGain 1.0 calculated angle of incidence on 1 January in Vancouver. Picture: Ilchmann (2016)

The second metric used to determine the simulation of a collector in SolGain 1.0 was the **irradiance onto the collector**. At this stage it is useful to explain to the reader the sky model used by SolGain 1.0.

SolGain 1.0 models the sky using an isotropic sky model, as discussed in Section 3.1.3. This is a very coarse model for determining diffuse irradiance from the sky on a tilted surface (G_{st}) and reflected irradiance from the ground on a tilted surface (G_{rt}). A more accurate model of diffuse sky and ground reflected irradiance is the Perez or anisotropic model (Hess, 2014). For the purposes of SolGain as a pre-assessment tool, the coarse isotropic model suffices.

The calculated irradiance falling on the collector G_t is dependent on the angle of incidence and the sky model used. A test was completed by Ilchmann (2016) to determine the accuracy of the isotropic sky model in SolGain 1.0. This was done by inputting the same weather data into TRNSYS and SolGain 1.0, while the values for angle of incidence θ were inputted directly into SolGain 1.0 from TRNSYS. This was done so that only the sky models were being compared, with no influence from differences in angle of incidence.

Once again Cape Town and Vancouver were used as test locations; however, the Vancouver case study will only be reviewed in this text. The input data was exactly the same as in Table 4.2 with the addition of ground reflectance, ρ_{grd} , being set to 0.2. The results for a randomly selected day (5 February) from this test are contained in Figure 4.5.

The errors displayed in Figure 4.5 are minimal. The annual daily deviations in total irradiance on the collector G_t between TRNSYS and SolGain 1.0 is less than 0.03%.

The final metric used to determine the validity of SolGain 1.0's FPC simulation

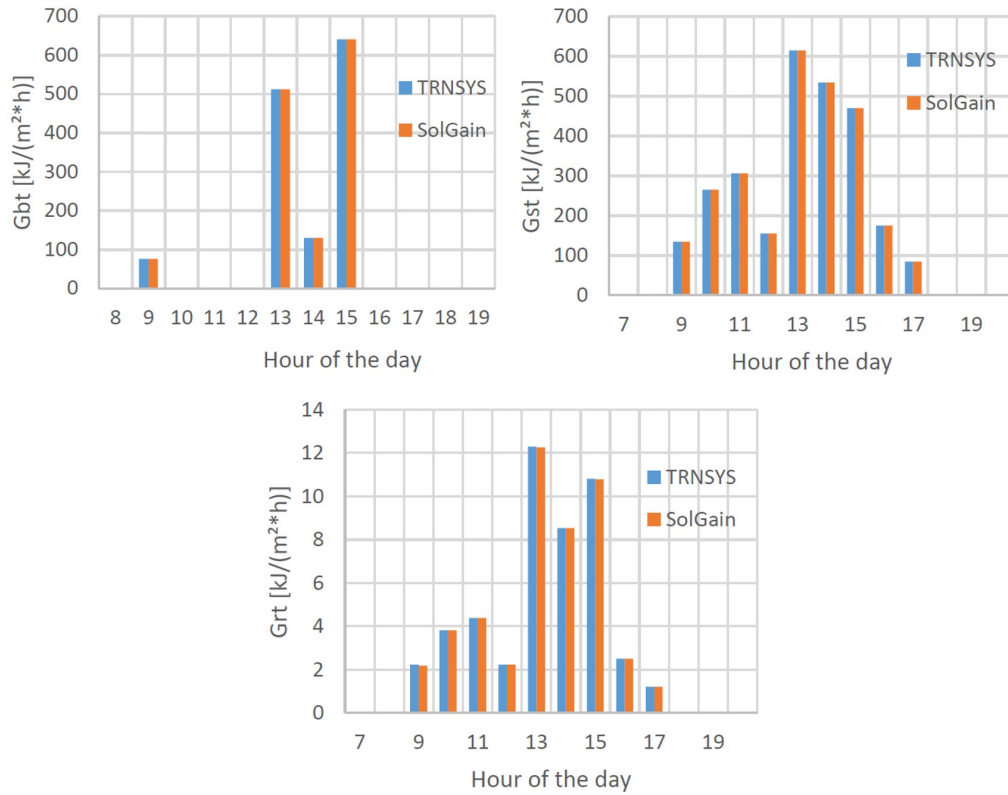


Figure 4.5: SolGain 1.0 irradiance on a collector (tilted) on 5 February for Vancouver **Left:** Beam irradiance (G_{bt}) **Right:** Diffuse sky irradiance (G_{dt}) **Bottom:** Ground reflected irradiance (G_{rt}). Picture: Ilchmann (2016)

was **collector heat output**. In order to adequately test this metric, values for G_{bt} , G_{st} and G_{rt} were inputted directly from TRNSYS into SolGain 1.0. This was done so that the previously measured inaccuracies in angle of incidence and irradiance onto the collector would be attenuated.

The collector selected in TRNSYS was a *Type1b*, which is a quadratic efficiency FPC - the same type of collector used by SolGain 1.0. The collector efficiency parameters in SolGain 1.0 and TRNSYS were set to the values contained in Tables 4.3 and 4.4.

Cape Town and Vancouver were used as test locations, but for the sake of brevity only the Vancouver case will only be reviewed. The results for a single day of testing in SolGain 1.0 and TRNSYS can be seen below in Figure 4.6.

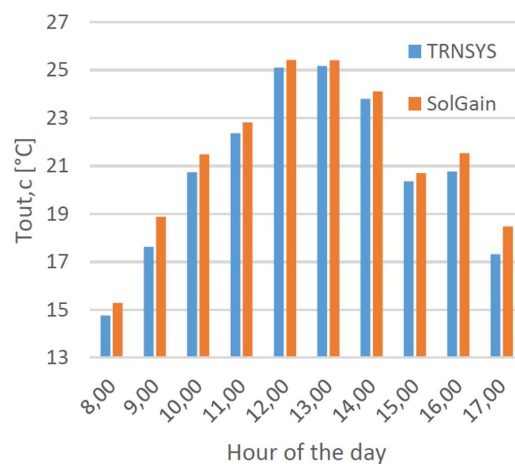
From Figure 4.6 it can be seen that SolGain 1.0 consistently gives outlet temperatures higher than TRNSYS. The total annual collector yield for Vancouver is also 9.05% higher in SolGain 1.0 than in TRNSYS (Ilchmann, 2016). This is an improvement that can be implemented in SolGain.

Table 4.3: Input data for collector output testing of SolGain 1.0

Term	Value	Unit	Description
A_{col}	5	m ²	Aperture area
c_p	3500	J/(kg K)	HTF specific heat
η_0	0.811	-	Intercept efficiency
c_1	2.71	W/(m ² K)	First order heat loss coefficient
c_2	0.01	W/(m ² K ²)	Second order heat loss coefficient
K_d	0.912	-	IAM for diffuse irradiance
c_{eff}	7.05	kJ/(m ² K)	Effective collector heat capacity
\dot{M}_{col}	250	kg/h	Mass flow rate through collector
$T_{col,in}$	15	°C	Collector inlet temperature

Table 4.4: IAM references for collector output testing of SolGain 1.0

θ_{ref}	50°
$K_b(\theta_{ref})$	0.96

**Figure 4.6:** SolGain 1.0 collector output test results for Vancouver on 26 February. Picture: Ilchmann (2016)

4.5 Chapter Conclusion

This chapter addressed the state of SolGain at the commencement of this project. Various deficiencies in SolGain 1.0 were addressed. Amongst the deficiencies are lack of user interface that queries input data, parameter assumptions not based on literature in the field, a primitive tank model, and inaccuracies in component modelling.

Chapter 5

Modifications to SolGain

This chapter outlines the changes that were made to SolGain during the course of this project. The SolGain source code was rewritten due to reasons that will be discussed in this chapter. Other modifications to SolGain include the development of a user interface, amendments to sun position calculations, development of evacuated tube and parabolic trough collector models, implementation of system controls, development of a more accurate tank model and development of an economic model.

5.1 Rewriting SolGain Code

SolGain 1.0 was written using minimal functions and subroutines, meaning that most of the code was contained in a long, nested subroutine. The code was also developed without variable declarations. This can cause difficulties when debugging and cause the software to be inefficient with memory usage as all variables are assumed to be *variants*, which is the largest data type. The author also found many discrepancies between the theory discussed in Chapter 3 and the implementation in SolGain 1.0. For the above reasons, it was decided to rewrite the SolGain code.

The code was rewritten using objects or classes as the basis for programming. The objects were structured so that most of the objects could represent an actual physical component of the system. These will be termed *physical objects*. The objects that do not represent a physical component will be referred to as *non-physical objects*. The purpose of each physical object is described below in Table 5.1 and of each non-physical object in Table 5.2.

A main subroutine is run in SolGain 2.0 whereby instances of all the classes in Tables 5.1 and 5.2 are created. For more information on the code structure of SolGain 2.0 the reader is referred to Appendix B.

Table 5.1: Physical object classes in SolGain 2.0

Physical Objects	
Name in SolGain 2.0	Description
SunClass	The SunClass contains all angles to determine the angles of the sun relative to earth (i.e. azimuth and zenith angle) and the collector (i.e. angle of incidence). These angles are calculated using subroutines and functions that implement the theory discussed in Section 3.1. This class also has subroutines to calculate the irradiance onto the collector using the theory discussed in Section 3.1.
CollectorClass	The CollectorClass contains subroutines and functions to determine the outlet temperature of a collector. This class also contains algorithms for determining a mass flow rate that results in a specified collector outlet temperature. The theory applied in this class can be seen in Section 3.2.
PipeClass	The PipeClass is responsible for modelling pipe heat losses and calculating the outlet temperature of a pipe. The theory used to do this is contained in Section 3.4.2.
HeatExchangerClass	The HeatExchangerClass models a heat exchanger based on the theory described in Section 3.4.1. This class takes both inlet temperatures to the heat exchanger and calculates both outlet temperatures.
TankClass	The TankClass models a thermocline storage tank using the theory discussed in Section 3.3. For each time step heat losses and gains of every node in the tank are modelled. The outlet temperatures to the heat source (heat exchanger) and to the heat sink (process) are determined by the TankClass.
HTFPropertiesClass	The HTFPropertiesClass stores the physical properties of the heat transfer fluid (HTF). At present the properties are static and don't change with temperature and pressure. The class is structured such that functions and subroutines to determine properties with changing temperature and pressure could be implemented at a later stage.

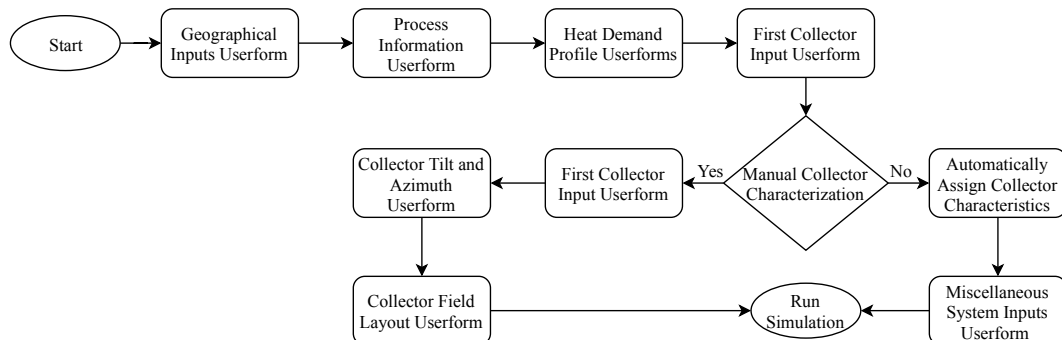
Table 5.2: Non-physical object classes in SolGain 2.0

Non-physical Objects	
Name in SolGain 2.0	Description
TemperatureClass	The TemperatureClass acts as an array for memory storage of all system temperatures. The added benefit of using a class instead of an array is that the variables can be indexed with a name instead of a number.
MassFlowClass	The MassFlowClass acts as an array that stores the values of all mass flows in the system. This class is also responsible for calculating the mass flow to the process based on the heat demand profile.
FinancialModelClass	The FinancialModelClass implements all the theory explored in Section 3.6. It is responsible for determining the levelised cost of heat (LCOH), net present value (NPV), internal rate of return (IRR) and other system performance parameters.

5.2 User Interface and Parameter Assumptions

A user interface was developed to assist users with using SolGain 2.0. This section will give a brief introduction, but the reader is referred to Appendix A for the complete documentation of the user interface and parameter assumptions. This appendix also functions as a user-manual for beginning a simulation in SolGain 2.0.

The user starts the process of a simulation by clicking on a button, which opens the first userform. The user then inputs values, which are queried by the userform code and then stored in a worksheet. Once the user has finished with inputting values a full year simulation is run. The flow diagram structure of userforms in SolGain 2.0 is displayed in Figure 5.1.

**Figure 5.1:** SolGain 2.0's userform structure

SolGain 2.0 was developed so that it would be useful to those familiar with SPH systems and those that are not. The user interface was designed to allow experienced users to make all design decisions, while inexperienced users can rely on SolGain 2.0 to make design decisions using assumptions. These assumptions differ from the ones made in SolGain 1.0 (discussed in Section 4.3) as they are formulated from available literature on sizing of SPH systems.

The reader is referred to Appendix A to view the complete documentation of userforms and parameter assumptions.

Miscellaneous System Inputs

***If unsure of a value, leave the default value.**

Heat Storage:	<input type="checkbox"/> Yes	Pipe Heat Loss Coefficient:	<input type="text" value="0.8"/> W/(m ² *K)
Heat Storage Volume:	<input type="text" value="10"/> m ³	Pipe Diameter:	<input type="text" value="0.1"/> m
Heat Storage Heat Loss Coefficient:	<input type="text" value="0.5"/> W/(m ² *K)	Distance between Collector (outside) and Heat Exchanger (inside):	<input type="text" value="10"/> m
Heat Exchanger UA:	<input type="text" value="6500"/> W/K		

< Previous Next >

Figure 5.2: A userform (*Miscellaneous System Inputs*) used for user inputs in SolGain 2.0

5.3 Sun Position

The position of the sun as calculated by SolGain 1.0 was slightly off for a reason that could not be determined by Ilchmann (2016). This inaccuracy was investigated and the calculation of zenith θ_z and azimuth γ_s angle were amended.

Two errors were found upon investigation of the formulas used by SolGain 1.0. These were:

- *Clock time* being used instead of *solar time* in the calculation of θ_z and γ_s .

- No longitude correction for differences between the time zone's meridian and the local meridian, as described by Equation 3.2.

These errors were amended by careful application of the formulas contained in Section 3.1.

5.4 Collector Modelling

SolGain 1.0 could model a one-dimensional flat plate collector (FPC). Alterations that were made to the collector model in SolGain during the duration of this project allow for the modelling of more complex collectors. Evacuated tube (ETC) and parabolic trough collectors (PTC) can be modelled by SolGain 2.0. This was achieved by applying the theory in Section 3.2.

The accuracy of SolGain 1.0's flat plate collector model was slightly off. This was due to the theory described in Section 3.2 not being strictly applied in SolGain 1.0. This was amended by strict application of the theory.

Another alteration made to SolGain's collector model is the ability to model collectors in series (N_{ser}) and flow loops in parallel (N_{par}) as seen in Figure 5.3. Collectors in series are modelled in SolGain 2.0 by setting the inlet of an individual collector i equal to the outlet of the previous collector $i - 1$, as seen in Equation 5.1:

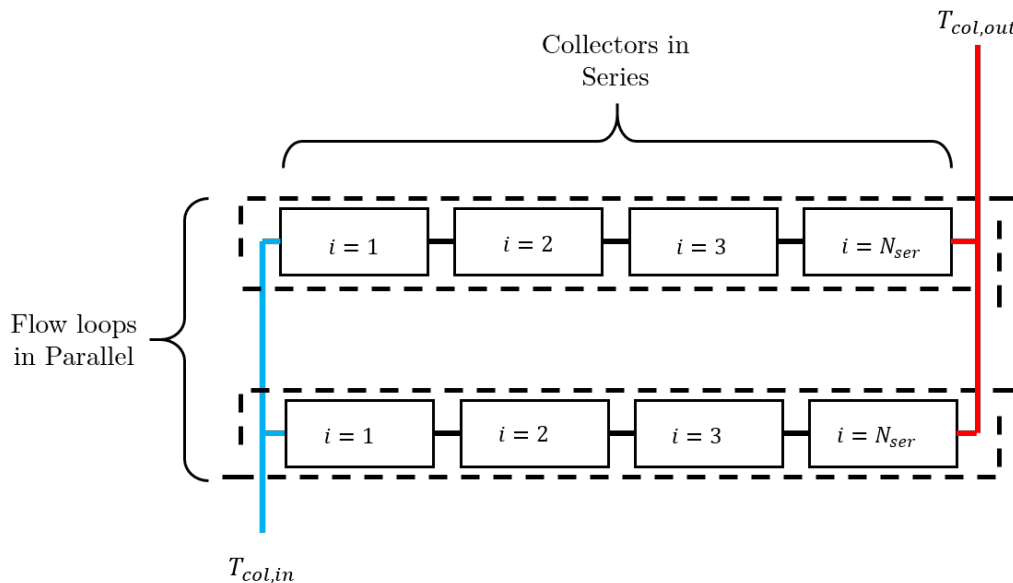


Figure 5.3: Collectors in series and parallel

$$T_{col,in,i} = T_{col,out,i-1} \quad (5.1)$$

Flow loops in parallel are modelled by setting the flow rate through each flow loop equal to:

$$\dot{M}_{loop} = \frac{\dot{M}_{col}}{N_{par}} \quad (5.2)$$

5.5 System Controls

Two strategies are applied in SolGain 2.0 for charging the storage using solar means. These are the *preheating* and *target temperature* strategies. The *preheating* strategy uses a set specific flow rate in the collector loop of $\dot{m}_{col} = 18 \text{ kg}/(\text{m}^2 \text{ h})$, based on the work of Furbo and Shah (1996), to charge the storage. The *target temperature* strategy on the other hand controls the value of mass flow in the collector loop \dot{M}_{col} such that the inlet to the tank is equal to some predefined *target temperature*.

The preheating strategy was implemented in SolGain 1.0, but there was no target temperature control. In SolGain 2.0 the target temperature strategy is implemented using various functions and subroutines that were developed. The method used by SolGain 2.0 to calculate \dot{M}_{col} will now be discussed. The reader is referred to Figure 5.4 for clarity on the system layout.

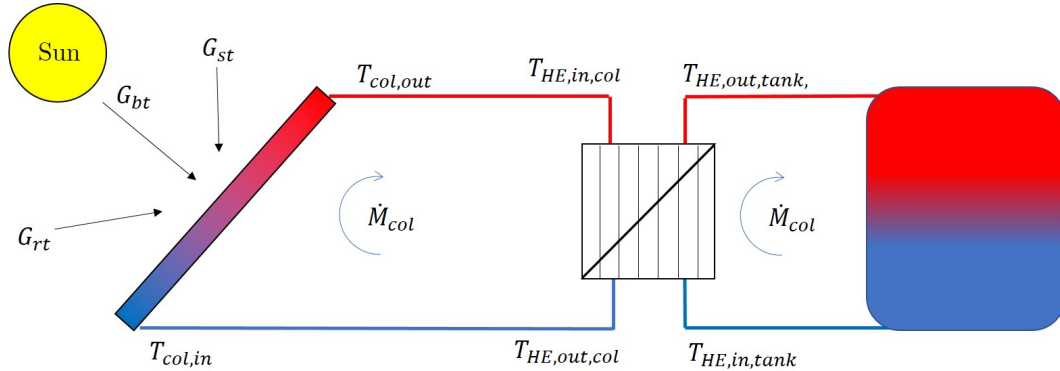


Figure 5.4: An isolated part of the SolGain 2.0 system relevant for storage charging using solar means

The value of the tank inlet temperature $T_{HE,out,tank}$ is assumed to be 5°C above the target process inlet temperature $T_{pro,in}$ (i.e. $T_{HE,out,tank} = T_{pro,in} + 5^\circ\text{C}$). This assumption along with a known $T_{HE,in,tank}$ allow us to reverse calculate

the \dot{M}_{col} . The value of \dot{M}_{col} is then calculated using the process displayed in Figure 5.5.

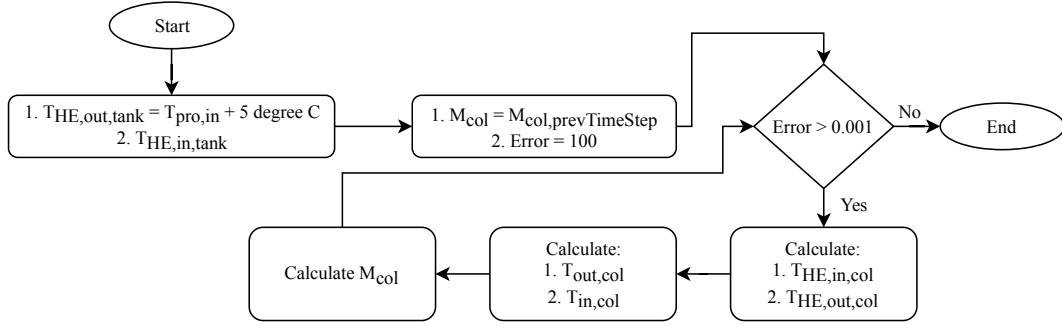


Figure 5.5: Target temperature mass flow control strategy

Each of the calculations contained in Figure 5.5 will now be discussed.

5.5.1 Calculation of collector side heat exchanger temperatures

In Figure 5.5 the values of $T_{HE,in,col}$ and $T_{HE,out,col}$ are calculated by a subroutine (named calcHotSideTemps). The subroutine uses the known cold side temperatures of the heat exchanger ($T_{HE,out,tank}$ and $T_{HE,in,tank}$) to determine the hot side temperatures ($T_{HE,in,col}$ and $T_{HE,out,col}$). The theory behind this calculation will now be addressed. The reader is referred to Section 3.4.1 for clarification on heat exchanger theory.

From heat transfer knowledge it is known that the heat transferred by a heat exchanger Q_{HE} can be expressed as:

$$\dot{Q}_{HE} = c_{p,pro} \dot{M}_{col} (T_{HE,out,tank} - T_{HE,in,tank}) \quad (5.3)$$

Or

$$\dot{Q}_{HE} = c_{p,col} \dot{M}_{col} (T_{HE,in,col} - T_{HE,out,col}) \quad (5.4)$$

From Equations 5.3 and 5.4 above as well as Equation 3.36 the following two equations for determining the hot side temperatures of the heat exchanger can be derived:

$$T_{HE,in,col} = T_{HE,in,tank} + \frac{\dot{Q}_{HE}}{\epsilon C_{min}} \quad (5.5)$$

$$T_{HE,out,col} = T_{HE,in,col} - \frac{\dot{Q}_{HE}}{c_p \dot{M}_{col}} \quad (5.6)$$

5.5.2 Calculation of collector inlet and outlet temperatures

Calculating collector side temperatures ($T_{col,out}$ and $T_{col,in}$) from the heat exchanger side temperatures ($T_{HE,in,col}$ and $T_{HE,out,col}$) will now be addressed. Calculating pipe outlet temperatures can be done using Equation 3.41, which can be used for determining $T_{col,in}$ from $T_{HE,out,col}$.

The calculation of $T_{col,out}$ from $T_{HE,in,col}$ on the other hand is more complex. An iterative process must be followed to do so. The procedure followed to determine pipe inlet temperatures from outlet temperatures can be seen in Figure 5.6.

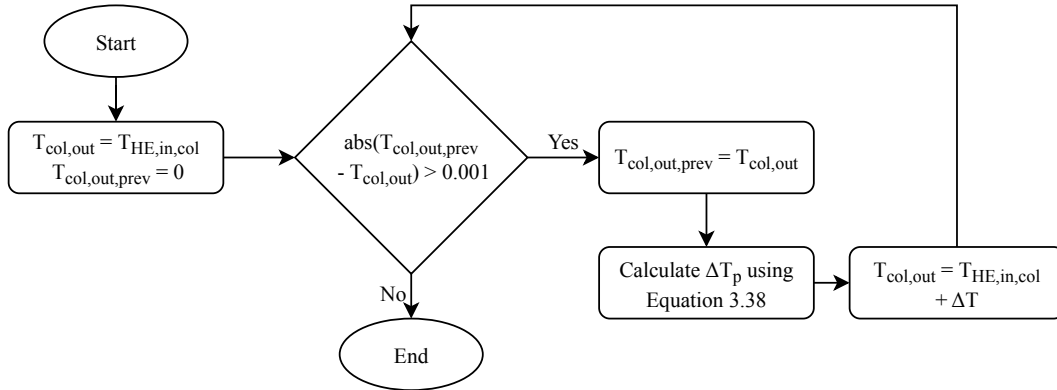


Figure 5.6: Pipe inlet temperature calculation from pipe outlet temperature

5.5.3 Calculation of collector loop mass flow rate

Finally, once $T_{col,out}$ and $T_{col,in}$ have been calculated, \dot{M}_{col} can be calculated. The value of \dot{M}_{col} is solved using a bisection root finding algorithm. The procedure used for doing this will now be briefly addressed.

For the purposes of determining \dot{M}_{col} using the bisection method, from now on the previously determined value of $T_{col,out}$ will be referred to as $T_{col,out,desired}$.

As discussed in Section 3.2, varying the mass flow rate through a collector will result in varied collector outlet temperatures i.e. $T_{col,out}(\dot{M}_{col}, T_{col,in})$. It is also known that once the mass flow rate has been solved that $T_{col,out}(\dot{M}_{col}, T_{col,in}) = T_{col,out,desired}$. From this a function can be set up whose root will give the value of \dot{M}_{col} :

$$f(\dot{M}_{col}, T_{col,in}) = 0 = T_{col,out,desired} - T_{col,out}(\dot{M}_{col}, T_{col,in}) \quad (5.7)$$

The bisection method requires the above Equation 5.7 and two initial estimates ($\dot{M}_{col,1}$ and $\dot{M}_{col,2}$) that will definitely lie on opposing sides of the root. These are given by:

- $\dot{M}_{col,1}$ is determined by the minimum specific flow rate $\dot{m}_{col,min} = 0.001 \text{ kg}/(\text{s m}^2)$ for which the collector model can run:

$$\dot{M}_{col,1} = \dot{m}_{col,min}(N_{par} \cdot A_{col}) \quad (5.8)$$

- $\dot{M}_{col,2}$ is set to a value of ten times an approximation of \dot{M}_{col} made by a SolGain 2.0 subroutine *collector.approxFlowRate*.

The bisection method can now be used to solve for \dot{M}_{col} . Once \dot{M}_{col} has been solved, the maximum error ("Error" in Figure 5.5) is calculated between the current and previous values of \dot{M}_{col} and all the temperatures. If this error value exceeds 0.001 then the process is iterated starting at the procedure in Section 5.5.1 again.

5.6 Tank Model

The tank model in SolGain 1.0 was a single temperature tank model or a lumped tank model. This model assumes that the tank is fully mixed. This is a coarse model and will generally result in lower solar gains than a more accurate model of a thermocline tank. A *multinode* tank model as described in Section 3.3 was implemented in SolGain 2.0.

The method of solving energy balance equations for the thermal storage in SolGain 1.0 was also not in line with the theory studied in Section 3.3. SolGain 2.0 makes use of a Crank-Nicolson method to solve the energy balance equations.

The number of nodes N_{nodes} by the tank model in SolGain 2.0 is 12. This number was selected as it is the number of nodes used in Polysun for tank simulations (Vela Solaris, 2017).

5.7 System Performance Measurements

This addition to SolGain was made to allow tangible results to be analysed by designers and possible investors. The non-financial system performance

measurements that are implemented in SolGain 2.0 are solar fraction SF , system efficiency η_{sys} , net present value NPV , internal rate of return IRR and levelised cost of heat $LCOH$.

Some assumptions are made by SolGain 2.0 to determine the performance parameters. Firstly the system lifetime is assumed to be 20 years. The second assumption is the system cost, which is determined using the line-of-best-fit in Figure 3.14. The last assumption is that the alternative system (to solar) is assumed to provide heat at the same cost as the auxiliary heater.

The process of determining system performance parameters starts with summing the heat provided by solar means Q_{sol} and auxiliary means Q_{aux} . At the end of a year of simulation net present value and internal rate of return are calculated using excel functions named NPV and $WorksheetFunction.IRR$. Levelised cost of heat, solar fraction and system efficiency are calculated by SolGain 2.0 functions using the methods described in Section 3.6.

Depending on the users selection (as described in Appendix A) of whether to manually enter collector characterisation or automatically enter collector characterization, a different simulation procedure will be followed by SolGain 2.0. This will now be addressed as well as the way that system performance measurements are displayed for both.

5.7.1 Manual collector inputs

If the user opted to manually input collector characteristics, the program will only run for the system size entered by the user. Two simulations will be run: one using a pre-heat strategy and one using a target temperature strategy (as described in Section 5.5). System performance parameters for each of the strategies are shown in a table. The user can then assess the performance of his/her design.

5.7.2 Automatic collector inputs

Alternatively if the user opted for automatic collector characterization, the program will run using five different system sizes. These system sizes are determined using the user input of *available space* (refer to Appendix A).

The first system size will only use one-fifth of the available space. The second two-fifths of the available space and so on until the fifth system size which will use all of the available space. The space is assumed to be filled with collectors in parallel.

System performance results are displayed for each system size, as seen below in Figure 5.7. A solar fraction and system efficiency versus system size graph

is plotted (as described in Section 3.6). This will allow the user to see the pros and cons of different system sizes.

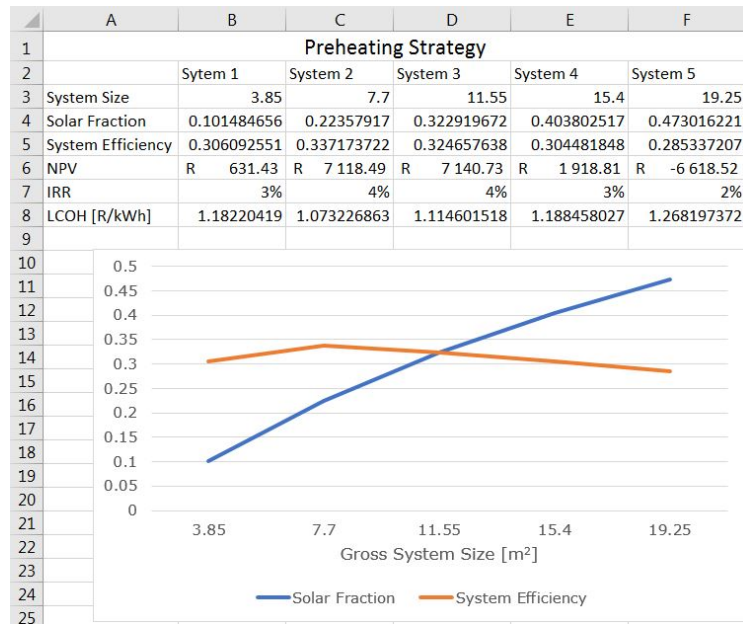


Figure 5.7: Simulation results in SolGain 2.0

This procedure is followed for both charging strategies, namely pre-heat and target temperature (as described in Section 5.5). A table and graph as seen in Figure 5.7 are displayed for both strategies.

5.8 Chapter Conclusion

This chapter outlined the work that was completed during this project. Sol-Gain's code was completely rewritten into an object orientated program with a more modular approach. A user interface was developed, that queries variables and makes parameter assumptions depending on the user's preference ¹. The inaccuracies in sun position determination of SolGain 1.0 were amended. The collector model was adapted to include evacuated tube collectors and parabolic troughs. An algorithm for controlling the collector loop flow rate was developed. The single temperature tank model was replaced with a more realistic model. Lastly, system performance measurements were implemented in SolGain 2.0, allowing user's to size SPH systems better.

¹For more in depth documentation of the user interface, the reader is referred to Appendix A.

Chapter 6

Component Validation

This chapter focuses on validating the separate system components used in SolGain 2.0. In order to do this simulations were run using TRNSYS and SolGain 2.0 with the same input variables. Results from these simulations are explored in this chapter.

All simulations were run using weather data for Cape Town, South Africa from the TRNSYS Meteoronorm database. For angle of incidence testing an extra location in the Northern hemisphere was used, namely London to validate determination of the sun's position in both hemisphere.

The specific heats c_p used for all simulations except for the parabolic trough simulation (Section 6.3.3) are based on water being used as a heat transfer fluid (HTF). A value of 4190 J/(kg K) was used as this is roughly the specific heat of water at room temperature (Çengel and Ghajar, 2015). For the parabolic trough simulation the specific heats were based on Therminol 66 used as the HTF. The properties sheet for Therminol 66 is contained in Appendix C.

6.1 Angle of Incidence

The angle of incidence θ , as explored in Section 3.1 is dependent on the position of the sun in the sky. Having an accurate angle of incidence is the foundation of an accurate collector model.

Year long simulations were run using TRNSYS and SolGain 2.0 to observe how SolGain 2.0's angle of incidence compares to that of TRNSYS. The input data for the Southern and Northern hemisphere simulations can be found below in Table 6.1 and Table 6.2, respectively.

The results from simulations seem to indicate that SolGain accurately deter-

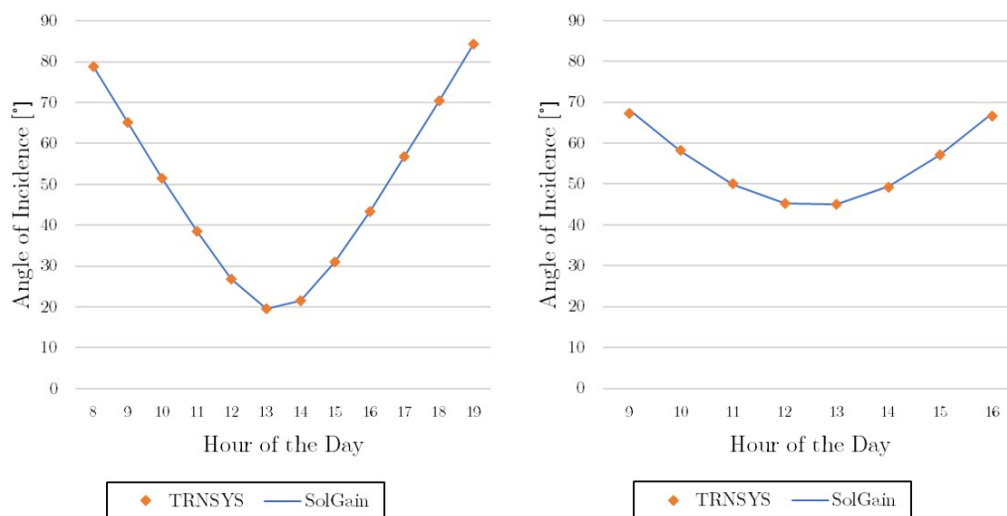
Table 6.1: Input data for angle of incidence testing in the southern hemisphere (location: Cape Town)

Term	Value	Unit	Description
ϕ	-33.96	degrees	Latitude
ψ	18.6	degrees	Longitude
β	30	degrees	Collector tilt
γ	0	degrees	Collector azimuth (0=North; 180=South)

Table 6.2: Input data for angle of incidence testing in the northern hemisphere (location: London)

Term	Value	Unit	Description
ϕ	51.516	degrees	Latitude
ψ	0.116	degrees	Longitude
β	30	degrees	Collector tilt
γ	180	degrees	Collector azimuth (0=North; 180=South)

mines the position of the sun. Three days were randomly selected to illustrate how well SolGain 2.0 Tracks with TRNSYS. Figures 6.1, 6.2 and 6.3 contain the results for these three days.

**Figure 6.1:** Angle of incidence for 1 January **Left:** Cape Town **Right:** London

It can be seen in Figures 6.1, 6.2 and 6.3 that SolGain 2.0 determines the position of the sun accurately for different seasons and for different locations. The maximum error for θ was 3.314° and 3.417° for Cape Town and London respectively. High error values (above 1°) only occur early in the morning and

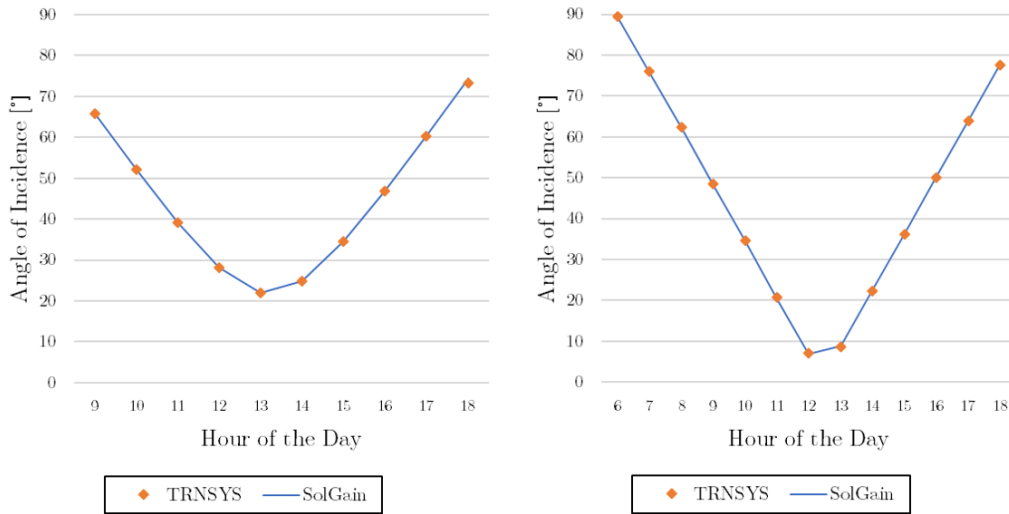


Figure 6.2: Angle of Incidence for 12 May **Left:** Cape Town **Right:** London

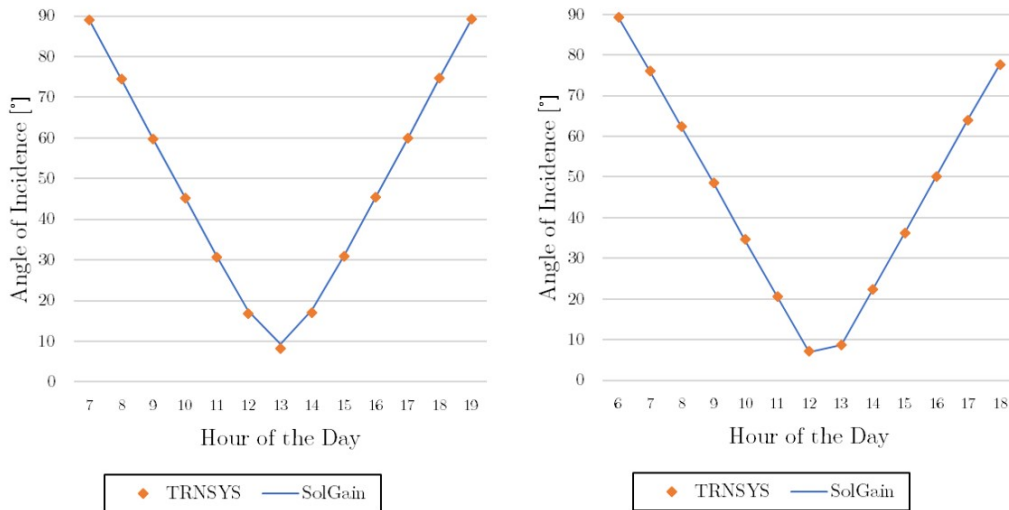


Figure 6.3: Angle of Incidence for 26 October **Left:** Cape Town **Right:** London

late in the evening when the strength of the sun is low, meaning that they will have minimal impact on system performance. The average error over the whole year of simulation was 0.181° for Cape Town and 0.404° for London.

6.2 Radiation on the Collector

The radiation landing on a collector is crucial to determining collector output. It is primarily dependent on the weather data, position of the sun, whether the collector tracks or not and the sky model used. The sole purpose of this test

was to analyse the functioning of the sky model. For this reason simulations were run in SolGain 2.0 whereby the position of the sun was set equal to that of TRNSYS for every time step.

SolGain 2.0 implements an isotropic model for sky diffuse G_{st} and reflected diffuse G_{rt} irradiance. The sky model used in TRNSYS was therefore set to an isotropic one. Cape Town was used as the location for radiation testing. The input data used for simulations was the same as in Table 6.1 with ground reflectance ρ_{grd} being set to 0.2.

After simulations were run using TRNSYS and SolGain 2.0, results for two irradiance measures were compared, namely total irradiance on the surface $G_t = G_{bt} + G_{st} + G_{rt}$ and beam irradiance on the surface G_{bt} . G_t is important for non-concentrating collectors and G_{bt} is important for concentrating collectors.

Results for G_t in SolGain 2.0 did display some deviation from TRNSYS. The maximum instantaneous error for total irradiance in SolGain 2.0 was 7.17 W/m. The cumulative error over the whole year for total irradiation was 10.76 kWh/m² which translates to a percentage error of 0.51 % per annum. Graphical results for a clear and an overcast day can be seen below in Figure 6.4.

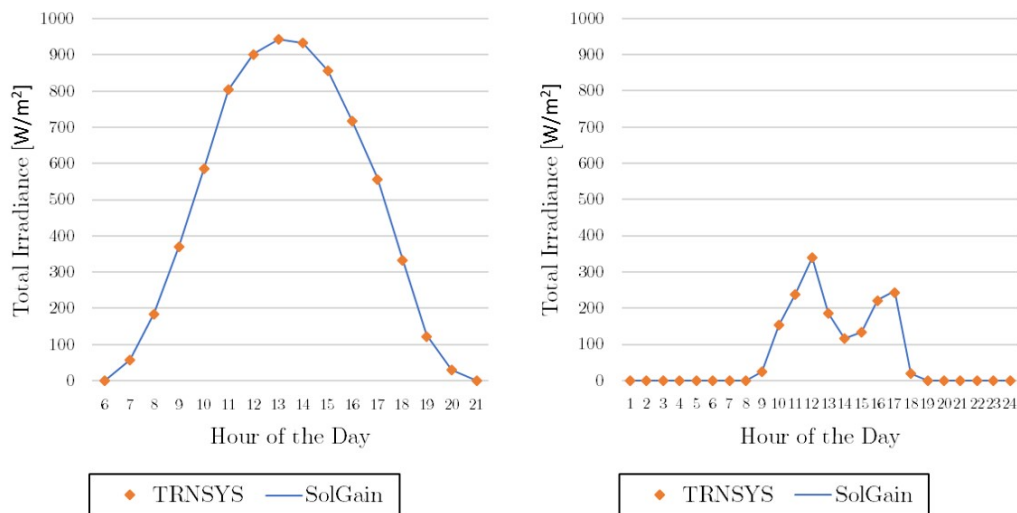


Figure 6.4: Total Irradiance onto collector **Left:** 1 January (clear day) **Right:** 20 June (overcast day)

The test results for beam irradiance G_{bt} indicated minimal deviation between TRNSYS and SolGain 2.0. The maximum instantaneous error on G_{bt} for SolGain 2.0 was 4.83×10^{-13} W/m² and the cumulative error of beam irradiation over the whole year was 6.99×10^{-13} kWh/m².

6.3 Collector Model Testing

Three types of collectors can be modelled in SolGain 2.0, namely flat plate (FPC), evacuated tube (ETC) and parabolic trough (PTC) collectors. Each one is modelled according to slightly different procedures discussed in Section 3.2.

In order to validate the collector model against TRNSYS a system was set up in TRNSYS with just a collector that receives irradiance values from a sky model. Irradiance values G_{bt} , G_{rt} and G_{st} and incidence angles θ_l and θ_t from TRNSYS were read directly into SolGain 2.0. This means that any differences between the output values would be purely due to the collector model.

6.3.1 Flat plate collector

The collector type used in TRNSYS to validate SolGain 2.0's FPC model was the *Type1c* collector. The TRNSYS collector type was selected and set up to be the same as the SolGain 2.0 model (theory in Section 3.2). Input parameters for both the SolGain 2.0 and TRNSYS simulations are contained below in Table 6.3. Water was used as the heat transfer fluid (HTF) and so the specific heat value c_p contained in Table 6.3 is approximately that of water at room temperature. The incidence angle modifier (IAM) references used for both simulations are contained in Table 6.4.

Table 6.3: Input data for FPC testing

Term	Value	Unit	Description
A_{col}	3.85	m ²	Aperture area
c_p	4190	J/(kg K)	HTF specific heat
η_0	0.811	-	Intercept efficiency
c_1	2.71	W/(m ² K)	First order heat loss coefficient
c_2	0.01	W/(m ² K ²)	Second order heat loss coefficient
K_d	0.912	-	IAM for diffuse irradiance
c_{eff}	7.05	kJ/(m ² K)	Effective collector heat capacity
\dot{M}_{col}	250	kg/h	Mass flow rate through collector
$T_{col,in}$	15	°C	Collector inlet temperature

Table 6.4: IAM references for FPC testing

θ_{ref}	50°	85°
$K_b(\theta_{ref})$	0.96	0.05

Results of the FPC test indicate that SolGain 2.0's FPC model is quite similar to TRNSYS's model. A graphical representation of both model's outlet temperatures $T_{col,out}$ for a clear day and an overcast day can be seen below in Figure 6.5. It can be seen that SolGain 2.0 tracks with TRNSYS closely except early in the morning and late at night. This could be due to differences in incidence angle modifier calculations in SolGain 2.0 and TRNSYS.

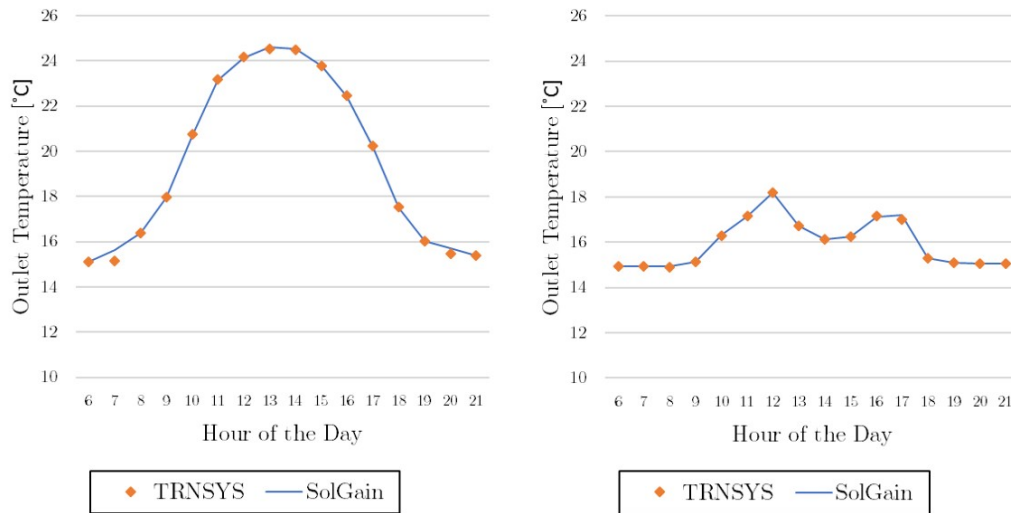


Figure 6.5: FPC outlet temperature ($T_{col,out}$) **Left:** 1 January (clear day) **Right:** 20 June (overcast day)

The maximum difference in $T_{col,out}$ for the whole year between SolGain 2.0 and TRNSYS is 0.60°C . Over a year simulation, SolGain 2.0's FPC model produces 10.69 kWh more heat than TRNSYS. This translates to 0.19% more heat per annum in SolGain 2.0.

6.3.2 Evacuated tube collector

The *Type71* collector was used in TRNSYS as a reference to validate SolGain 2.0's ETC model. The inputs for ETC testing are given in Table 6.5, while the IAM reference values can be seen in Table 6.6. Water was once again used as the HTF for simulations.

A graphical representation of the results from ETC testing for a clear day and an overcast day can be seen in Figure 6.6. It can be seen that the value of $T_{col,coll}$ in SolGain 2.0 is slightly less than TRNSYS before and after solar noon, but than equal at noon. This is most probably to do with differences in IAM calculations between SolGain 2.0 and TRNSYS.

Table 6.5: Input data for ETC testing

Term	Value	Unit	Description
A_{col}	3.00	m ²	Aperture area
c_p	4190	J/(kg K)	HTF specific heat
η_0	0.687	-	Intercept efficiency
c_1	0.613	W/(m ² K)	First order heat loss coefficient
c_2	0.003	W/(m ² K ²)	Second order heat loss coefficient
K_d	0.912	-	IAM for diffuse irradiance
c_{eff}	8.78	kJ/(m ² K)	Effective collector heat capacity
\dot{M}_{col}	250	kg/h	Mass flow rate through collector
$T_{col,in}$	15	°C	Collector inlet temperature

Table 6.6: IAM references for ETC testing

$\theta_{l,ref}$	10°	20°	30°	40°	60°	70°
$K(\theta_{l,ref}, 0)$	1.00	0.99	0.97	0.94	0.86	0.85
$\theta_{t,ref}$	10°	20°	30°	40°	60°	70°
$K(0, \theta_{t,ref})$	1.01	1.02	1.02	1.02	1.06	1.20

The maximum instantaneous error of $T_{col,out}$ for SolGain 2.0 is 0.46 °C. SolGain 2.0 produced 127.58 kWh less useful energy than TRNSYS over a year of simulation. This translates to 3.00% less energy per year compared to TRNSYS.

6.3.3 Parabolic trough collector

The *Type1245* was used in TRNSYS as it is the closest model to the parabolic trough collector (PTC) model provided by SolGain 2.0 (refer to Section 3.2 review the theory behind the SolGain 2.0 PTC model). The input data used for both TRNSYS and SolGain 2.0 simulations can be seen below in Table 6.7, while the IAM references can be seen in Table 6.8.

The results from two days of simulation (a clear day and an overcast day) are displayed below in Figure 6.7. It can be seen that SolGain 2.0 tracks fairly well with TRNSYS; SolGain 2.0 however does slightly underestimate collector performance around noon. The reason for this is unknown to the author. The deviation seems to be minimal though.

The maximum instantaneous difference between $T_{col,out}$ in SolGain 2.0 and TRNSYS is 1.04 °C. This may seem quite large, but the average instantaneous difference over the whole year is only 0.15 °C. For a whole year the difference in useful heat generated Q_{use} between SolGain 2.0 and TRNSYS is 341.92 kWh

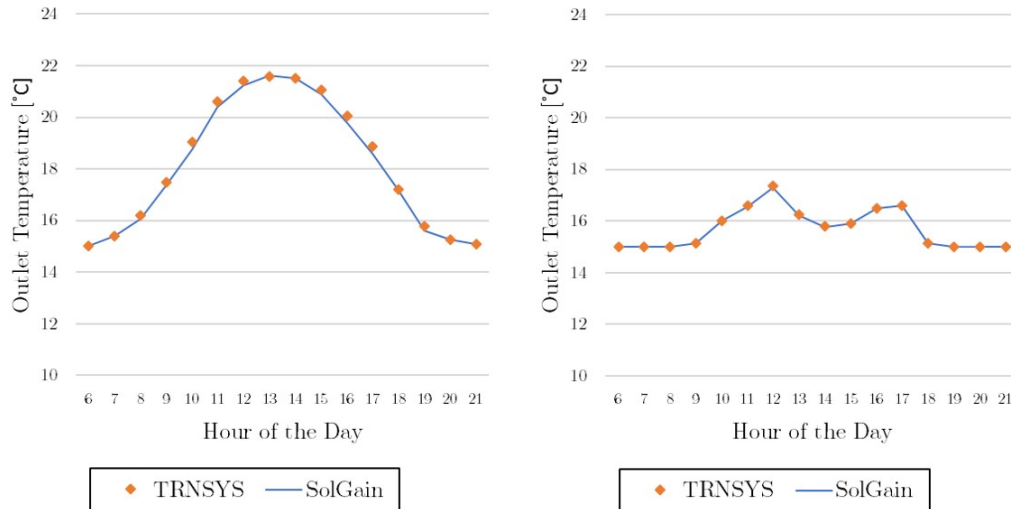


Figure 6.6: ETC outlet temperature ($T_{out,col}$) **Left:** 1 January (clear day) **Right:** 20 June (overcast day)

Table 6.7: Input data for PTC testing

Term	Value	Unit	Description
A_{col}	9.225	m ²	Aperture area
L_{col}	5.00	m	Aperture length
w_{col}	1.845	m	Aperture width
L_{fo}	0.65	m	Focal length
c_p	4190	J/(kg K)	HTF specific heat
η_0	0.6	-	Intercept efficiency
c_1	0.36	W/(m ² K)	First order heat loss coefficient
c_2	0.0011	W/(m ² K ²)	Second order heat loss coefficient
K_d	0.912	-	IAM for diffuse irradiance
c_{eff}	5.2249	kJ/(m ² K)	Effective collector heat capacity
\dot{M}_{col}	250	kg/h	Mass flow rate through collector
$T_{col,in}$	15	°C	Collector inlet temperature

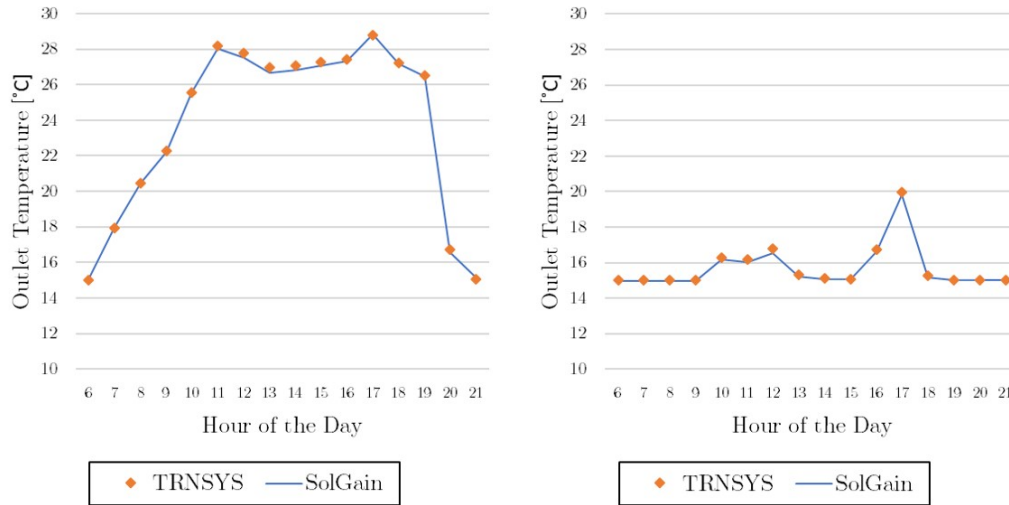
with SolGain 2.0 estimating less heat generation. This means the SolGain 2.0 PTC model estimates 3.30% less heat production than TRNSYS.

6.4 Pipes

Heat transfer losses between the collector field and storage tank are accounted for in SolGain 2.0 with a pipe model. The theory for this pipe model is discussed in Section 3.4.2.

Table 6.8: Input data for PTC testing.

$\theta_{l,ref}$	10°	20°	30°	40°	50°	60°	70°	80°
$K(\theta_{l,ref})$	0.99	0.99	0.98	0.96	0.93	0.88	0.75	0.46

**Figure 6.7:** PTC outlet temperature ($T_{out,col}$) **Left:** 1 January (clear day) **Right:** 20 June (overcast day)

In order to represent a solar process heat system accurately, simulations were run in TRNSYS using a system represented conceptually in Figure 6.8. Inlet temperatures $T_{col,out}$ in SolGain 2.0 were set equal to that of TRNSYS for each time step. The pipe model was tested by comparing the outlet temperatures $T_{HE,in,col}$ for TRNSYS and SolGain 2.0. The input data for both TRNSYS and SolGain 2.0 was set to the values contained in Table 6.9.

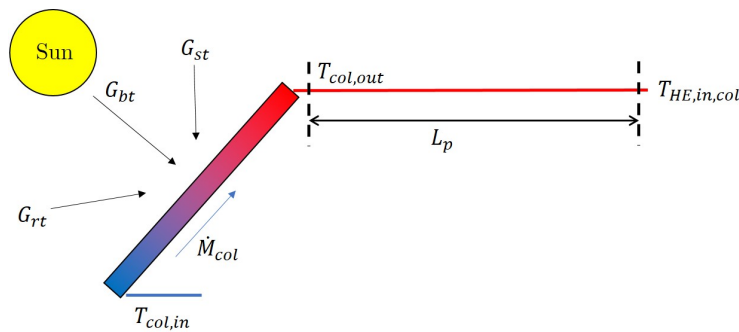
**Figure 6.8:** Schematic representation of the system modelled in TRNSYS for pipe tests

Table 6.9: Input data for Pipe testing

Term	Value	Unit	Description
L_p	20	m	Pipe length
d_p	0.01	m	Pipe diameter
c_p	4190	J/(kg K)	Heat transfer fluid specific heat
U_p	0.8	W/(m ² K)	Pipe heat loss coefficient
\dot{M}	250	kg/h	Mass flow rate through the pipe

Over a whole year of simulation the maximum instantaneous difference between TRNSYS and SolGain 2.0's pipe outlet temperature $T_{HE,in,col}$ was 0.083 °C. SolGain 2.0 estimated 0.018 kWh more heat loss Q_{loss} than TRNSYS over the year simulation. This is equivalent to a 0.088 % discrepancy per annum.

6.5 Heat Exchanger

The heat exchanger model was tested by running a simulation in TRNSYS using the system concept in Figure 6.9. The values for $T_{HE,in,col}$ and $T_{HE,in,tank}$ were inputted from TRNSYS into SolGain 2.0, so that a direct comparison could be made between TRNSYS and SolGain 2.0's heat exchanger model. The input parameters used for both simulations are contained in Table 6.10.

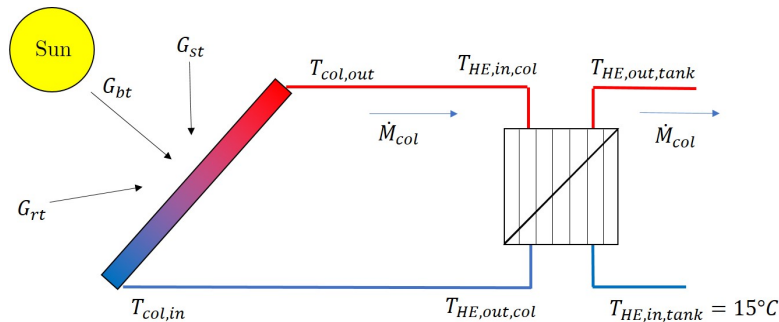


Figure 6.9: Schematic representation of the system modelled in TRNSYS for heat exchanger tests

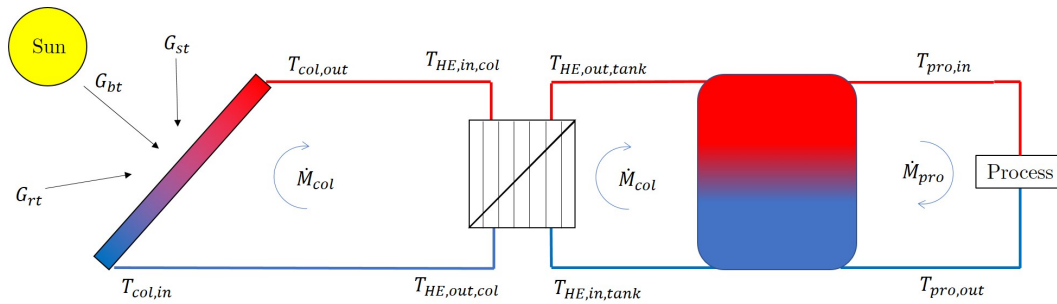
SolGain 2.0's heat exchanger proved highly accurate with an annual deviation in total energy transferred Q_{HE} of only 3.02×10^{-5} kWh from TRNSYS. This is a negligible difference i.e. less than 0.01 % of the total annual energy transferred.

Table 6.10: Input data for heat exchanger testing

Term	Value	Unit	Description
UA_{HE}	6500	W/K	Heat transfer factor of heat exchanger
\dot{M}_{col}	250	kg/h	Mass flow through the hot and cold side
$(c_p)_{col}$	4190	J/(kg K)	Specific heat on the hot side
$(c_p)_{pro}$	4190	J/(kg K)	Specific heat on the cold side
$T_{HE,in,tank}$	10	°C	Cold side inlet temperature

6.6 Thermal Energy Storage Tank

The storage tank model was tested against TRNSYS by using the system concept in Figure 6.10. The input parameters used for both TRNSYS and SolGain 2.0 are contained in Table 6.11. The values for $T_{HE,out,tank}$ were inputted directly from TRNSYS into SolGain 2.0 for each time step to ensure that all inputs to the tank models in TRNSYS and SolGain 2.0 were equal.

**Figure 6.10:** Schematic representation of the system modelled in TRNSYS for storage tank tests**Table 6.11:** Input data for thermal storage tank testing

Term	Value	Unit	Description
V_{tank}	5	m ³	Volume of storage tank
c_p	4190	J/(kg K)	Specific heat of HTF
U_{tank}	0.5	W/(m ² K)	Heat loss coefficient of tank
N_{nodes}	12	-	Number of nodes used for tank model
\dot{M}_{pro}	40	kg/h	Mass flow rate to the process
\dot{M}_{col}	90	kg/h	Mass flow rate from the collector side
$T_{pro,out}$	15	°C	Process outlet temperature
T'_a	20	°C	Ambient temperature at tank

To graphically display the results of the tank model, the 5th of March was randomly selected as a case study. Results for the temperatures of selected nodes on the 5th of March can be seen in Figure 6.11. The results indicate that SolGain 2.0 tracks fairly accurately with TRNSYS. SolGain 2.0's node temperatures seem to be slightly ahead of those of TRNSYS.

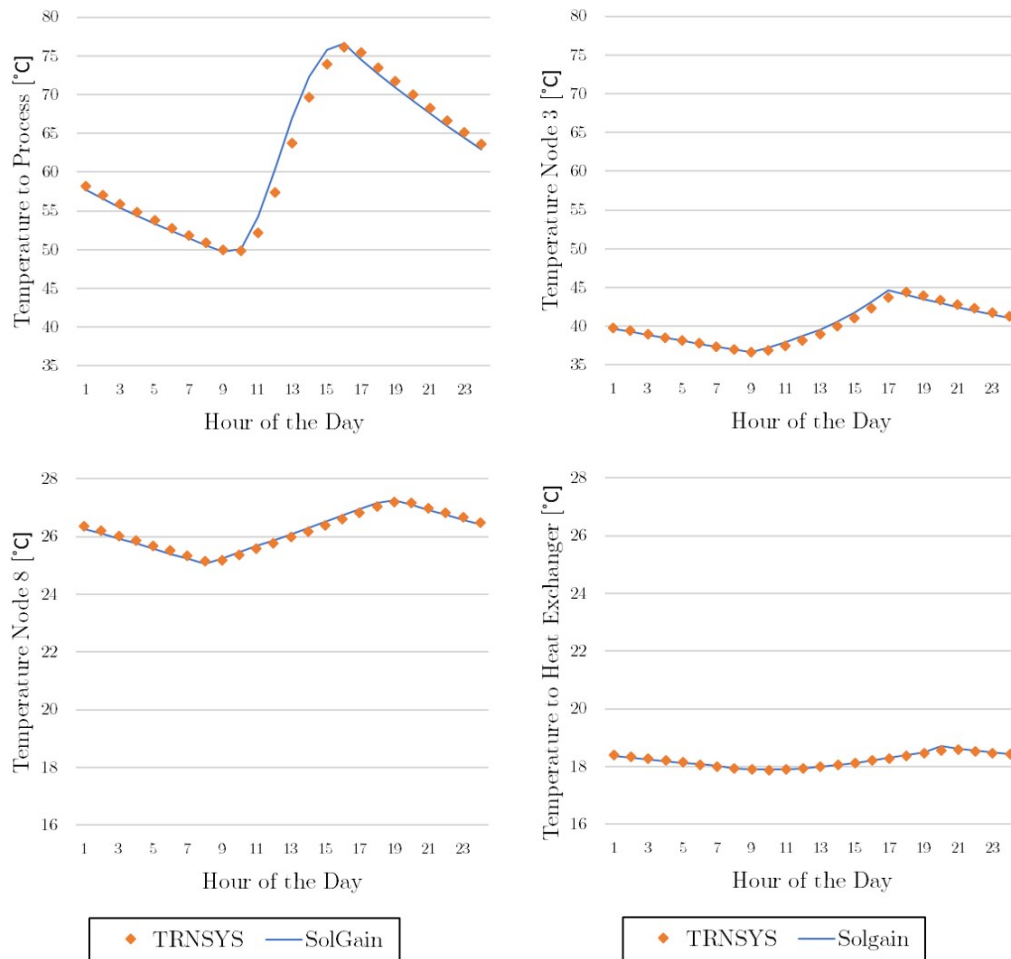


Figure 6.11: Tank model node temperatures on the 5th of March **Top left:** node one (i.e. $T_{pro,in}$) **Top right:** node three **Bottom left:** node eight **Bottom right:** node twelve (i.e. $T_{HE,tank,in}$)

Over a year of simulation TRNSYS supplied 14801.82 kWh of heat to the process and SolGain 2.0 14809.95 kWh. This means that SolGain 2.0 supplied 0.055% more energy than TRNSYS. This value seems to indicate that SolGain 2.0's tank model is fairly accurate.

6.7 Chapter Conclusion

The chapter documents the result of component testing of SolGain 2.0. TRNSYS was used as a reference to compare SolGain 2.0 to. The tests indicate that all of SolGain 2.0's components operate within a 5% margin of TRNSYS. This can be considered satisfactory for the purpose of SolGain 2.0. The components that were recoded for SolGain 2.0 are either more accurate than or as accurate as SolGain 1.0.

Chapter 7

System Validation

This chapter focuses on the validation of solar process heat (SPH) systems in SolGain 2.0. Two system tests were done; one with non-tracking, non-concentrating collector and one with tracking, concentrating collectors. Yearly simulations were run in TRNSYS and SolGain 2.0 to compare outputs. Heat supplied to the process is the main output investigated in this chapter as it is the most important to a user of SolGain 2.0. Points in the system that were identified as sources of inaccuracy are also investigated in this chapter.

Simulations were run using Cape Town, South Africa as a case study. The weather data is from the TRNSYS Meteororm database.

7.1 System with Non-concentrating Collectors

The SPH system that was implemented in SolGain 2.0 and in TRNSYS is conceptually displayed in Figure 7.1. Due to the evacuated tube collector (ETC) model providing the highest error of the non-concentrating collectors in component validation it was decided to implement an ETC for system validation.

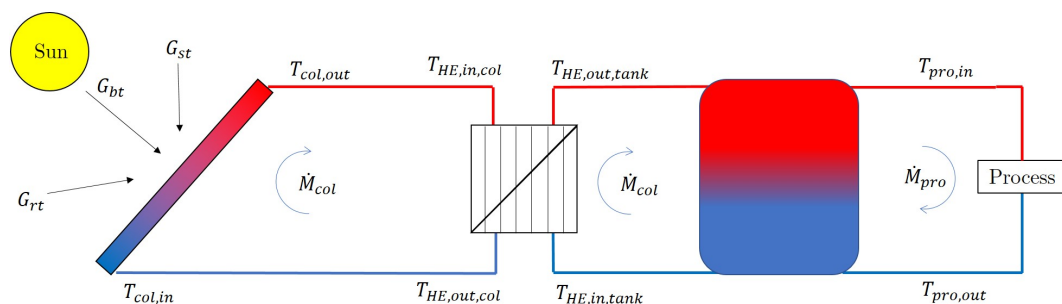


Figure 7.1: Schematic representation of the system modelled in TRNSYS for pipe tests

The input data for simulations run in both TRNSYS and SolGain 2.0 is contained in Table 7.1. Additionally the ETC was modelled using the same collector characterization data used in component validation (contained in Table 6.5 and 6.6). In order to test whether SolGain 2.0 can effectively model collectors in series, two collectors were modelled in series.

Table 7.1: Input data for system with non-concentrating collectors testing

Term	Value	Unit	Description
ϕ	-33.96	degree	Latitude
ψ	18.6	degree	Longitude
β	33	degree	Collector tilt
γ	0	degree	Collector azimuth (0=North; 180=South)
N_{ser}	2	-	Number of collectors in series
N_{par}	1	-	Number of collector flow loops in parallel
$c_{p,col}$	4190	J/(kg K)	Specific heat of collector loop HTF
\dot{M}_{col}	90	kg/h	Mass flow rate in the collector loop
L_p	10	meter	Pipe length
d_p	0.02	meter	Pipe diameter
U_p	0.8	W/(m ² K)	Pipe heat loss coefficient
UA_{HE}	6500	W/K	Heat transfer factor of heat exchanger
$c_{p,pro}$	4190	J/(kg K)	Specific heat of process loop HTF
V_{tank}	5	m ³	Volume of storage tank
U_{tank}	0.5	W/(m ² K)	Heat loss coefficient of tank
N_{nodes}	12	-	Number of nodes used for tank model
$T_{pro,out}$	20	°C	Process return temperature
\dot{M}_{pro}	40	kg/h	Mass flow rate to the process
T'_a	20	°C	Ambient temperature at tank

Monthly heat supplied to the process for both TRNSYS and SolGain 2.0 can be seen in Figure 7.2. The graph indicates that for each month of the year, SolGain 2.0 provided less heat to the process than TRNSYS.

The total energy provided to the process by SolGain 2.0 was 7424.42 kWh as opposed to 7784.47 kWh by TRNSYS. This is an annual discrepancy of 4.63% less heat to the process in SolGain 2.0. The reason for this error is suspected to be the ETC model in SolGain 2.0 which provided less solar gains than TRNSYS in component validation.

SolGain 2.0's ETC provided 8043.96 kWh of useful energy Q_{use} over the whole year, while TRNSYS provided 8455.08 kWh. This seems to confirm that the discrepancy in heat provided to the process is due to SolGain 2.0's ETC model.

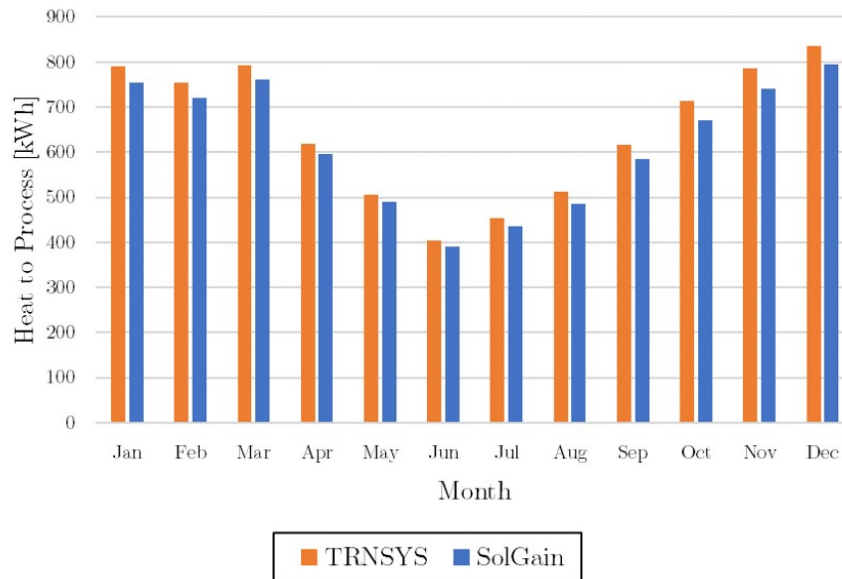


Figure 7.2: Monthly heat supplied to the process by a non-concentrating collector system for TRNSYS and SolGain 2.0

It should be noted that modelling collectors in series accentuates the difference between SolGain 2.0 and TRNSYS.

The error in energy supplied to the process is fairly low (less than 10%) and SolGain 2.0 underestimates heat supplied compared to TRNSYS.

7.2 System with Concentrating Collectors

The system concept implemented to validate simulations with tracking concentrating collectors was exactly the same as for non-concentrating collectors (refer to Figure 7.1) with the only difference being the collector type implemented. The collector that was used for validation is a parabolic trough collector (PTC) as this is the only concentrating collector implemented in SolGain 2.0. The PTC modelled is exactly the same as the one used in component validation and is characterised by the values contained in Table 6.7 and Table 7.2.

The input data used for simulations in both SolGain 2.0 and TRNSYS is the same as that used in Table 7.1 above, with the exceptions contained in Table 7.2 below.

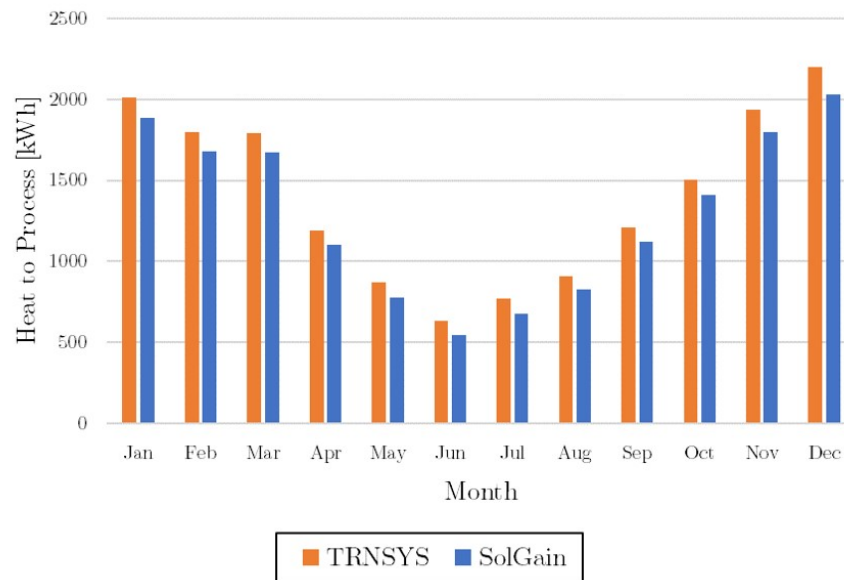
Due to temperatures of above boiling point of water present in the system with concentrating collectors, *Therminol 66* was used as the HTF. *Therminol 66* is an HTF that is commonly used in process heat systems. The properties sheet for *Therminol 66* can be found in Appendix C.

Table 7.2: Changes made to input data contained in Table 7.1 for system validation with concentrating collectors

Term	Value	Unit	Description
β	0	degree	Collector tilt
$c_{p,col}$	1873	J/(kg K)	Specific heat of collector loop HTF
M_{col}	180	kg/h	Mass flow rate in the collector loop
$c_{p,pro}$	1873	J/(kg K)	Specific heat of process loop HTF

The specific heats of both the collector loop HTF $c_{p,col}$ and the process loop HTF $c_{p,pro}$ are affected by the change in HTF. These were both set to a value of 1873 J/(kg K), which correlates the the specific heat of *Therminol 66* at 110 °C (the approximate operation temperature of the system).

The monthly results for heat supplied to the process are contained in Figure 7.3. The results indicate that SolGain 2.0 supplied less energy to the process than TRNSYS for every month of the year.

**Figure 7.3:** Monthly heat supplied to the process by a concentrating collector for TRNSYS and SolGain 2.0

The annual energy supplied to the process by SolGain 2.0 was 15 534.16 kWh. TRNSYS on the other hand supplied 16 824.09 kWh to the process. This means that SolGain 2.0 provided 7.67% less energy than TRNSYS. This error was once again suspected to be due to differing collector models in SolGain 2.0 and TRNSYS.

SolGain 2.0's PTC provided 36 195.78 kW h of useful energy Q_{use} , while TRNSYS's PTC provided 40 518.80 kW h. This translates to SolGain 2.0 providing 10.67% less collector gains than TRNSYS. This confirms that the error in annual energy provided to the process in SolGain 2.0 is most probably due to the PTC model. Once again it is important to note that collectors in series will accentuate the difference in collector performance of SolGain 2.0 and TRNSYS.

The difference between energy supplied to the process in SolGain 2.0 and TRNSYS is fairly low (less than 10%) with SolGain 2.0 underestimating energy to the process compared to TRNSYS.

7.3 Chapter Conclusion

System validation was reviewed in this chapter. SolGain 2.0 was tested against TRNSYS as a benchmark. A system with non-concentrating collectors and a system with concentrating collectors were tested. Both systems provide accuracy values of within 10% compared to TRNSYS, with the collector model rendering the highest source of error.

Chapter 8

Conclusion and Recommendations

This chapter aims to bring all of the content of this thesis to closure. This entails outlining the work that was completed during this project and its relevance. Recommendations are finally given to conclude.

8.1 Conclusion

The main purpose of this project was to develop SolGain to a state where it is ready for release on the Solar Thermal Research Group (STERG) web page. This included improving SolGain's functionality, accuracy and user-friendliness. Chapter 5 outlines the changes that were made in all of these areas to SolGain 2.0. Changes to SolGain include recoding SolGain to be more modular, improved user control and friendliness, and development of system analysis tools.

The accuracy of SolGain 2.0 is confirmed by component validation in Chapter 6. All component models in SolGain 2.0 provided accuracy of within 5% of TRNSYS (an industry trusted simulation package). The system validation in Chapter 7 provided an overall system error of less than 10% when compared to TRNSYS.

SolGain 2.0 is a pre-assessment simulation package package for solar process heat (SPH) systems. It can be used by system designer, end-user and investors of SPH systems to gauge the performance of such a system.

8.2 Recommendations

The main inaccuracies when compared to TRNSYS in SolGain 2.0 stem from the collector model. The flat plate (FPC) model was very accurate (i.e. 0.19% error per annum), but the evacuated tube (ETC) and parabolic trough (PTC)

collector models were not as accurate. The ETC and PTC both underestimate heat generation. It is suspected by the author that this is due to the incidence angle modifier calculations. More collector types could also be introduced to SolGain.

A better method for determining the system size could be implemented if the user selects automatic collector selection. The current procedure of using the available space, as described in Section 5.7.2, is a coarse way of doing this and could be improved.

Complete comparison of SolGain 2.0 to another software, including system controls and system performance measurements (including financial performance) is recommended. Simulations could be run alongside Polysun to determine solar fractions and system efficiencies of different system sizes. The financial parameters from Polysun could also be compared to SolGain 2.0. To take this a step further, SolGain 2.0 results could be compared to data from an existing solar process heat installation.

Carbon savings is a parameter that is becoming more and more applicable in renewable energy investments. It could be useful for SolGain to calculate carbon savings of an SPH system.

The final recommendation is that industry experts in SPH could review the simulation package and make recommendations. This could be useful regarding the user interface, parameter assumptions and system performance representation.

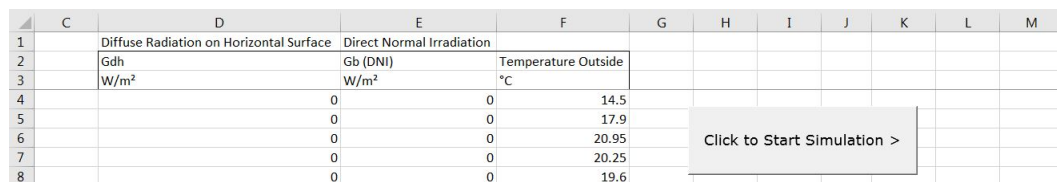
Appendices

Appendix A

Userforms and Parameter Assumptions

This appendix aims at describing in detail the flow of userforms for user inputs before a simulation is run. SolGain 2.0, makes various assumptions as the user goes along depending on the user's inputs. These assumptions are also discussed in this section providing rationale behind each assumption. The flow of userforms is contained in Figure 5.1. The reader is referred to this figure before reading the rest of this appendix.

User input is initiated by the user by clicking on a button in the *Weather Data* spreadsheet. This is displayed in Figure A.1. If the user has not yet inputted hourly weather data for the whole year, the user will be prompted with an error message to do so before continuing. Weather data for the whole year consists of 8760 data points for diffuse horizontal irradiance G_{dh} , direct normal irradiance G_b and ambient temperature T_a .



	C	D	E	F	G	H	I	J	K	L	M
1		Diffuse Radiation on Horizontal Surface	Direct Normal Irradiation								
2		Gdh	Gb (DNI)	Temperature Outside							
3		W/m ²	W/m ²	°C							
4		0	0	14.5							
5			0	0	17.9						
6			0	0	20.95						
7			0	0	20.25						
8			0	0	19.6						

Figure A.1: A screen-shot of the *Weather Data* spreadsheet in SolGain 2.0

Each of the userforms will now be sequentially described, explaining assumptions made depending on the user's inputs.

A.1 Geographical Inputs Userform

The *Geographical Inputs* userform is displayed below in Figure A.2. The user must input values for *Latitude*, *Longitude* and *Time Zone*. *Location* is an optional input. The values for *Latitude* and *Longitude* are inputted into a text box and queried by the code when the user clicks *Next* to ensure they are valid. The rest of inputs are done using combo boxes, so that only valid inputs may be selected. Once the user clicks *Next* and all inputs are valid, the *Process Information* userform opens.

Figure A.2: A screen-shot of the *Geographical Inputs* userform in SolGain 2.0

A.2 Process Information Userform

The *Process Information* userform is displayed below in Figure A.3. The user must input values for *Process Feed Temperature* $T_{pro,in}$, *Process Return Temperature* $T_{pro,out}$, *Max Mass Flow of Process Medium* $M_{pro,max}$ and *Heat Capacity of Process Medium* $c_{p,pro}$ via text boxes. These values are queried by the code to check whether they are valid. If the user chooses not to enter a value for *Heat Capacity of Process Medium*, SolGain 2.0 assumes a value of 4.18 kJ/(kg K) (roughly the heat capacity of water at room temperature).

Figure A.3: A screen-shot of the *Process Information* userform in SolGain 2.0

SolGain 2.0 calculates the maximum heat demand of the process $\dot{Q}_{need,max}$ using:

$$\dot{Q}_{need,max} = \dot{M}_{pro,max} c_{p,pro} (T_{pro,in} - T_{pro,out}) \quad (A.1)$$

If all inputs are valid and the user clicks *next* the *Daily Demand* userform opens.

A.3 Daily, Weekly and Monthly Demand Userforms

The purpose of these three userforms is to establish a user demand profile. The *Weekly Demand* userform is used as an example in Figure A.4 to illustrate how the user defines a demand profile. The user must input values for *Percent of Max Demand* for each hour of the day x_{hour} , each day of the week x_{day} and each week of the year x_{week} .

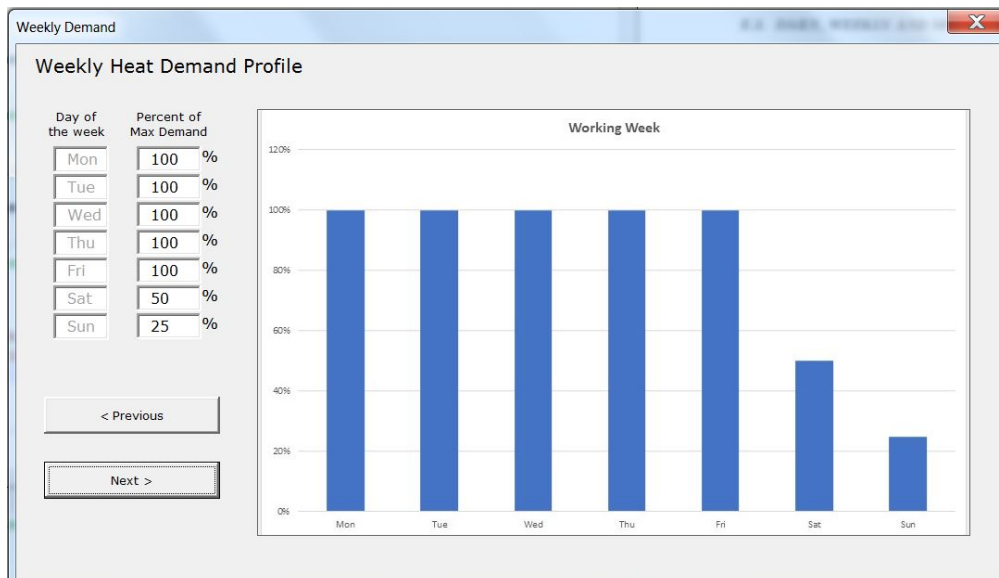


Figure A.4: A screen-shot of the *Weekly Demand* userform in SolGain 2.0

In Figure A.4, it can be seen that the user has inputted a value of 100 % for all week days, 50 % for Saturdays and 25 % for Sundays. The heat demand \dot{Q}_{need} for any hour of the year is calculated using:

$$\dot{Q}_{need} = \dot{Q}_{need,max}(x_{hour} x_{day} x_{week}) \quad (A.2)$$

Once the user has filled in all the *Demand* userforms, the *First Collector Input* userform is opened.

A.4 First Collector Input Userform

The *First Collector Input* userform is used to allow the user to make a decision whether they would like to input the collector efficiency parameters (described in Section 3.2) or whether SolGain 2.0 should assume them. This is done by clicking on the option button in Figure A.5 of the user's choice.

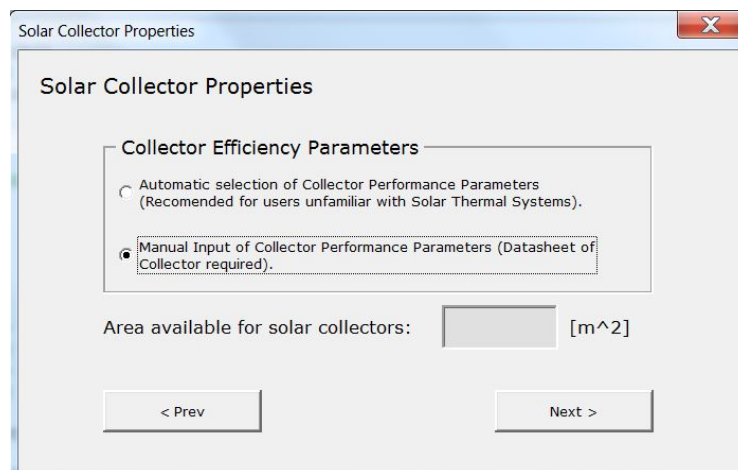


Figure A.5: A screen-shot of the *First Collector Input* userform in SolGain 2.0

If the user selects the ***Automatic Selection of Collector Performance Parameters*** option button, the *Area available for solar collectors* text box will become enabled. The user then inputs the available space. The number of solar collectors used in simulations will be based on this value. If the user then clicks *next*, the *Miscellaneous Inputs* user form will open after SolGain 2.0 has made decisions regarding the solar field.

SolGain 2.0 will determine the collector type used based on the previously entered process inlet temperature $T_{pro,in}$. For $T_{pro,in} \leq 80^\circ\text{C}$ SolGain 2.0 selects a flat plate collector (FPC). For temperatures of $80^\circ\text{C} < T_{pro,in} \leq 110^\circ\text{C}$, SolGain 2.0 selects an evacuated tube collector (ETC). Finally for temperatures of $T_{pro,in} > 110^\circ\text{C}$, SolGain 2.0 selects a parabolic trough collector (PTC). The collector parameters for all three collector types are assumed to be that of the collectors contained in Appendix D.

SolGain 2.0 also assumes the collector azimuth γ and tilt β for *Automatic Selection of Collector Performance Parameters* option. For FPCs and ETCs the tilt is set to the latitude angle i.e. $\beta = |\phi|$. For PTCs the tilt is set to zero.

The collector azimuth is set towards the equator for all collector types i.e. $\gamma = 0^\circ$ in the southern hemisphere and $\gamma = 180^\circ$ in the northern hemisphere. These assumptions are based on general rule-of-thumb approaches to solar thermal system design.

On the other hand, if the user selects the *Manual Input of Collector Performance Parameters* once the user clicks *next* a userform, *Manual Collector Inputs*, will be opened for the user to input performance parameters. The user will also be required to specify the system size and layout in later userforms.

A.5 Manual Collector Inputs Userform

The *Manual Collector Inputs* userform displayed in Figure A.6 allows the user to manually enter collector properties. The user must first select a collector type: FPC, ETC or PTC. The user will then be required to input all the parameters contained in Figure A.6. The *Incidence Angle Modifier References* tables at the bottom will enable text boxes based on the *Number of References* selected by the user. All inputs are queried once the user clicks *next* the *Collector Tilt and Azimuth* userform is opened.

Figure A.6: A screen-shot of the *Manual Collector Inputs* userform in SolGain 2.0

A.6 Collector Tilt and Azimuth Userform

There are three *Collector Tilt and Azimuth* userforms for each of the three collector types that can be modelled in SolGain 2.0. Figure A.7 displays a screen-shot of the ETC userform. The FPC userform is identical except without the *Tube Configuration* visual and combo box on the right. The PTC userform is displayed in Figure A.8. Different pictures were used in this userform to clearly depict collector tilt and azimuth of a PTC to the user.

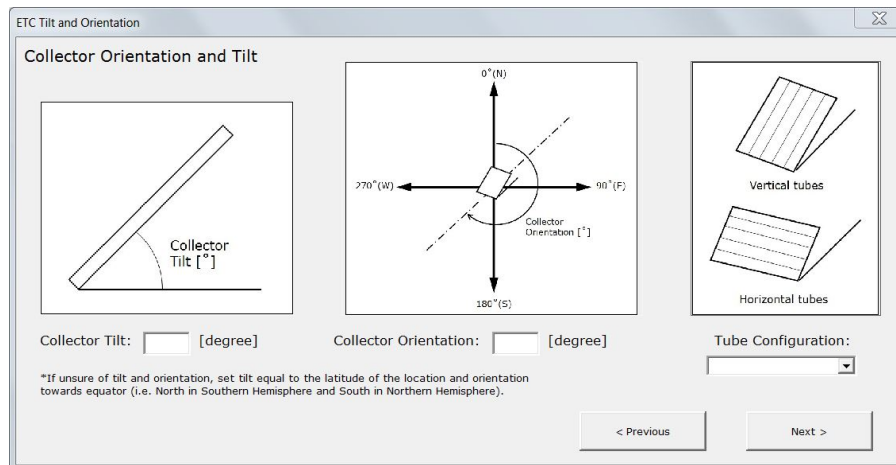


Figure A.7: A screen-shot of the *Evacuated Tube Collector Tilt and Azimuth* userform in SolGain 2.0

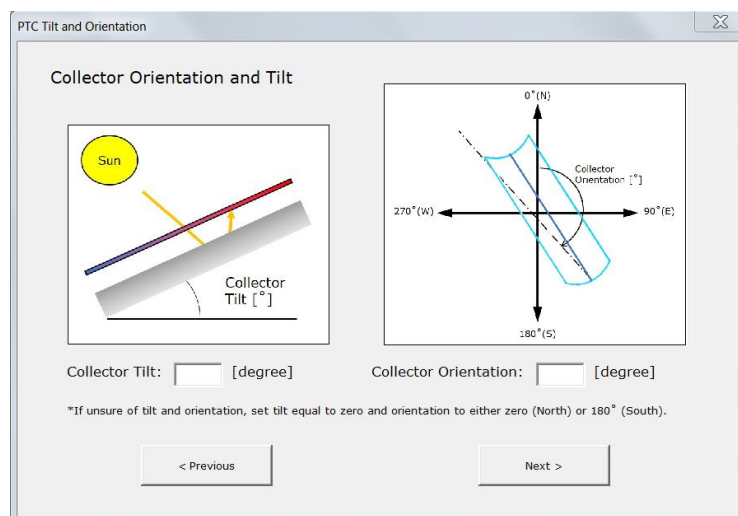


Figure A.8: A screen-shot of the *Parabolic Trough Collector Tilt and Azimuth* userform in SolGain 2.0

The angles inputted by the user are queried by the code once the user clicks *Next*. If the inputs are all valid the *Collector Field Layout* userform will open.

A.7 Collector Field Layout Userform

There are two *Collector Field Layout* userforms, one for non-concentrating collector fields and one for concentrating collector field. More specifications are required for concentrating than non-concentrating collectors so that end losses, as described in Section 3.2, can be calculated.

The *Collector Field Layout* user form for concentrating collectors is displayed below in Figure A.9. The non-concentrating version of this form only requires the user to input the *Number of Collectors in Series* and *Number of Modules in Parallel*. Once the user clicks *Next*, the user inputs are queried to make sure they are not nonsensical i.e. negative values, a decimal input when it should be an integer, etc. If they are indeed not nonsensical the *Miscellaneous System Inputs* userform is opened.

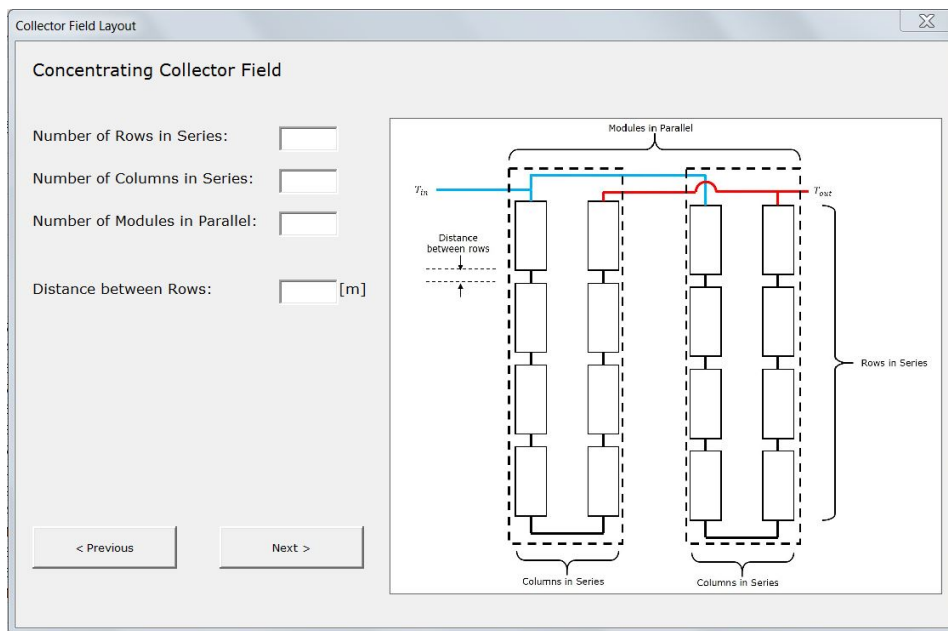


Figure A.9: A screen-shot of the *Concentrating Collector Field Layout* userform in SolGain 2.0

A.8 Miscellaneous System Inputs Userform

The *Miscellaneous System Inputs* userform is the last userform and can be seen in Figure A.10. The user can choose to input values or leave the values on

their default. The default value will be based on assumptions that SolGain 2.0 makes using rule-of-thumb approaches.

The screenshot shows the 'Miscellaneous System Inputs' userform. At the top, there is a diagram illustrating the system components: Sun, Collector, Pipe, Heat Exchanger, Heat Storage, and Process. The diagram labels 'Distance between Collector and Heat Exchanger', 'Pipe Heat Losses', 'Pipe Diameter', 'Heat Exchanger', 'Storage Heat Losses', and 'Process'. Below the diagram, there is a note: '*If unsure of a value, leave the default value.' The input fields are as follows:

Heat Storage:	Yes	Pipe Heat Loss Coefficient:	0.8	W/(m ² *K)
Heat Storage Volume:	10	Pipe Diameter:	0.1	m
Heat Storage Heat Loss Coefficient:	0.5	Distance between Collector (outside) and Heat Exchanger (inside):	10	m
Heat Exchanger UA:	6500			

Buttons for '< Previous' and 'Next >' are located at the bottom right of the form.

Figure A.10: A screen-shot of the *Miscellaneous System Inputs* userform in SolGain 2.0

The first assumption that SolGain 2.0 can make is the default value for **Heat Storage Volume**. SolGain 2.0 will assume there is a storage tank and will size the tank according to the guidelines set out by the AEE - Institute for Sustainable Technologies (2009a). These guidelines advise a storage volume size of between 0.8 and 1.2 times the daily process demand volume. Storage volume is thus calculated using:

$$V_{tank} = 1.2(V_{pro,day}) = 1.2 \left(\Delta t_{day} \frac{\dot{M}_{pro}}{\rho_{pro}} \right) \quad (A.3)$$

After the volume of the tank is known, the tank height h_{tank} and diameter d_{tank} are selected by SolGain 2.0 so that the surface area of the tank is minimized. This occurs when (Ilchmann, 2016):

$$\frac{d_{tank}}{h_{tank}} = 1 \quad (A.4)$$

And the volume of a cylinder is given by:

$$V_{tank} = \frac{\pi}{4} d_{tank}^2 h_{tank} \quad (\text{A.5})$$

From Equations A.4 and A.5 the diameter and height of the tank can be determined:

$$d_{tank} = h_{tank} = \sqrt[3]{\frac{4V_{tank}}{\pi}} \quad (\text{A.6})$$

The second default value that SolGain 2.0 can assume is the **Heat Storage Heat Loss Coefficient**. This value is assumed to be $0.3 \text{ W}/(\text{m}^2 \text{ K})$, which is roughly what the heat loss coefficient would be for 100 mm of polyurethane foam (Vela Solaris, 2017).

The third default value that can be assumed by SolGain 2.0 is the **Heat Exchanger UA**. U_{HE} is the heat transfer coefficient and A_{HE} is the surface area of the heat exchanger. SolGain 2.0 assumes the value of U_{HE} to be $500 \text{ W}/(\text{m}^2 \text{ K})$, in line with the specification for heat exchangers in a solar thermal system given by AEE - Institute for Sustainable Technologies (2009a). The value of A_{HE} is also assumed to be in line with these specifications which advise (AEE - Institute for Sustainable Technologies, 2009a):

$$A_{HE} = 0.2 \cdot A_{col,tot} \quad (\text{A.7})$$

Where $A_{col,tot}$ is the total collector aperture area of the collector field.

The fourth assumption made by SolGain 2.0 is the default value for **Pipe Heat Loss Coefficient**. This value is assumed to be equal to $0.8 \text{ W K}/\text{m}^2$, which is roughly the insulation that 37.5 mm of polyurethane foam would provide (Vela Solaris, 2017).

The fifth and second last default value assumption made by SolGain 2.0 is for the **Pipe diameter**. SolGain 2.0 assumes this value to be in line with the empirical specification made by Regulus (2007):

$$d_p = \sqrt{0.35 \dot{V}_{col}} \quad [\text{mm}] \quad (\text{A.8})$$

Where \dot{V}_{col} is the volumetric flow rate through the collector in l/h. \dot{V}_{col} can be determined from the mass flow rate through the collector \dot{M}_{col} and the density of the heat transfer fluid through the collector loop ρ_{col} . For the calculation of pipe diameter using Equation A.8, it is assumed that the specific mass flow

through the collector loop $\dot{m}_{col} = 18 \text{ kg}/(\text{m}^2 \text{ h})$. This is the value used for *preheating* strategy as described in Section 5.5.

The final assumption made by SolGain 2.0 as a default value is the ***Distance between Collector (outside) and Heat Exchanger (inside)***. This value is assumed to be 10 m.

Once the user clicks *Next* and if all the values inputted into the *Miscellaneous System Inputs* userform are valid, the *Financial Inputs Userform* is opened up.

A.9 Financial Inputs Userform

The *Financial Inputs* userform is used to gather information so that the system performance parameters discussed in Section 3.6 can be determined. The userform is displayed in Figure A.11. The user needs to enter values for *Price of Auxiliary Heat*, *Price Increase* rate (of auxiliary heat), *Discount Rate* and *Exchange Rate*. The *Price of Auxiliary Heat* is the cost of heat from a non-solar source.

The screenshot shows a software window titled "Financial Inputs". Inside the window, there are four input fields arranged in two rows. The first row contains "Price of Auxiliary Heat: R [] /kWh" and "Price Increase: [] %/annum". The second row contains "Discount Rate: [] %" and "Exchange Rate: [] ZAR/EUR". To the right of the input fields, there are two buttons: "< Previous" and "Run Simulation".

Figure A.11: A screen-shot of the *Financial Inputs* userform in SolGain 2.0

Once the user clicks *Run Simulation*, the software queries user inputs. If the all inputs are valid, the simulation is fully set up and starts running. Before this appendix is concluded, another important assumption must be addressed, namely the heat transfer fluid in the collector loop.

A.10 Heat Transfer Fluid in the Collector Loop

The selection of heat transfer fluid (HTF) in the collector loop is based on the weather data provided by the user as well as the collector type. For concentrating collectors the HTF used will always be *Therminol 66*. This is due to the high operating temperatures present in concentrating collector systems. The properties of *Therminol 66* are contained in Appendix C.

If a non-concentrating collector is used, the HTF in the collector loop will either be water or a mixture of glycol and water. A higher water content is preferable due to its higher specific heat capacity. The HTF will be selected so that freezing will not occur in the collector loop. This is done by selecting a mixture from Table C.1 with a freezing point that is below the the lowest ambient temperature contained in the weather data. The properties of glycol and water are contained in Appendix C.

Appendix B

SolGain 2.0 Program Structure

This appendix will focus on the SolGain 2.0 code. The flow structure that a year simulation follows in SolGain 2.0 is displayed in Figure B.1 on the following page.

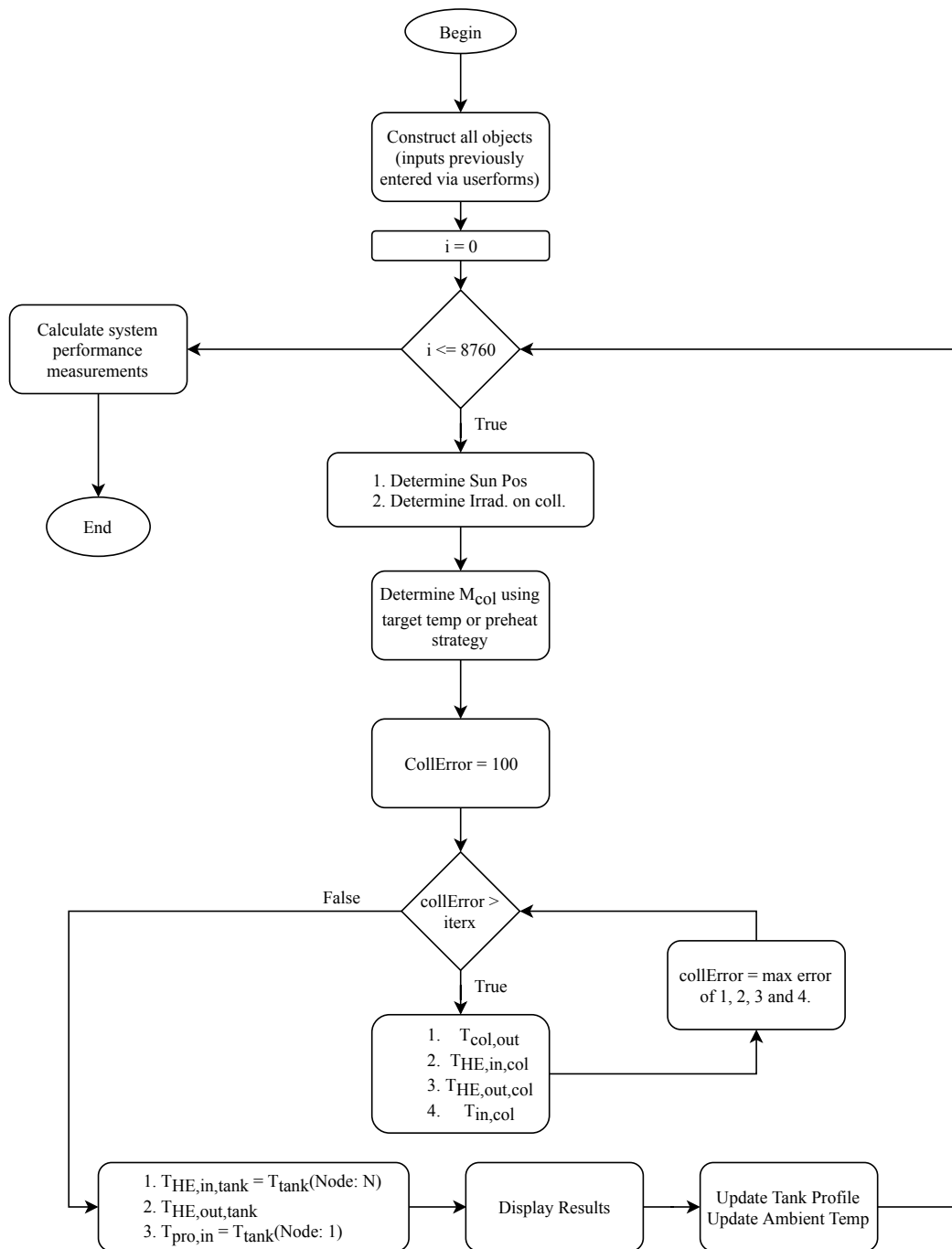


Figure B.1: Flow structure of a year simulation in SolGain 2.0

Appendix C

Heat Transfer Fluids Properties

There are three heat transfer fluids (HTFs) that are used by SolGain 2.0, namely water, glycol and *Therminol 66*. This appendix will focus on the fluid properties of the HTFs. Firstly water and glycol will be addressed and then *Therminol 66*.

C.1 Water and Glycol

The non-concentrating collectors in SolGain 2.0 use either water or a mixture of water and glycol as an HTF. The ratio of water to glycol is based on the freezing point of the HTF to ensure that freezing does not occur in the collector loop. The freezing points of various glycol-water mixtures is contained in Table C.1 below.

Table C.1: Glycol and water mixtures and their freezing points (Alvarez, 2010)

Freezing point	Volume % water	Volume % glycol
0 °C	100 %	0 %
-10.6 °C	80 %	20 %
-19.3 °C	70 %	30 %
-27.8 °C	60 %	40 %
-30 °C	58 %	42 %
-45 °C	50 %	50 %

The densities of glycol and water are roughly the same at room temperature i.e. $\rho_{water} \approx \rho_{glycol} \approx 1000 \text{ kg/m}^3$ (Alvarez, 2010). For this reason, the heat capacities of mixtures of glycol and water can be calculated using:

$$c_p = x_{water} c_{p,water} + (1 - x_{water}) c_{p,glycol} \quad (\text{C.1})$$

Where x_{water} is the volume percentage of water in the mix. The values for the heat capacities are assumed to be at room temperature in SolGain 2.0, which corresponds to values of $c_{p,water} = 4180 \text{ J}/(\text{kg K})$ and $c_{p,glycol} = 2500 \text{ J}/(\text{kg K})$.

C.2 Therminol 66

The properties of *Therminol 66* can be found in the datasheet below.

Therminol 66

Properties of Therminol®66 vs Temperatures

Temperature °C	Density kg/m ³	Thermal Conductivity W/m.K	Heat Capacity kJ/kg.K	Viscosity		Vapour pressure (absolute) kPa*
				Dynamic mPa.s	Kinematic mm ² /s**	
0	1021.5	0.118	1.495	1324.87	1297.01	-
10	1014.9	0.118	1.529	344.26	339.20	-
20	1008.4	0.118	1.562	123.47	122.45	-
30	1001.8	0.117	1.596	55.60	55.51	-
40	995.2	0.117	1.630	29.50	29.64	-
50	988.6	0.116	1.665	17.64	17.84	-
60	981.9	0.116	1.699	11.53	11.74	-
70	975.2	0.115	1.733	8.06	8.26	0.01
80	968.5	0.115	1.768	5.93	6.12	0.02
90	961.8	0.114	1.803	4.55	4.73	0.03
100	955.0	0.114	1.837	3.60	3.77	0.05
110	948.2	0.113	1.873	2.92	3.08	0.08
120	941.4	0.112	1.908	2.42	2.58	0.12
130	934.5	0.111	1.943	2.05	2.19	0.18
140	927.6	0.111	1.978	1.75	1.89	0.27
150	920.6	0.110	2.014	1.52	1.65	0.40
160	913.6	0.109	2.050	1.34	1.46	0.58
170	906.6	0.108	2.086	1.18	1.30	0.83
180	899.5	0.107	2.122	1.06	1.17	1.17
190	892.3	0.107	2.158	0.95	1.06	1.62
200	885.1	0.106	2.195	0.86	0.97	2.23
210	877.8	0.105	2.231	0.78	0.89	3.02
220	870.4	0.104	2.268	0.72	0.82	4.06
230	863.0	0.103	2.305	0.66	0.77	5.39
240	855.5	0.102	2.342	0.61	0.71	7.10
250	847.9	0.100	2.379	0.57	0.67	9.25
260	840.3	0.099	2.417	0.53	0.63	11.95
270	832.5	0.098	2.455	0.49	0.59	15.31
280	824.6	0.097	2.492	0.46	0.56	19.46
290	816.6	0.096	2.531	0.44	0.54	24.55
300	808.5	0.095	2.569	0.41	0.51	30.73
310	800.3	0.093	2.608	0.39	0.49	38.22
320	792.0	0.092	2.647	0.37	0.47	47.20
330	783.5	0.091	2.686	0.35	0.45	57.94
340	774.8	0.089	2.726	0.34	0.43	70.68
350	765.9	0.088	2.766	0.32	0.42	85.74
360	756.9	0.086	2.806	0.31	0.41	103.42
370	747.7	0.085	2.847	0.30	0.39	124.09
380	738.2	0.084	2.889	0.28	0.38	148.13

Note: Values quoted are typical values obtained in the laboratory from production samples. Other samples might exhibit slightly different data. Specifications are subject to change. Write to Solutia for current sales specifications.

* 1 bar = 100 kPa - ** 1 mm²/s = 1 cSt

Physical Property Formulae

$$\text{Density (kg/m}^3\text{)} = -0.614254 \cdot T \text{ (}^\circ\text{C)} - 0.000321 \cdot T^2 \text{ (}^\circ\text{C)} + 1020.62$$

$$\text{Heat capacity (kJ/kg.K)} = 0.003313 \cdot T \text{ (}^\circ\text{C)} + 0.000008970785 \cdot T^2 \text{ (}^\circ\text{C)} + 1.496005$$

$$\text{Thermal Conductivity (W/m.K)} = -0.000033 \cdot T \text{ (}^\circ\text{C)} - 0.00000015 \cdot T^2 \text{ (}^\circ\text{C)} + 0.118294$$

$$\text{Kinematic Viscosity (mm}^2\text{/s)} = e^{\left(\frac{586.375}{T \text{ (}^\circ\text{C)} + 62.5} - 2.2809\right)}$$




$$\text{Vapour Pressure (kPa)} = e^{\left(\frac{-9094.51}{T \text{ (}^\circ\text{C)} + 340} + 17.6371\right)}$$

Appendix D

Collector Datasheets

This appendix contains the datasheets that were used to specify generic performance parameters for flat plate (FPC), evacuated tube (ETC) and parabolic trough (PTC) collectors in SolGain 2.0. They are also the collector parameters used in Chapter 6 for component validation and Chapter 7 for system validation. The datasheets are included in the pages after this one, starting with the FPC, then the ETC and finally the PTC. Only the relevant pages of each datasheet are shown.

D.1 Flat Plate Collector

 TÜVRheinland® 		 AUSTRIAN INSTITUTE OF TECHNOLOGY								
Summary of EN 12975 Test Results, annex to Solar KEYMARK Certificate Kurzfassung EN 12975 Test Ergebnisse, Anlage zum Solar KEYMARK-Zertifikat Synthèse des résultats d'essais selon EN 12975, annexe au certificat Solar KEYMARK			Registration No. Registernummer Numéro d'enregistrement 011-7S839 F							
Company / Firma / Société S.O.L.I.D. Gesellschaft für Solarinstallation und Design GmbH			Country/Land/Pays Austria							
Street / Straße / Rue Puchstraße 85		Website www.solid.at								
Postal Code, Place / PLZ, Ort / Code postal, Place 8020 Graz		E-mail office@solid.at								
		Tel. / Fax +43 316/292840								
Collector Type / Kollektorbauart / type de capteur Flat plate / Flachkollektor / Capteur plan										
To be roof integrated / im Dach eingegliedert zu sein / pour être intégré dans le toit			Yes / ja / oui							
Product name Produktbezeichnung Modèle	Aperture area Aperturfläche Superficie d'entrée	Gross length Länge(Außenmaß) Longueur hors tout	Gross width Breite (Außenmaß) largeur hors tout	Gross height Höhe (Außenmaß) épaisseur hors tout	Gross area Bruttofläche Superficie hors-tout	Power output per collector unit Leistung je Kollektormodul Puissance fournie par le capteur (note 1) G = 1000 W/m ² T _m -T _a :				
	[m ²]	[mm]	[mm]	[mm]	[m ²]	0 K	10 K	30 K	50 K	70 K
Glutmugl HT 4,2 m ²	3,85	2.050	2.076	170	4,26	3.117	3.009	2.769	2.499	2.196
Glutmugl HT 16,7 m ²	15,23	2.363	7.173	179	16,95	12.351	11.923	10.974	9.901	8.704
Collector efficiency parameters related to aperture area Kollektorleistungsparameter bezogen auf die Aperturfläche Paramètres de performances thermiques rapportées à la superficie d'entrée (note 1)						η _{10a}	0,811	-		
						η _{1a}	2,710	W/(m ² K)		
						η _{2a}	0,010	W/(m ² K ²)		
Stagnation temperature / Stagnationstemperatur / Temperature de stagnation (note 2)						t _{stg}	197,0 °C			
Effective thermal capacity / Effektive Wärmekapazität / Capacité thermique effective						C _{eff} = C/A _a	7,05 kJ/(m ² K)			
Max. operation pressure / max. Betriebsdruck / pression d'opération de maximum (note 3)						p _{max}	1000 kPa			
Incidence angle modifiers K_θ(θ) Einfallswinkelkorrekturfaktoren K _θ (θ) Facteur d'angle d'incidence K _θ (θ)	C _{DIF} /C _{TOT}		θ _r / θ _l	50°	10°	20°	30°	40°	60°	70°
	min	max	K _θ (θ _r)	0,96						
	0,06	0,2	K _θ (θ _l)	0,96						
C _{DIF} /C _{TOT} : min&max while measuring / min&max während messen / min&max pendant qu'essayant						Optional values / Angaben optional / Données optionnelles				
Testing Laboratory / Prüflaboratorium / Laboratoire d'essais ÖFPZ Arsenal Ges.m.b.H.						Website www.ait.ac.at				
Test report id. number / Prüfberichtsnummer / numéro d'identification de rapport des essais 2.04.00667.1.0-2-LT(1) / 2.04.00667.1.0-2- QT(1)						Date of test report / Datum des Prüfberichts / date de rapport des essais 29.06.2009				
Perf. test method / Leistungstestmethode / méthode d'essai de performance EN 12975-2 6.1.5 (indoor/innen/intérieur)						Comments of testing laboratory / Kommentare des Prüflaboratoriums / commentaires du laboratoire d'essais : 				
Note 1	Test conditions Prüfbedingungen conditions d'essais	Fluid Flüssigkeit Liquide	Water Wasser Eau	Flow rate Durchfluss Débit	0,018	kg/s per m ²	Österreichisches Forschungs- und Prüfzentrum Arsenal Ges.m.b.H. A-1210 Wien, Giefinggasse 2 Tel.: +43(0)50 550-0 Fax: +43(0)50 550-6666			
Note 2	Irradiance / Bestrahlungsstärke / Irradiance G_s=1000 W/m² Ambient temperature / Umgebungstemperature / Temperature ambiante: t_a=30 °C									
Note 3	Given by manufacturer / Herstellerangaben / donnée par le fabricant									

DIN CERTCO • Alboinstraße 56 • 12103 Berlin

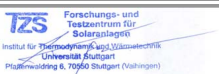
Tel: +49 30 7562-1131 • Fax: +49 30 7562-1141 • E-Mail: info@dincertco.de • www.dincertco.de

D.2 Evacuated Tube Collector



Page 1/2

Summary of EN 12975 Test Results, annex to Solar KEYMARK Certificate						Certificate No. 011-7S1889 R					
						Date of issue 29.05.2012					
Company Ritter Energie- & Umwelttechnik GmbH & Co				Country Germany							
Brand (optional)				Website www.ritter-gruppe.com							
Street, number Kuchenäckerstraße 2				E-mail T.Weidemann@ritter-gruppe.com							
Postal Code 72135				Tel. +49 (0)7202 922 134							
City Dettenhausen				Fax +49 (0)7202 922 100							
Collector Type (flat plate / evacuate tubular / un-glazed) Evacuated tubular collector											
Integration in the roof possible ? No											
	Aperture area (A _a) [m ²]	Gross length [mm]	Gross width [mm]	Gross height [mm]	Gross area (A _g) [m ²]	Power output per collector unit G = 1000 W/m ² T _m -T _a :					
						0 K [W]	10 K [W]	30 K [W]	50 K [W]	70 K [W]	
Collector name											
AQUA PLASMA 19/17 *	1.49	2,058	823	110	1.69	1,024	1,014	992	967	938	
AQUA PLASMA 19/34 *	3.00	2,058	1,628	110	3.35	2,061	2,042	1,998	1,947	1,888	
AQUA PLASMA 19/50 *	4.50	2,058	2,433	110	5.01	3,092	3,063	2,997	2,920	2,832	
Collector efficiency parameters related to aperture area (A_a)						η _{0a}	0.687	-			
Type of fluid and flow rate see note 1						β _{1a}	0.613	W/(m ² K)			
						β _{2a}	0.003	W/(m ² K ²)			
Stagnation temperature - Weather conditions see note 2						t _{stg}	338 °C				
Effective thermal capacity						C _{eff} = C/A _a	8.78 kJ/(m ² K)				
Max. operation pressure - see note 3						p _{max}	1000 kPa				
Incidence angle modifiers K_θ(θ)	G _{DIF} /G _{TOT}		θ _r / θ _i	50°	10°	20°	30°	40°	60°	70°	
	min	max	K _θ (θ _r)	0.96	1.01	1.02	1.02	1.02	1.06	1.20	
G _{DIF} /G _{TOT} : min&max - while measuring			K _θ (θ _i)	0.90	1.00	0.99	0.97	0.94	0.86	0.85	
						<i>Optional values</i>					
Testing Laboratory						TZS, ITW University of Stuttgart					
Website						www.tzs.uni-stuttgart.de					
Test report id. number						11COL1008/1, 11COL1007/1, 11COL1007Q/1					
Date of test report						29.05.2012					
Perf. test method						EN 12975-2 6.1.4 (outdoor)					
Comments of testing laboratory : * dimensions according to manufacturer											
Note 1	Fluid	Water	Flow rate	0.020 kg/s per m ²							
Note 2	Irradiance, G _s =1000 W/m ² Ambient temperature , T _a =30 °C										
Note 3	Given by manufacturer										



VERSION 3.6, 2012.01.13

DIN CERTCO • Alboinstraße 56 • 12103 Berlin
 Tel: +49 30 7562-1131 • Fax: +49 30 7562-1141 • E-Mail: info@dincertco.de • www.dincertco.de



Annual collector output based on EN 12975 Test Results, annex to Solar KEYMARK Certificate	Certificate No.	011-751889 R
	Issued	29.05.2012

Annual collector output kWh													
Collector name	Location and collector temperature (T _m)												
	Athens			Davos			Stockholm			Würzburg			
	25°C	50°C	75°C	25°C	50°C	75°C	25°C	50°C	75°C	25°C	50°C	75°C	
AQUA PLASMA 19/17 *	1,768	1,664	1,544	1,659	1,551	1,430	1,128	1,032	934	1,207	1,106	1,001	
AQUA PLASMA 19/34 *	3,560	3,350	3,109	3,340	3,123	2,879	2,271	2,078	1,881	2,430	2,227	2,015	
AQUA PLASMA 19/50 *	5,340	5,026	4,663	5,010	4,684	4,319	3,407	3,117	2,821	3,645	3,340	3,023	

Collector mounting: Fixed or tracking Fixed; slope = latitude - 15° (rounded to nearest 5°)

Overview of locations				
Location	Latitude °	Gtot kWh/m ²	Ta °C	Collector orientation or tracking mode
Athens	38	1,765	18.5	South, 25°
Davos	47	1,714	3.2	South, 30°
Stockholm	59	1,166	7.5	South, 45°
Würzburg	50	1,244	9.0	South, 35°

Gtot	Annual total irradiation on collector plane	kWh/m ²
Ta	Mean annual ambient air temperature	°C
Tm	Constant collector operating temperature (mean of in- and outlet temperatures)	°C

Calculation of the annual collector performance is done by the official Solar Keymark spreadsheet tool. Hour by hour the collector output is calculated according to the efficiency parameters from the Keymark test using constant collector operating temperature (T_m). Detailed description with all equations used is available from the Solar Keymark web site (direct link: <http://www.estif.org/solarkeymark/annexb1.php>)

DIN CERTCO • Alboinstraße 56 • 12103 Berlin Tel: +49 30 7562-1131 • Fax: +49 30 7562-1141 • E-Mail: info@dincertco.de • www.dincertco.de	Datasheet version: VERSION 3.6, 2012.01.13 Calculation program version: 3.07, October 2011 (SP)
---	--

D.3 Parabolic Trough Collector




Technical Data for the PolyTrough 1800

General Description

The PolyTrough 1800 is a roof and ground-mountable parabolic trough collector developed for:

- High performance up to 250°C outlet temperature
- Ease of installation
- Flexible configurations
- Efficient shipping in ISO compliant containers
- Low cost per kWh delivered

The solar heat is used in thermal applications such as:

- Industrial processes (steam, water or oil)
- Solar cooling systems
- Organic Rankine Cycles (ORC) for power generation
- Desalination

Technical Data for the Base Module

Geometry

Refer to Drawing 'Polytrough 1800_1250_2_2' for a detailed drawing of the collector module.

Aperture area: 36.9 m²

Aperture width: 1.845 m

Length: 20.9 m

Height: 1.75 m

Focal length: 0.65 m

Rim angle: 71°

Concentration ratio: 54 (geometric)

Weight

Weight of complete module: 1,100 kg (30 kg/m² aperture area)

NEP Solar AG
Technoparkstrasse 1 | 8005 Zürich | Switzerland

P: +41 44 445 16 95

F: +41 43 411 90 08

www.nep-solar.com

NEP Solar Pty Ltd
21/14 Jubilee Ave | Warriewood | NSW 2102 | Australia

P: +61 2 9998 4700

F: +61 2 9999 2077

www.nep-solar.com



1 Description of Collector

1.1 Technical Data of the Sample

Product information		Absorber	
Manufacturer	NEP SOLAR AG	Absorber element	Stainless steel pipe
Model	PolyTrough 1800	Length of absorber element	10305.0 mm
Type	Tracking concentrating collector	Width of absorber element	34.0 mm
Flow	Direct flow	Thickness of absorber element	1.50 mm
Serial product	Yes	Coating	Black chrome
Drawing number	A complete set of technical drawings is filed at the test institute	Flowed through element	Stainless steel pipe
Serial number	--	Joining technique	Orbitally welded
Date of manufacture	01.05.2012	Joining seam	Blank
Physical parameters		Installation	
Gross length	11.085 m	On tilted roof	No
Gross width	1.965 m	In tilted roof	No
Gross height	1.819 m	On flat roof	Yes
Gross area	21.782 m ²	On flat roof with stand	No
Aperture area	18.450 m ²	Facade	No
Absorber area	1.079 m ²	Casing and insulation	
Weight empty	700.0 kg	Casing material	Aluminium
Fluid capacity	9.8 l	Sealing material	--
Construction		Insulation material	Rockwool, Braided fiberglass
Type	Tracking concentrating collector	Thickness (in mm)	50, 30
Number of absorber elements	1	Aperture dimensions	5.000 m * 1.845 m * 2
Absorber pitch	--	Limitations (manufacturer information)	
Number of hydraulically parallel tubes	1	Max. temperature	230°C
Number of thermally serial glazings	1	Max. operating pressure	40 bar
Material of glazing(s)	Borosilicate glass	Other	--
Thickness of glazing(s)	2.5 mm	Remarks on collector design	
Heat transfer fluid (manufacturers' recommendation)		Parabolic trough collector	
Type	Water	Test schedule	
Specifications	Can be operated with water-antifreeze and thermal oil	Test procedure	EN12975:2006, Outdoor test
Flow range (manufacturers' recommendation)		Sample received	27.07.2012
Flow range	900 - 3600 l/h	Start of test	13.08.2012
Rated flow rate	1800 l/h	End of test	16.11.2012



2.3.3 Efficiency curve based on aperture area and direct solar irradiance

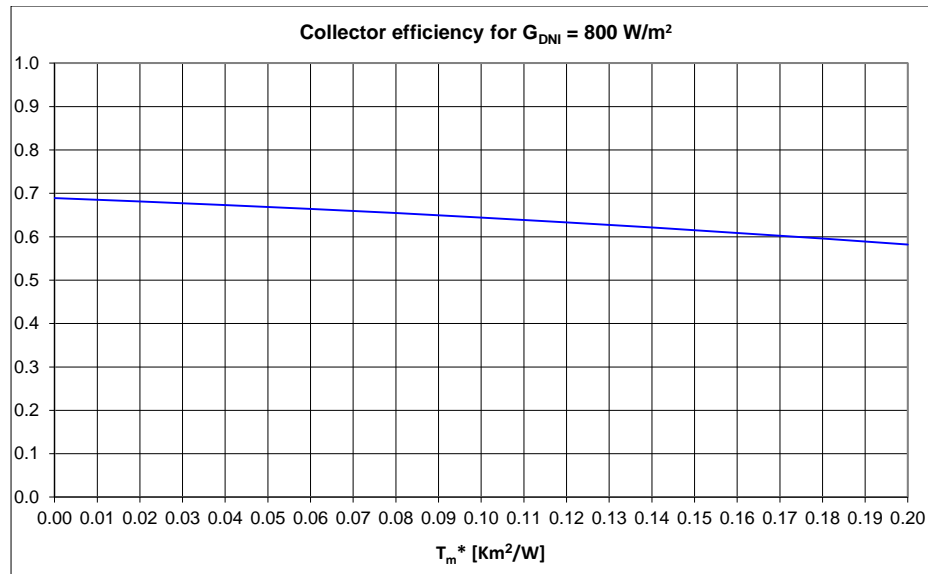


Fig. 2.3: Efficiency diagram for $G_{DNI} = 800 \text{ W/m}^2$

2.3.3.1 Parameters for efficiency equation

The collector parameters below are based on direct solar irradiance and derived from the collector parameters determined from the measurements under quasi-dynamic conditions.

$\eta_{0,DNI} (-)$	0.689
$a_1 \text{ (W/m}^2\text{K)}$	0.36
$a_2 \text{ (W/m}^2\text{K}^2)$	0.0011



2.4 Incidence Angle Factor

2.4.1 Table of the Incidence Angle Modifier (IAM)

	0°	10°	20°	30°	40°	50°	60°	70°	80°	90°
K_{θ} (transversal)	1.00	0.99	0.99	0.98	0.96	0.93	0.88	0.75	0.46	0.00
K_{θ} (longitudinal)	--	--	--	--	--	--	--	--	--	--

2.4.2 Diagram of the Incidence Angle Modifier

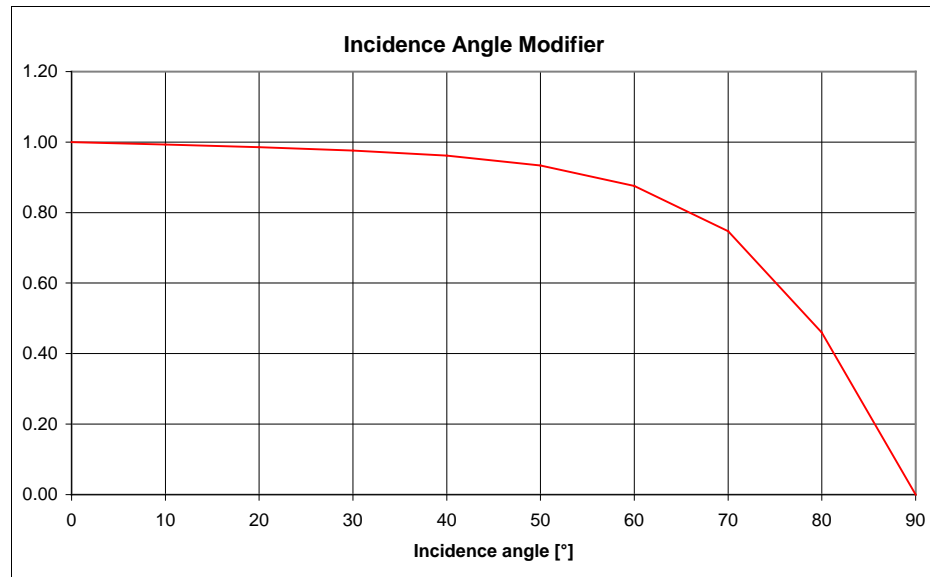


Fig. 2.5: Incidence angle modifier



2.5 Time Constant

$$\tau_c = 27 \text{ s}$$

2.6 Effective Thermal Capacity

2.6.1 Determination according to EN12975-2:2006, Section 6.3.5

Determination based on the measurements under quasi-dynamic conditions.

$$C_{\text{eff, qd}} = 56.5 \text{ kJ/K (Effective thermal capacity of collector filled with fluid)}$$

Additional information: The thermal capacity was measured with the properties of „Water “. For other fluids, the thermal capacity is calculated as follows:

$$C_{\text{eff, qd}} = 17.5 \text{ l} * \text{density} * \text{specific heat capacity of fluid} + 15.5 \text{ kJ/K}$$

2.6.2 Determination according to EN12975-2:2006, Section 6.1.6.2

Estimation based on material properties.

$$C_{\text{eff, 6162}} = 48.2 \text{ kJ/K (Effective thermal capacity of collector filled with fluid)}$$

Additional information: The thermal capacity was measured with the properties of „Water “. For other fluids, the thermal capacity is calculated as follows:

$$C_{\text{eff, 6162}} = 17.5 \text{ l} * \text{density} * \text{specific heat capacity of fluid} + 7.2 \text{ kJ/K}$$

List of References

- AEE - Institute for Sustainable Technologies (2009*a*). Dimensioning and Design of Solar Thermal Systems. Tech. Rep..
- AEE - Institute for Sustainable Technologies (2009*b*). Thermal use of solar energy. Tech. Rep., AEE INTEC.
- Alvarez, M.L. (2010). Propylene Glycol Fluid and Thermal Properties. Tech. Rep., Fermilab.
- Arcon-Sunmark (2017). Codelco's Pampa Elvira Solar installation in Chile. Available at: <http://arcon-sunmark.com/newsandmedia/work-aboard-1>
- British Petroleum (2017). BP Statistical Review of World Energy 2017. *British Petroleum*, , no. 66, pp. 1–52. ISSN 1098-6596. arXiv:1011.1669v3.
- Brooks, M.J., Du Clou, S., Van Niekerk, J.L., Gauche, P., Leonard, C., Mouzouris, M.J., Meyer, A.J., Van der Westhuizen, N., Van Dyk, E. and Vorster, F.J. (2015). SAURAN: A new resource for solar radiometric data in Southern Africa. *Journal of Energy in Southern Africa*, vol. 26, no. 1, pp. 2–10. ISSN 1021447X.
- Carvalho, M.J., Horta, P., Mendes, J.F. and Pereira, M.C. (2007). Incidence Angle Modifiers: a General Approach for Energy Calculations. *Proceedings of ISES World Congress*, vol. 1 - 5, no. 3, pp. 608–612.
- Çengel, Y.A. and Ghajar, A.J. (2015). *Heat and Mass Transfer: Fundamentals & Applications*. 5th edn. McGraw-Hill Education, New York.
- Deutsche Gesellschaft für Sonnenenergie (2010). *Planning & Installing Solar Thermal Systems*. 2nd edn. James & James. ISBN 9781844077601.
- Duffie, J.A. and Beckman, W.A. (2013). *Solar Engineering of Thermal Processes Solar Engineering*. 4th edn. John Wiley & Sons, Inc., Hoboken. ISBN 9780470873663. arXiv:1011.1669v3.
- Energy Research Centre (2013). Assumptions and Methodologies in the South African TIMES (SATIM) Energy Model. vol. 2.1, p. 97.
- Frasquet, M. (2016). SHIPcal: Solar Heat for Industrial Processes Online Calculator. *Energy Procedia*, vol. 91, pp. 611–619. ISSN 18766102.

- Furbo, S. and Shah, L.J. (1996). Optimum solar collector fluid flow rates. In: *EuroSun. 10. Internationales Sonnenforum*, pp. 189–193.
- Hess, S. (2014). *Low-Concentrating, Stationary Solar Thermal Collectors for Process Heat Generation*. Ph.D. thesis, De Montfort University Leicester.
Available at: http://www.reiner-lemoine-stiftung.de/en/pdf/dissertationen/Diss_Hess_Final_view_sh.pdf
- IDAE (2015). Informes Técnicos Ramsar. Tech. Rep., IDAE, Madrid.
- Ilchmann, C. (2016). *Modeling of Solar Process Heat Systems in an Open Source Simulation Environment*. Ph.D. thesis, Brandenburgische Technische Universität Cottbus-Senftenberg.
Available at: http://sterg.sun.ac.za/wp-content/uploads/2016/04/3_C_Ilchmann.pdf
- International Energy Agency (2017). *Key World Energy Statistics*. Paris. ISBN 9788578110796.
- Iqbal, M. (1983). *An Introduction to Solar Radiation*. Academic Press Canada, Ontario.
- ISO 9806:2017 (2017). Solar energy - solar thermal collectors - test methods, edition. Tech. Rep..
- Joubert, E.C., Hess, S. and Van Niekerk, J.L. (2016). Large-scale solar water heating in South Africa: Status, barriers and recommendations. *Renewable Energy*, vol. 97, pp. 809–822. ISSN 18790682.
- Kleinbach, E., Beckman, W. and Klein, S. (1993). Performance study of one dimensional models for stratified thermal storage tanks. *Solar Energy*, vol. 50, no. 2, pp. 155–166. ISSN 0038092X.
- McIntire, W.R. (1982). Factored approximations for biaxial incident angle modifiers. *Solar Energy*, vol. 29, no. 4, pp. 315–322. ISSN 0038092X.
- Meteotest, Remund, J., Müller, S., Kunz, S., Huguenin-Landl, B., Studer, C. and Cattin, R. (2017). *Meteonorm Handbook part I: Software*.
- Newton, B.J. (1995). *Modeling of Solar Storage Tanks*. Ph.D. thesis, University of Wisconsin-Madison.
- Perez, R., Seals, R., Ineichen, P., Stewart, R. and Menicucci, D. (1987). A new simplified version of the perez diffuse irradiance model for tilted surfaces. *Solar Energy*, vol. 39, no. 3, pp. 221–231. ISSN 0038092X.
- Pizzolato, A., Donato, F., Verda, V. and Santarelli, M. (2015). CFD-based reduced model for the simulation of thermocline thermal energy storage systems. *Applied Thermal Engineering*, vol. 76, pp. 391–399. ISSN 13594311.
- Regulus (2007). Solar Systems Design and Sizing. Tech. Rep..

- Short, W., Packey, D. and Holt, T. (1995). A manual for the economic evaluation of energy efficiency and renewable energy technologies. Tech. Rep. March, NREL, Golden.
- Solar Energy Laboratory, U.o.W.-M. (2007). TRNSYS 16 Getting Started.
- Stine, W.B. and Geyer, M. (2001). *PowerFromTheSun*.
Available at: <http://www.powerfromthesun.net/book.html>
- Theunissen, P. and Beckman, W. (1985). Solar Transmittance Characteristics of Evacuated Tubular Collectors with Diffuse Back Reflectors. *Solar Energy*, vol. 35, no. 4, pp. 311–320.
- Vela Solaris (2017). Polysun Simulation Software - User Manual.
- Wagner, M.J. and Gilman, P. (2011). Technical Manual for the SAM Physical Trough Model Technical Manual for the SAM Physical Trough Model. Tech. Rep. June.